Ministero dell'Università e della Ricerca Scientifica e Tecnologica

Università Degli Studi di Palermo

"Development and application of active and passive DOAS instrumentation for the remote sensing measurement of volcanic gas emissions and continuous geochemical monitoring of degassing volcanoes"

PhD Thesis by:
FABIO VITA

Tutor Prof. F. Parello
Co - Tutor Dott. S. Inguaggiato

DOTTORATO DI RICERCA IN GEOCHIMICA XXII CICLO

Facoltà di Scienze Matematiche, Fisiche e Naturali
Dipartimento di Chimica e Fisica della Terra ed Applicazioni Alle Risorse ed ai Rischi Naturali (C.F.T.A)

1 INTRODUCTION

From the geochemical point of view the fluids released from volcanic systems represent the only surface manifestation of magma degassing at depth. Volatiles are dissolved in magma at well established thermodynamic conditions (P, T and fO_2), and any variation in the starting conditions at depth determine a new state of equilibrium. Usually, a decrease in total pressure caused by the fracturing of the rock around the conduit and/or the rise of a magma batch triggers the exsolution of dissolved volatiles that easily reach the surface, thus providing information on the physico-chemical conditions of the volcanic system.(Inguaggiato et al.2011)

In particular, "intensive" parameters such as the chemical composition of the discharged gases and their relative proportions (ratios) give useful information on Pressure, temperature and oxygen fugacity (P, T and fO2) conditions (Gerlach and Nordlie 1975; Giggenbach 1980, 1996; Gerlach 1993; Giammanco et al. 1998; Taran et al. 1998; Paonita et al. 2002). Isotopic compositions (such as He, C, Ar, N, H, O) mainly indicate the origin of the gases and give an indication of the physico-chemical processes that took place during exsolution and migration towards the surface (Allard 1983; Taran et al. 1986; Capasso et al. 1997; Nuccio and Paonita 2001; Inguaggiato et al. 2000, 2004). Moreover, the measure of the plume's compositional ratios such as F/Cl, S/Cl, C/S (Oppenheimer et al. 1998; Aiuppa and Federico 2004; Aiuppa et al. 2004; Allard et al. 2005) gives information about the depth of the exsolution of volatiles. In detail, C/S ratio measurements were performed by Aiuppa et al. (2009) during the 2007 Stromboli eruption with the aim of identifying the depth of the source of the degassing system.

Over the last few years, numerous studies have focused on the volcanic system using an "extensive" approach to quantify the "masses" involved in the degassing processes occurring both during quiescent and active states of degassing (Allard et al. 1994; Italiano et al. 1997; Aiuppa et al. 2005; Allard et al. 2005). Quantification of extensive parameters in volcanic systems results in estimates regarding the volume of magma involved in volcanic degassing. By coupling intensive parameters with extensive parameters, monitored simultaneously over a period of time, it is possible to obtain a more complete description of the state of the volcanic activity, making it possible to better evaluate the nature (i.e. explosive or effusive) and timing of eruptions.

Generally, CO_2 represents the main constituent of dry fumarolic gases emitted from the summit of a volcano through plume and/or crater fumarolic areas (Chiodini et al. 2005; Inguaggiato et al. 2005). CO_2 flux measurements has been successfully applied to volatile budget studies (Chiodini et al. 1996; Favara et al. 2001; Cardellini et al. 2003; Chiodini et al. 2005; Pecoraino et al. 2005), and to programs of geochemical monitoring of fluids, the aims of which are to forecast changes in volcanic activity (Brusca et al. 2004; Carapezza et al. 2004).

SO2 is the main sulphur species in high-temperature fumarolic gases (Aiuppa et al. 2005), SO_2 emission flux has been used to calculate the volume of magma batches in volcanic systems applied to volcanic surveillance activities (Bruno et al. 1999; Edmonds et al. 2003). Over the past few years many investigations have been carried out on SO_2 flux measurements of plumes (Bruno et al. 1999; Edmonds et al. 2001). Technological advancements in the SO_2 flux measurements have recently been made, which have simplified monitoring this parameter in the plume (Galle et al. 2003). Moreover, considering that SO_2 is absent in clean atmospheres, it is simple to measure the plume compared to the ambient background. By contrast, it is more difficult to measure CO_2 in the plume because CO_2 is present in the clean atmosphere, 388 ppm by volume (Annual Mean Growth Rate for Mauna Loa, Hawaii, http://www.esrl.noaa.gov/gmd/ccgg/trends/#mlo_growth. Retrieved 28 April 2010) and the telemetric measurement of this parameter is only possible over short distances in the atmosphere, where the plume occupies a large percentage of the path. In fact, for long-path CO_2 measurements, the contrast between plume and atmosphere is not well defined, and the amount measured in the atmospheric layers can be comparable to or greater than the amount of CO_2 in the plume.

For this reason, we have focused the development of this thesis on the measurements in the active volcanic areas of CO_2 flux emitted from the soils and of the SO_2 flux measured in the plume.

In particular during the realization of this thesis-work we investigate the fluids discharged from active volcanoes located in the Aeolian Archipelago (Vulcano and Stromboli) of Sicily island. These studied volcanic systems, Vulcano and Stromboli, are characterized by closed and open conduct systems respectively.

International joint projects are utilized to improve the quality of the investigation and to compare the relative high scientific technology reached in the different European countries.

The investigation on Vulcano Island was carried out inside of the NOVAC project (Network for Observation of Volcanic and Atmospheric Change) while for Stromboli Island the research investigation was performed inside a joint project with Heidelberg University.

Finally we utilize part of this PhD-work to the realization of a active DOAS equipment, to investigate SO_2 and trace molecular species inside of the volcanic plume.

1.2 Aeolian Islands

The Aeolian Islands represent the emerged portions of an extended submarine volcanic arc. This archipelago is related to the subduction of the African plate underneath the European Plate [Keller, 1980; Ellam et al., 1989]

Volcanic activity of the archipelago started at the westernmost part and then move towards East and South, defining three different sectors showing different evolutions, structural and volcanological features (De Astis et al., 2003).

(1) a western sector(Alicudi and Filicudi islands) dominated by NW–SE oriented tectonic lineaments;

(2) a central sector (Salina, Lipari and Vulcano islands)aligned along the NNW–SSE tectonic trend;

(3) an eastern sector (Panarea and Stromboli islands) characterized by prevailing NE–SW oriented SE to NNW–SSE-trending faults (Ventura, 1994).

Salina, Lipari, and Vulcano are three islands aligned along a NNW–SSE trend, distinct with respect to the arc layout. The development of these islands is strongly influenced by an active crustal discontinuity related to the Tindari–Letojanni dextral strike-slip fault system formed in the continuation of the Malta escarpment (Barberi et al., 1994; Ventura, 1994; Ghisetti, 1979)

Since 1983, more than 800 earthquakes (M > 2.5) have occurred in the southern portion of the Aeolian archipelago. Most seismicity occurred inside the Gulf of Patti area, showing a mix of dextral strike-slip and extensional fault-plane solutions, in agreement with the tectonic pattern of the northern shore of Sicily at this longitude (Billi et al., 2006). The remaining seismicity is clustered around the Salina, Lipari and Vulcano islands, in particular on their western side, showing reverse focal mechanisms with NNW–SSE and NW–SE compressive axes.

2 STROMBOLI ISLAND

2.1 Previous studies

Stromboli, the northernmost island of the Aeolian Arc (Tyrrhenian Sea; ***fig. 1***), is characterized by open conduit degassing and by a persistent, albeit, mildly explosive activity (e.g. “Strombolian activity”, Rosi et al. 2000). Intermittent explosions, which usually occur at intervals of 10-20 minutes, throw up melted scoriae, ash and solid blocks to heights of up to a few hundred meters.

This “normal” activity is episodically interrupted by more violent explosions, called “major explosions” or, if larger, “paroxysms” (Barberi et al. 1993), and by effusive events like the ones of the 2002-2003 and 2007 crises. The main difference between normal Strombolian activity and “major or paroxysm” events has been explained in terms of the petrology of the products and energy involved. In fact, normal Strombolian activity is characterized by high porphyritic products while “major or paroxysm” events are characterized by the presence of highly vesicular, crystal poor, light-coloured pumice (called golden pumice) (Bertagnini et al. 2008 and insight references).

Fig. 1 - Stromboli volcano is the northernmost island of Aeolian Islands archipelago

Moreover, these last events are characterized by higher energy than that of the normal Strombolian activity and by a deeper (i.e. several kilometres) feeding source (Bertagnini et al. 2008 and references therein). Major explosions occur on average two or three times a year (Barberi et al. 1993; Bertagnini et al. 2003). Paroxysms are Stromboli's most powerful explosive events and occur every 5-15 years; they last from a few hours to several days and produce a fallout of bombs and blocks, ash showers and glowing avalanches, such as those of the 1930, 1944, 2003 and 2007 events (Barberi et al. 1993; Calvari et al. 2005). Paroxysms often affect the inhabited areas of the island (i.e. the villages of Stromboli and Ginostra).

Stromboli's hydrothermal system has a marine-dominated aquifer located in the NE part of the island; this was recognized through wells drilled for thermal water (up to 40°C) that contains dissolved magmatic-derived fluids (mainly CO_2 and ^3He) (Inguaggiato and Rizzo 2004; Capasso et al. 2005, Grassa et al. 2008).

Zones of structural weakness (faults, fractures, etc.) on active volcanoes have proved to be the most representative sites for monitoring soil diffuse CO_2 flux (Finizola et al. 2002; Werner and Cardellini 2006; Mazot et al. 2010). On Stromboli, the most extensive and intense soil degassing areas, which

are sometimes associated with thermal anomalies, are located at the summit area (Pizzo Sopra la Fossa) and on structural zones (Carapezza and Federico 2000; Finizola et al. 2003; Brusca et al. 2004).

Plume degassing is the main way in which an open-conduit volcano such as Stromboli discharges fluids; this is another good site for investigating the compositional ratios and the relative fluxes of the fluids emitted (Aiuppa and Federico 2004, Allard et al. 2005; Burton et al 2007a; Allard et al. 2008).

On 27 February, 2007 the "normal" Strombolian activity was interrupted by a new effusive phase that lasted several weeks, finishing on 2 April of that year (Rizzo et al. 2009). During this effusive period a paroxysmal event occurred on 15 March with ejection of pyroclastic materials that ejected reached the village of Stromboli. This eruption was the first paroxysm to occur since the 5 April 2003 event.

2.2 *Dynamic volatiles equilibrium model*

Stromboli is an open conduit volcano characterized by "Strombolian" activity, which over the past few years has been interrupted by two effusive eruptions. We have been able to refine our previous models by using the experience gained over the last ten years through geochemical and volcanological observations at Stromboli.

The "normal" Strombolian activity is the result of a "delicate" dynamic equilibrium between continuous refilling of deep volatiles exsolved from the magma batch and superficial degassing (Allard et al. 2008, Grassa et al. 2008, Inguaggiato et al. 2011). When the volatiles reach the surface they interact with the superficial fluids, thereby modifying the peripheral and summit degassing processes. In particular, the main peripheral manifestations are represented by volatiles dissolved in the basal hydrothermal aquifer, and by structurally controlled soil degassing in the lower parts of the volcanic edifice (Capasso et al. 2005; Federico et al. 2008). Summit degassing is both active (i.e. explosions from the conduit) and passive (i.e. plume from the conduit and diffuse soil degassing). During "normal" Strombolian activity this dynamic equilibrium allows the volatiles, rising from deep down, to discharge into the atmosphere (***fig. 2a***). When the deep volatile flux increases, the system initially reacts with an increase in the diffuse volatile discharge from the superficial system. Indeed, the result is an increase in the Strombolian activity (i.e. increase in the frequency and energy of the explosions due to the increase in the total volatiles pressure) and/or an increase in the total dissolved volatiles in the hydrothermal aquifer and in the anomalous soil flux (***fig. 2b***).

Dynamic equilibrium
Pressure IN ≅ Pressure OUT

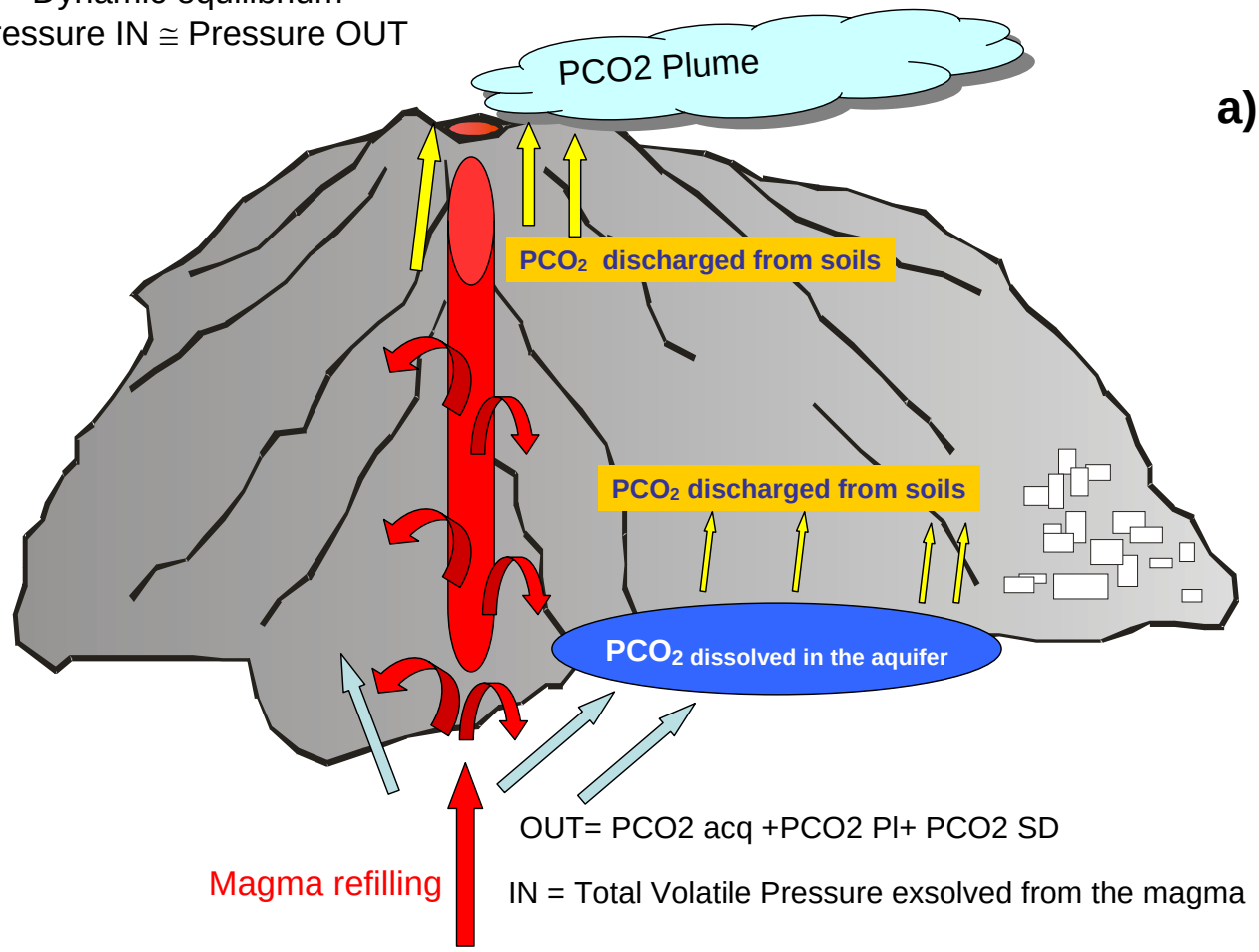

Dynamic equilibrium
Pressure IN >> Pressure OUT

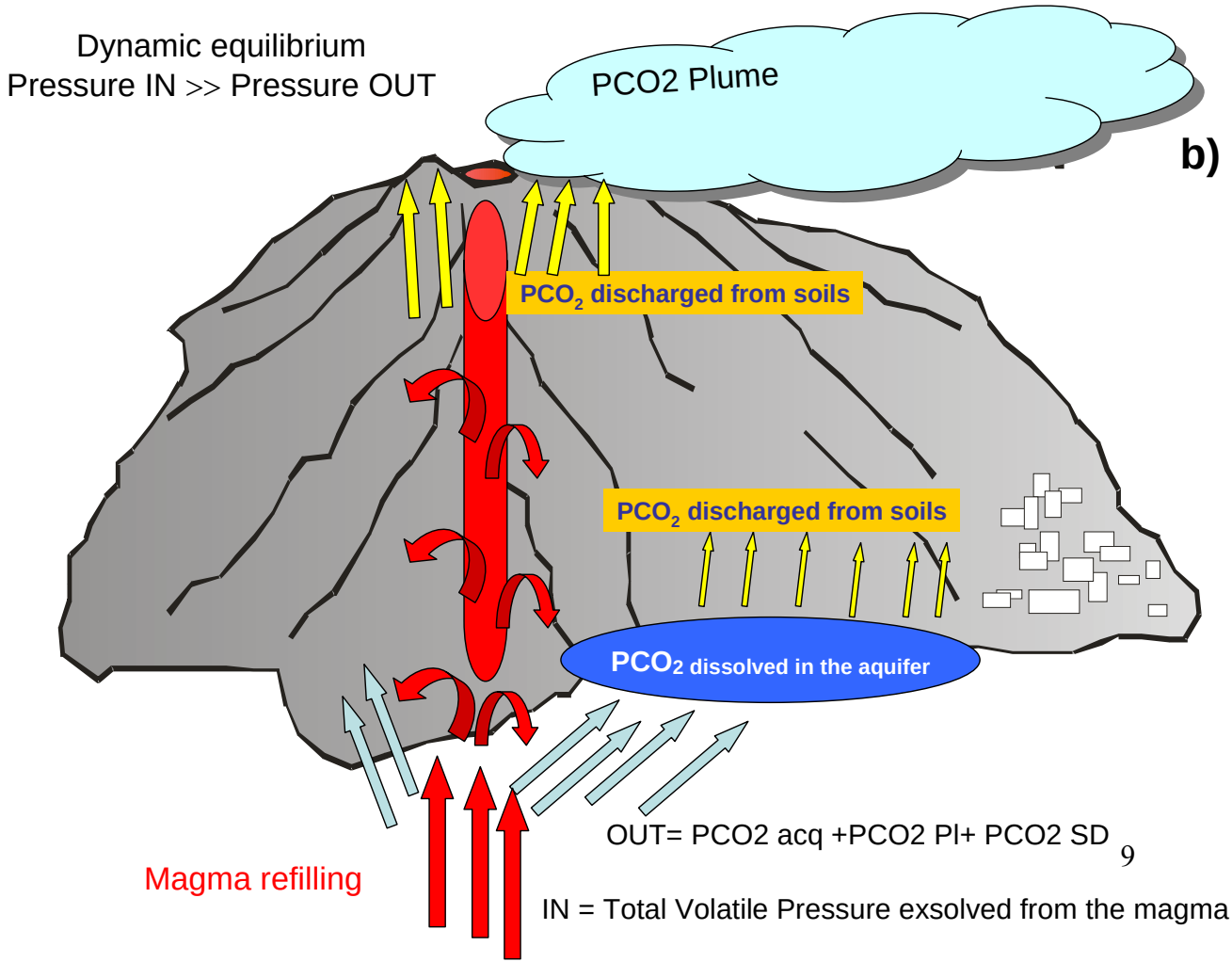

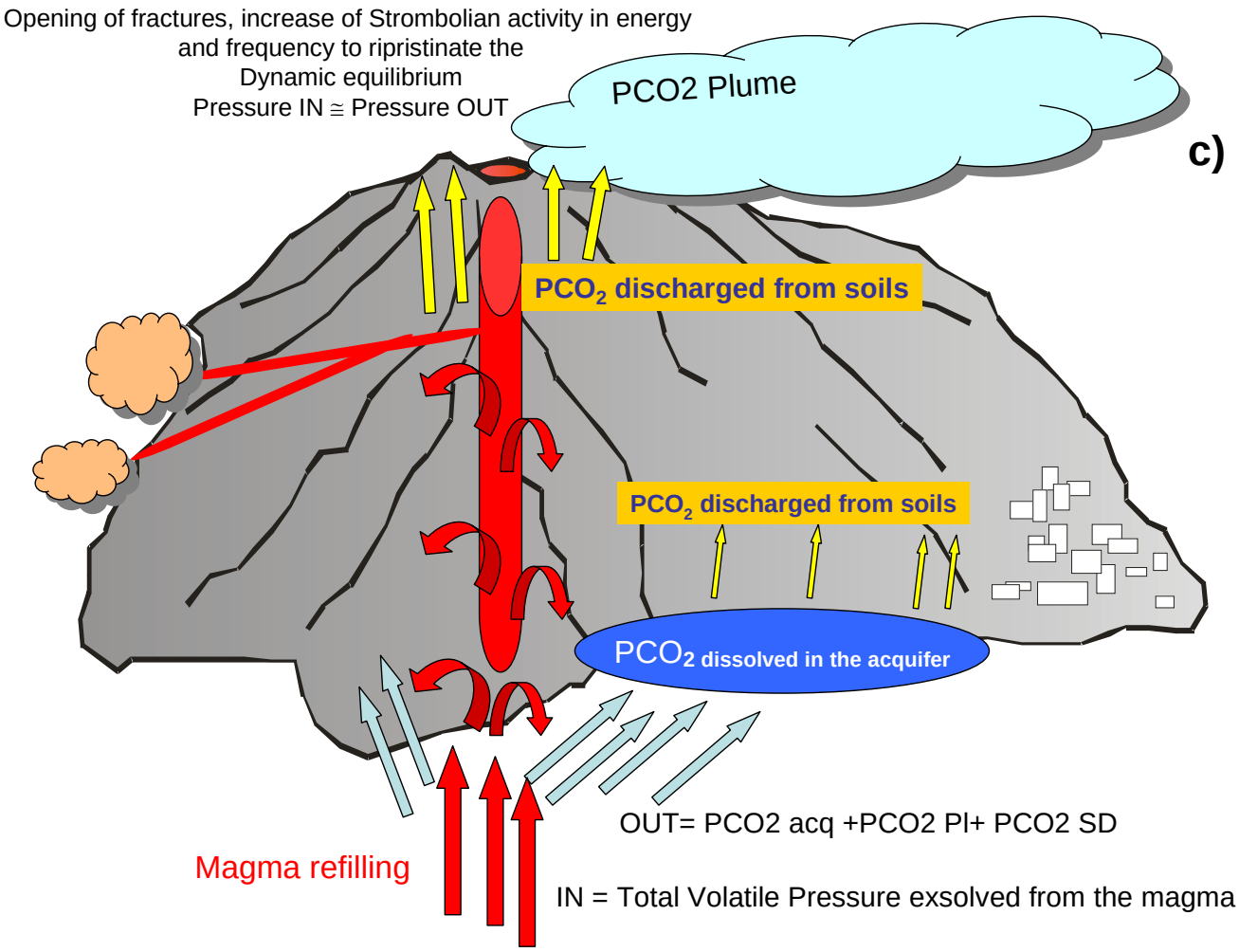

Fig. 2 - Sketch map of the "dynamic equilibrium" between deep and shallow fluids. **a)** "normal" Strombolian activity; **b)** "High" volcanic activity; **c)** "Paroxystic" volcanic activity.

During overpressure of the plumbing system, paroxystic activity is necessary to maintain the dynamic pressure equilibrium, which allows the dynamic equilibrium between the deep and superficial volatiles to be maintained. Indeed, due to the opening of new fractures and ensuing lava flow, or because of major explosions and paroxysms, there is a decrease in the total pressure of the volatiles that thus restores the dynamic equilibrium of the Stromboli plumbing system (***fig. 2c***).

2.3 *Data acquisition and field measurement procedures*

2.3.1 Continuous CO_2 flux measurements

Since 2000, the continuous monitoring of CO_2 flux emitted from the soil at Pizzo Sopra la Fossa (STR02) has been carried out on hourly basis (Brusca et al. 2004; Madonia et al. 2009) by means of an accumulation chamber (***Fig. 3***) (West Systems LTD, Chiodini et al. 1998). Data are transmitted to the COA Civil Protection volcano observatory at Stromboli via a radio link (STR02), whereby they are sent to the INGV-Palermo geochemical monitoring centre through a virtual private network link (VPN).

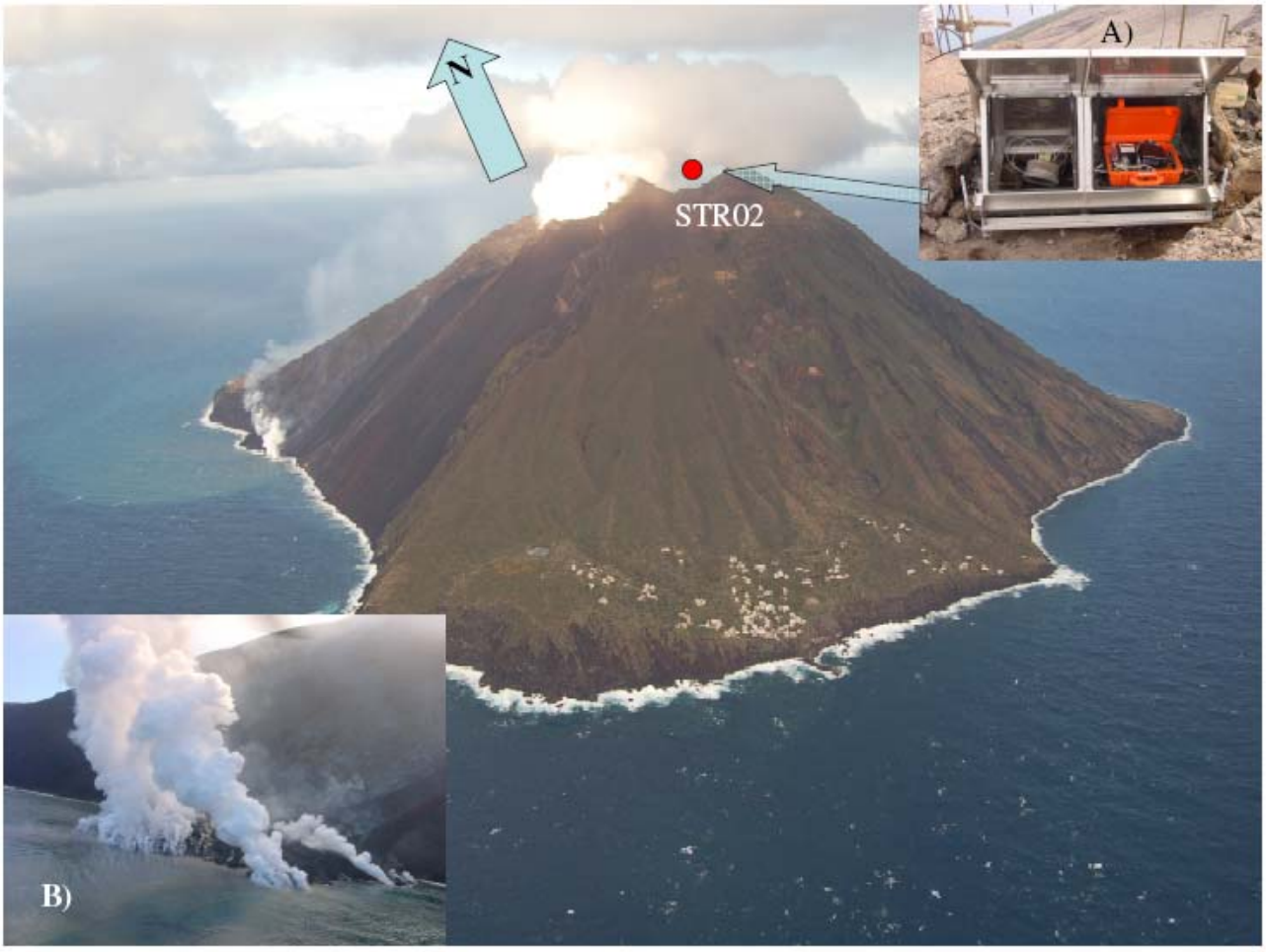

Fig. 3 - Location Map: a) monitoring CO_2 station (STR02), accumulation chamber (West Systems LTD); b) photo of the 2007 effusive eruption: the lava flow reached the sea; c) inset of Stromboli Island map with STR02 location;

Carbon dioxide is measured with a Dräger Polytron IR spectrometer, which operates in the range of 0-9999 ppm (precision of ±5 ppm); environmental parameters (wind direction and speed, soil and atmosphere temperatures, atmospheric pressure, soil and atmospheric relative humidity) are acquired at the same time (Brusca et al. 2004).

The daily average of the CO_2 flux (2005-2008 period) is reported in ***Fig. 5a***, while the Natural Daily Variation (NDV, see caption of figure 5b for explanation) in the CO_2 flux (for the same period), expressed as normalized standard deviation is reported in ***fig. 5b***.

2.3.2 SO_2 flux measurements

Initially SO_2 flux measurements were carried out on the plume using Mini-DOAS instruments consisting of a USB2000 ultra-violet spectrometer (spectral range 245-400 nm, resolution about 0.7 nm, manufactured by Ocean Optics Inc.) and a vertically pointing telescope of 7 mrad field of view with a circular-to-linear converter 4x200 μm fibre bundle which connects the telescope to the fibre. A USB cable connects the spectrometer to a laptop computer providing power and means of data transfer. Software control of the USB2000 was achieved using J-scripts executed in DOASIS software (https://doasis.iup.uni-heidelberg.de/bugtracker/projects/doasis/), to save and analyse spectra, providing real time concentration readings. Geographic coordinates for each spectrum were obtained using a hand held GPS receiver. Details of the DOAS routine used and the flux calculations can be found in Galle et al. (2003).

Considering the morphology of Stromboli, and on the basis of the dominant wind direction, the monthly measurements were carried out by performing several traverses of measurement a day (i.e. usually about five) from a boat moving beneath the plume. The used plume speed was assumed to be equally with the wind speed in a height of about 950m measured by a whether station located in the summit area at "Pizzo sopra la Fossa". To improve the frequency of data acquisition, in the beginning of March 2007 first two NOVAC mark II instruments (Kern 2009) were installed on the island, in agreement with University of Heidelberg for Long-time measurement (see below 2.5)

2.4 *Long-time variations*

2.4.1 Soil CO_2 flux at Pizzo Sopra la Fossa

We analyzed the complete soil CO_2 flux data from station STR02 during the period 2005-2008, in order to improve our knowledge of the behaviour of summit soil CO_2 flux and to relate variations to the different degassing regimes and eruptive states of Stromboli volcano.

We processed the CO_2 flux data through a cumulated probability graph (Sinclair 1974). In this graph (***Fig. 4a***), the log CO_2 flux is plotted against the cumulated probability for the entire data set of CO_2 flux at Pizzo sopra La Fossa (2005-2008). On the basis of the thresholds identified, we divided our data into 3 different families (L, M, and H). Their range is respectively between 2000-4000; 4000-10000; 10000-80000 g m^{-2} d^{-1}. Group M (i.e. medium CO_2 flux) includes about 85% of

the total acquired data, where the CO_2 flux ranges from 4000 to 10000 g m^{-2} d^{-1}. Group L (i.e. low CO_2 flux) includes about 12% of the total acquired data and it is to be referred to a low degassing regime between 2000 and 4000 g m^{-2} d^{-1}. Group H (i.e. high CO_2 flux) includes little more than 2% of the CO_2 flux data, having the highest values that range between 10000 and 80000 g m^{-2} d^{-1}.

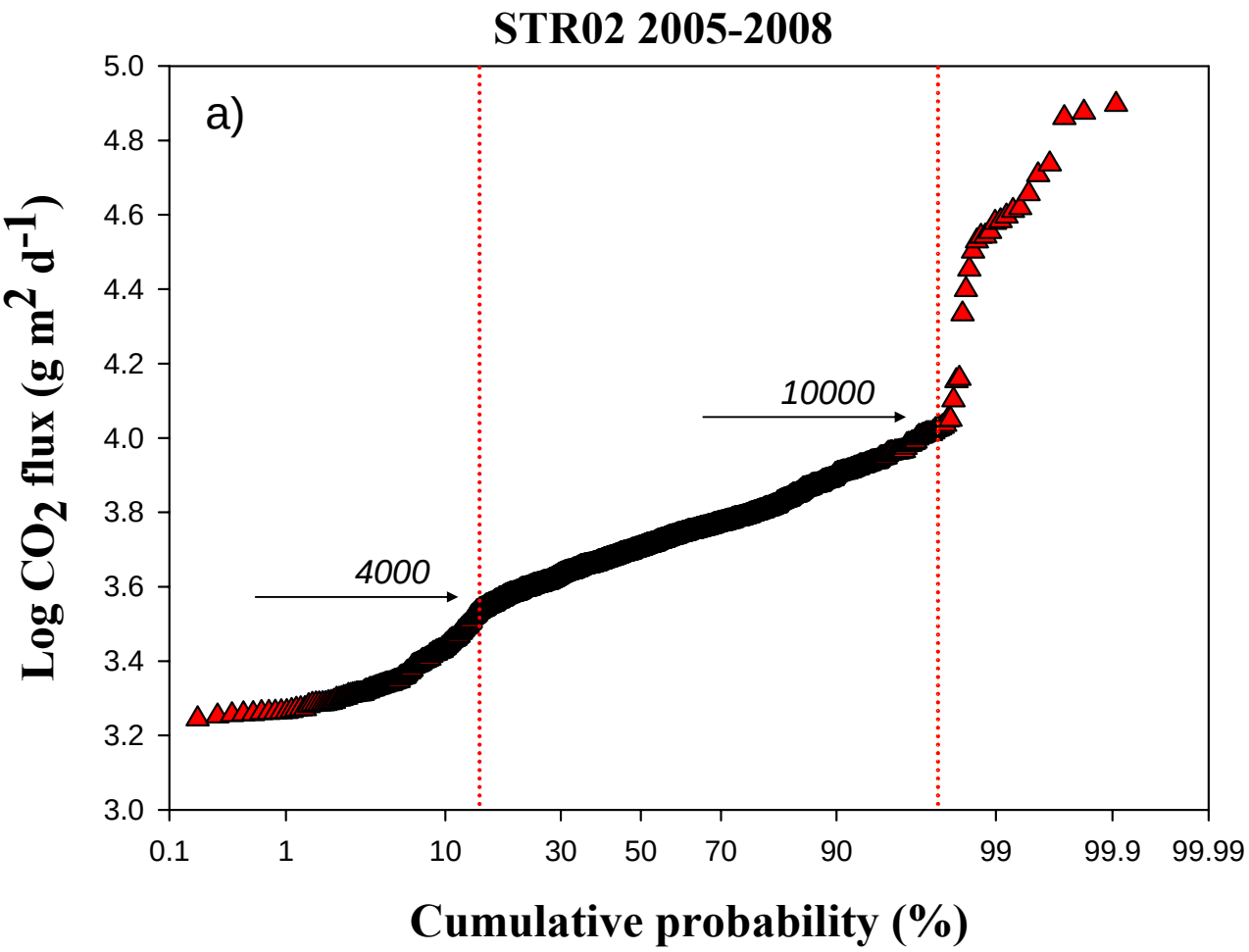

Fig. 4**a)** - STR02 Log CO_2 flux vs cumulated probability – period 2005-2008; The distribution of the plotted data has allowed us to divide it into three families: Low, Medium and High.

The histogram of the totality of the acquired data (***Fig 4b***) it's consistent with a unimodal distribution of log CO_2 centred around 3.7 (~5000 g m^{-2} d^{-1}) with two residual tail values. The average values of CO_2 flux, 5000±1000 g m^{-2} d^{-1}, computed from the data in Group M, represents the background value to be found during "normal" Strombolian activity at the permanent station. The left residual tail values represent the values below 4000 g m^{-2} d^{-1} (Group L). The right residual tail values represented by Group H deserve a separate discussion and elaboration. In fact, even though these latter include only about 2% of the CO_2 flux data, which is insufficient for statistical elaboration, this data group represents a higher than background CO_2 degassing regime.

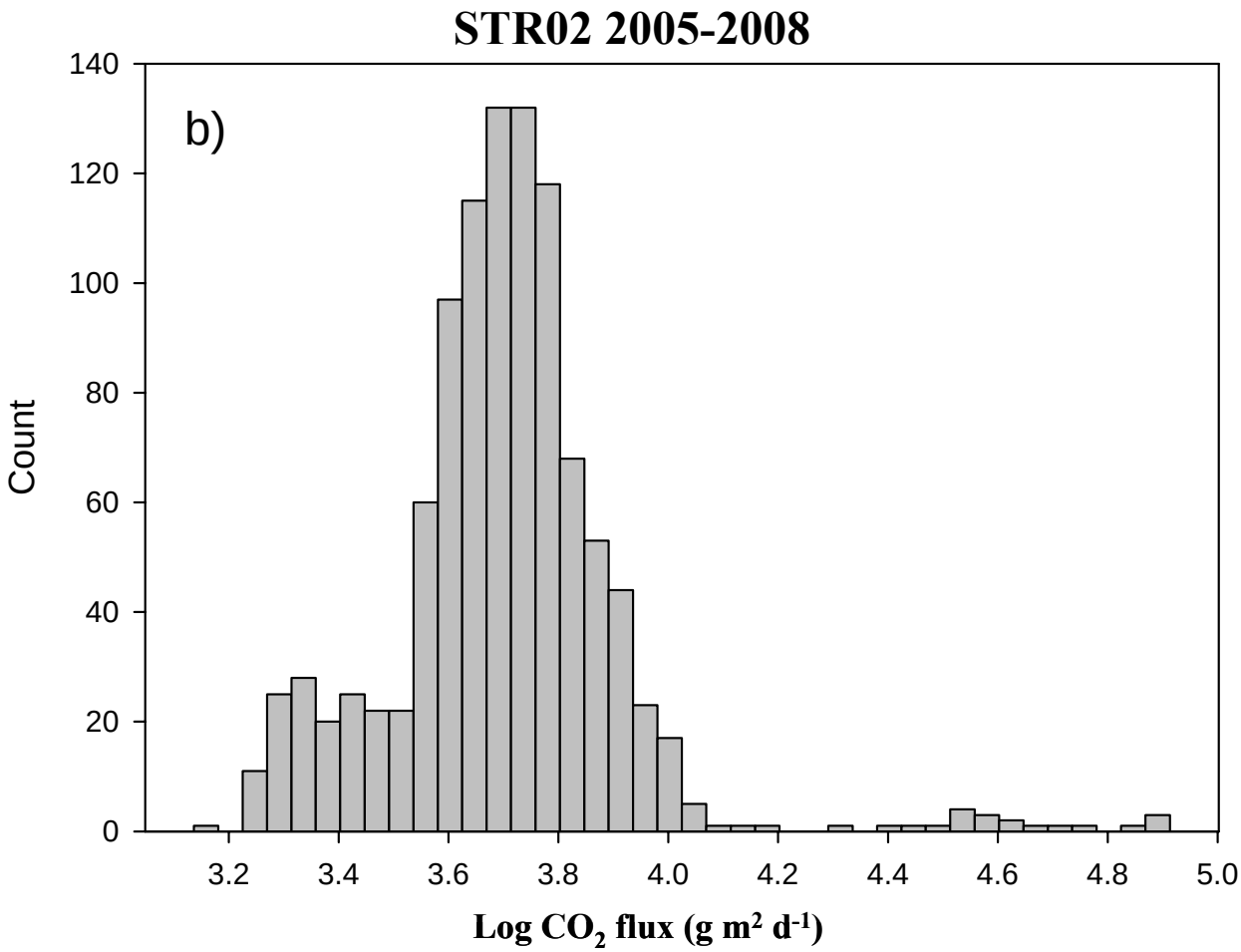

Fig. 4**b)** - Histogram of STR02 log CO_2 flux data. The plotted data show a unimodal distribution centred at 3.7 value.

Furthermore, this group is characterized by a wide NDV of flux, thus indicating an unstable degassing regime while providing important geochemical information during the transition phases. The thresholds defined in the CO_2 flux are marked on the temporal graph (***Fig. 5a***) where the daily average values of CO_2 flux for the period 2005-2008 have been plotted. The variations recorded highlight background values of around 5000 g m^2 d^{-1}, thus confirming regular Strombolian activity, and a high anomalous period (Group H) with values up to 80000 g m^2 d^{-1}. This clear and univocal peak coincides with the February-March 2007 effusive phase. In ***Fig. 5a*** it can be observed that the CO_2 fluxes recorded over the last 4 years have only reached Group H values a few times. In each of these cases the explosive activity at Stromboli increased significantly, leading to major explosive events (22 May 2006; 15 March 2007; 29 February 2008; 6 December 2008), or even to effusive activity accompanied by a paroxysm (27 February-2 April 2007, with a paroxysm on 15 March 2007). The NDV values have been calculated for the entire CO_2 flux data set (2005-2008) and plotted on the diagram given in ***Fig. 5b***. It is very interesting to observe that each increase in CO_2

flux corresponds to an increase in the NDV values; that highlights the instability of the soil CO_2 degassing system.

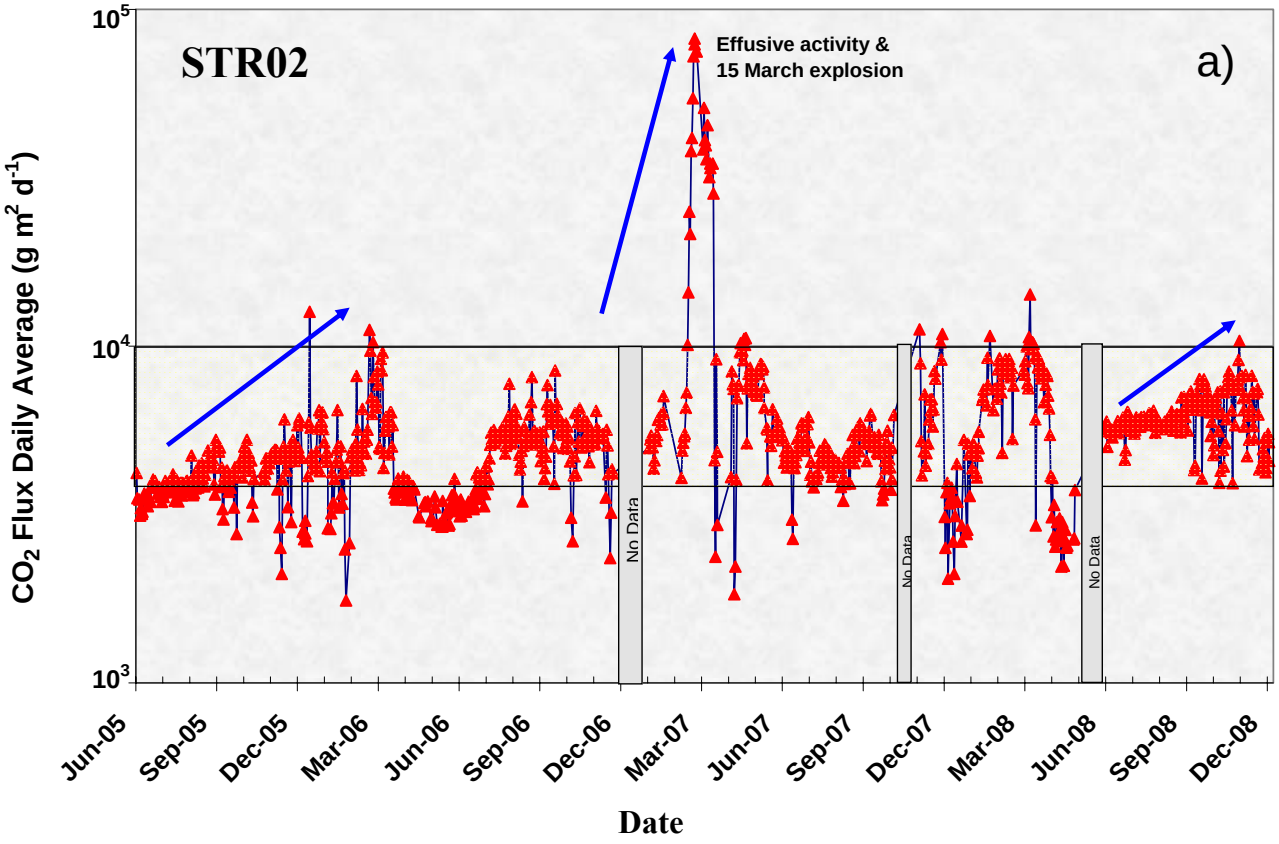

Fig. 5 - **a)** Daily average values (g $m^{-2}d^{-1}$) of summit CO_2 flux (STR02) for the period 2005-2008;

In particular, we recorded a significant change in the degassing style of the CO_2 flux from the STR02 station during the end-of-2005/first semester of 2006 period (***Fig. 5b***); the daily average degassing flux increased from 4000 to 12000 g m^2 d^{-1} with peaks in the hourly measurements of up to 20000 g m^{-2} d^{-1}. A simultaneous strong increase in NDV was recorded during the same period with values from 10 to 40%. An increase in the number of Very Long Period events (VLP) coincident with this anomalous passive style of CO_2 degassing was also recorded, thus confirming an increase in the degassing of volatiles in the magma column. This behaviour revealed the instability of the volcanic degassing system which had received numerous new impulses of volatiles exsolved from the magma. This anomalous behaviour of the geochemical and geophysical parameters culminated in the April–May 2006 period, when several earthquakes were recorded in the Aeolian Archipelago (the epicentre of which was close to the island of Stromboli) and when a major explosion from the north crater occurred on 22 May 2006.

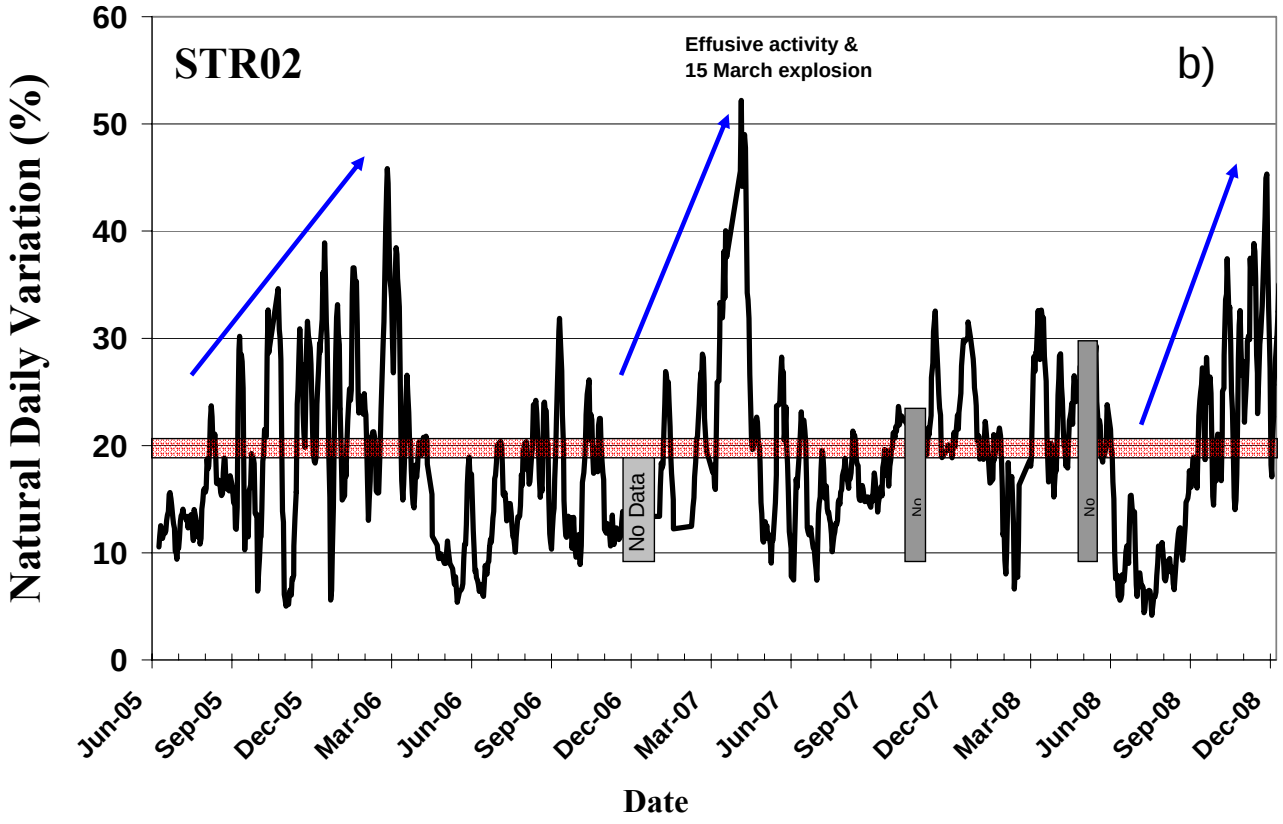

Fig 5 - **b)** Natural Daily Variation (NDV) of CO_2 flux (STR02) for the period 2005-2008; The NDV is expressed as normalized standard deviation in %. $NDV = \frac{\sigma_x}{\bar{x}}$ where $\sigma_x = \sqrt{\frac{\sum_{i=1}^{n}(x_i - \bar{x})}{n-1}}$ and $\bar{x}$ is the arithmetic mean of the daily measurements (hourly measurements, n=24). The red bar at 20% represents the average value of NDV for the whole period of observation. The blue arrows added to both figures (5a,5b) highlight similar behaviours and the simultaneous increase in these parameters.

The anomalous degassing stopped in the second half of April 2006 when it reached low values of around 4000 g m^{-2} d^{-1} (***Fig. 5a***). These low CO_2 flux values remained stable until the end of June 2006, thus highlighting very low passive degassing in the summit area. The CO_2 flux and the NDV increased again in the period July 2006-February 2007 with values of 5-7 thousand g m^2 d^{-1} and 10-30% respectively. No data was acquired due to technical problems encountered in December 2006.

2.4.2 2007 effusive eruptive phase

We will now focus on the variations observed in the CO_2 flux just before, during, and after the 2007 effusive eruptive phase. Between 23 and 26 February 2007, the CO_2 flux increased sharply, exceeding 15000 g m^2 d^{-1}, i.e. 3 times higher than the average values recorded during periods of "normal" Strombolian activity (***Fig. 5a***). On 27 February 2007 a lava effusion started at Sciara del

Fuoco. The CO_2 flux continued its increasing trend, reaching about 80000 g m^2 d^{-1} and NDV values of over 50% on 5-8 March 2007, a few days before the 15 March 2007 paroxysm. After this paroxysm, the CO_2 flux decreased drastically, dropping to about 4600 g m^2 d^{-1} on 28 March 2007, a few days before the end of the effusive event (2 April 2007). During the ensuing period (28 March to 23 May 2007) the CO_2 fluxes fluctuated between 5000 and 10000 g m^2 d^{-1}. Finally, in the last period (end May-early July) the CO_2 flux decreased, dropping to values of around 5000 g m^2 d^{-1}, a characteristic of "normal" Strombolian activity.

The year 2008 was characterized by normal Strombolian activity; in fact, only two major explosions occurred on February 29 and December 6 respectively. Both of these events were preceded by an increase in the CO_2 flux and NDV values, although they were more apparent on December 6 when the values reached 11000 g m^{-2} d^{-1} and up to 45 % respectively.

2.4.3 Plume SO_2 flux

In the past, SO_2 fluxes at Stromboli were measured using an ultraviolet correlation spectrometer (COSPEC), (Stoiber et al. 1983). The first studies on SO_2 flux at Stromboli focused on the sulphur budget involved in degassing during Strombolian activity (Millan and Hoff 1978; Allard et al. 1994; Bruno et al. 1999). However, the monitoring frequency has increased since the 2002-2003 effusive eruption and the large data set available has made it possible to fix the value of SO2 flux during periods of "normal" Strombolian activity at around 250±50 t d^{-1} (Burton et al. 2007b). We first measured the SO_2 flux on June 27, 2006.

The SO_2 fluxes, which were recorded nearly monthly (although the frequency of the measurements was higher during the 2007 eruptive period), show an average flux of 190±50 t d^{-1}; this refers to the 2006-2007 period with the exception of the effusive period (February 27-April 4 2007) and is a similar figure to that given by Burton et al. (2007b). On January 19, 2007, the first increase in the SO_2 flux (i.e. up to 730 t d^{-1}) was recorded, although by January 22 it had returned to the baseline. The flux showed a further increase on February 28, 2007 when it reached 1280 t d^{-1}, the day after the onset of the effusive activity (***Fig. 6a***). The flux showed generally higher than "normal" values during the entire effusive period (600±200 t d^{-1}), moreover there was a sudden increase on 14 March, just one day before the 15 March 2007 paroxysm, when it reached its maximum value of 2900 t d^{-1}. Over the following days, the SO_2 flux decreased but remained "anomalous" with values around 500 t d^{-1}. After the lava effusion ceased (i.e. on 2 April 2007) it took ~2 months for the SO_2 fluxes to drop back to typical Strombolian values (around 200 t d^{-1}).

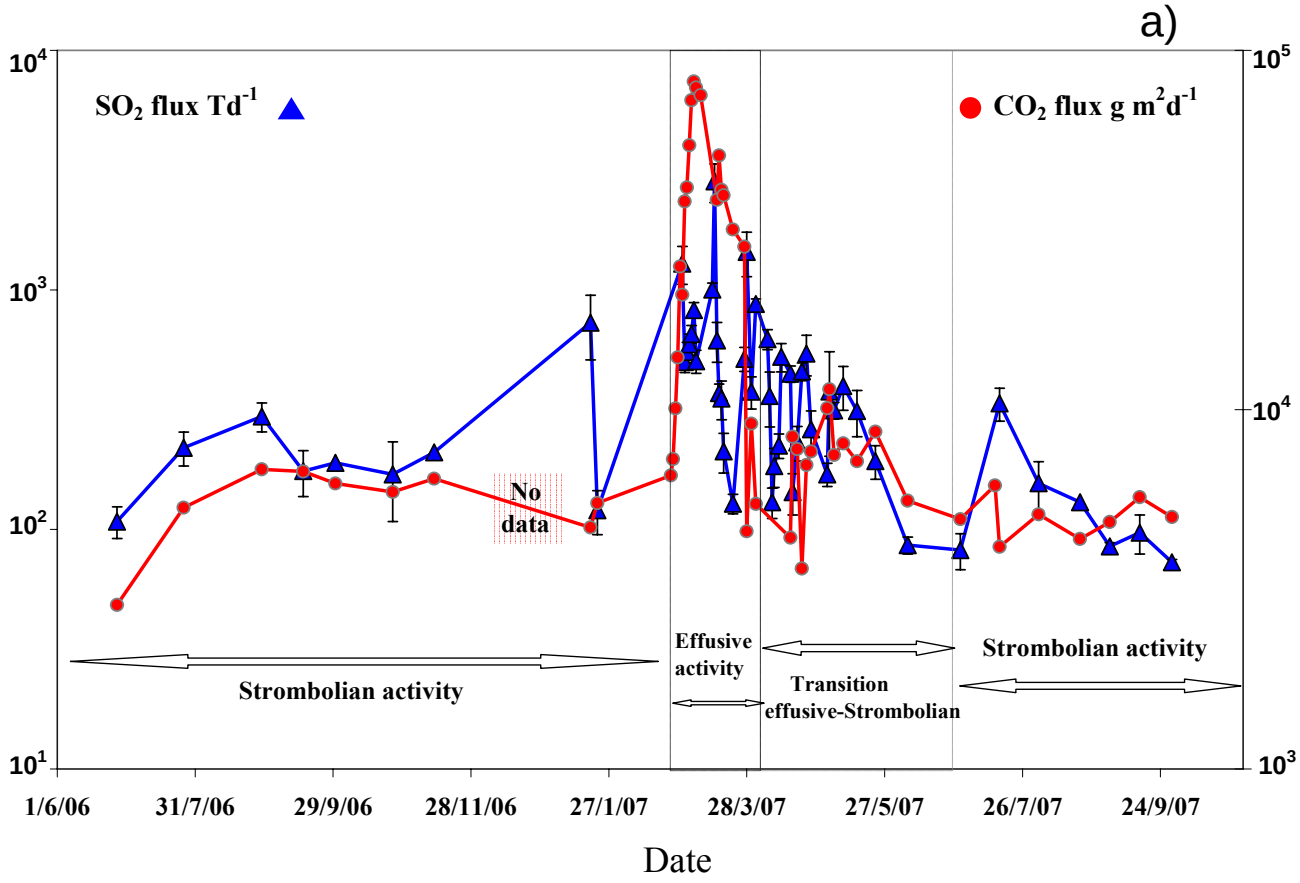

Fig.6 - **a)** Plume-SO_2 flux expressed in T/d^{-1} , time variation for the 2006-2007 period of discontinuous data set; The STR02-CO_2 flux (g $m^{-2}d^{-1}$) time variations for the same period (selected data of the continuous data set) have been plotted for comparison;

2.5 Discussion

The 2007 effusive eruption, timing and geochemical variations

On the basis of the CO_2 and SO_2 long-time data set, we have been able to define the values during "normal" Strombolian activity at 5000±1000 g m^{-2} d^{-1} and at 250±50 t d^{-1}, respectively.

February 2007 was characterized by an increase in the Strombolian activity: the level of the magma in the central conduit was high and summit soil degassing increased (CO_2 flux = 14000 g m^{-2} d^{-1} on 26 February 2007). This situation culminated on 27 February 2007 (CO_2 flux = 25000 g m^{-2} d^{-1}) with the opening of a fracture (c.13:00 GMT) in the lower Sciara del Fuoco at 650-600 m a.s.l. and with the consequent onset of effusive activity (Neri et al. 2008). On the same day (c.18:30) another vent opened at the lower elevation of ~400 m a.s.l. while the previous vent terminated its activity (Barberi and Rosi 2007) (***Fig. 6a,6b***). An initially fast lava flow of about 22 m^3 s^{-1} (Neri et al. 2008 and insight references) discharged through these fractures, a result of the emptying of the upper parts of the magma column. The fast drop in the lithostatic pressure triggered the uprising of a fresh magma batch (richer in volatiles), which caused a strong degassing of the lower parts of the magma column and a further increase in the CO_2 (>70000 g m^{-2} d^{-1}) and SO_2 (>1000 t d^{-1}) fluxes at the summit (***Fig. 6a,6b***).

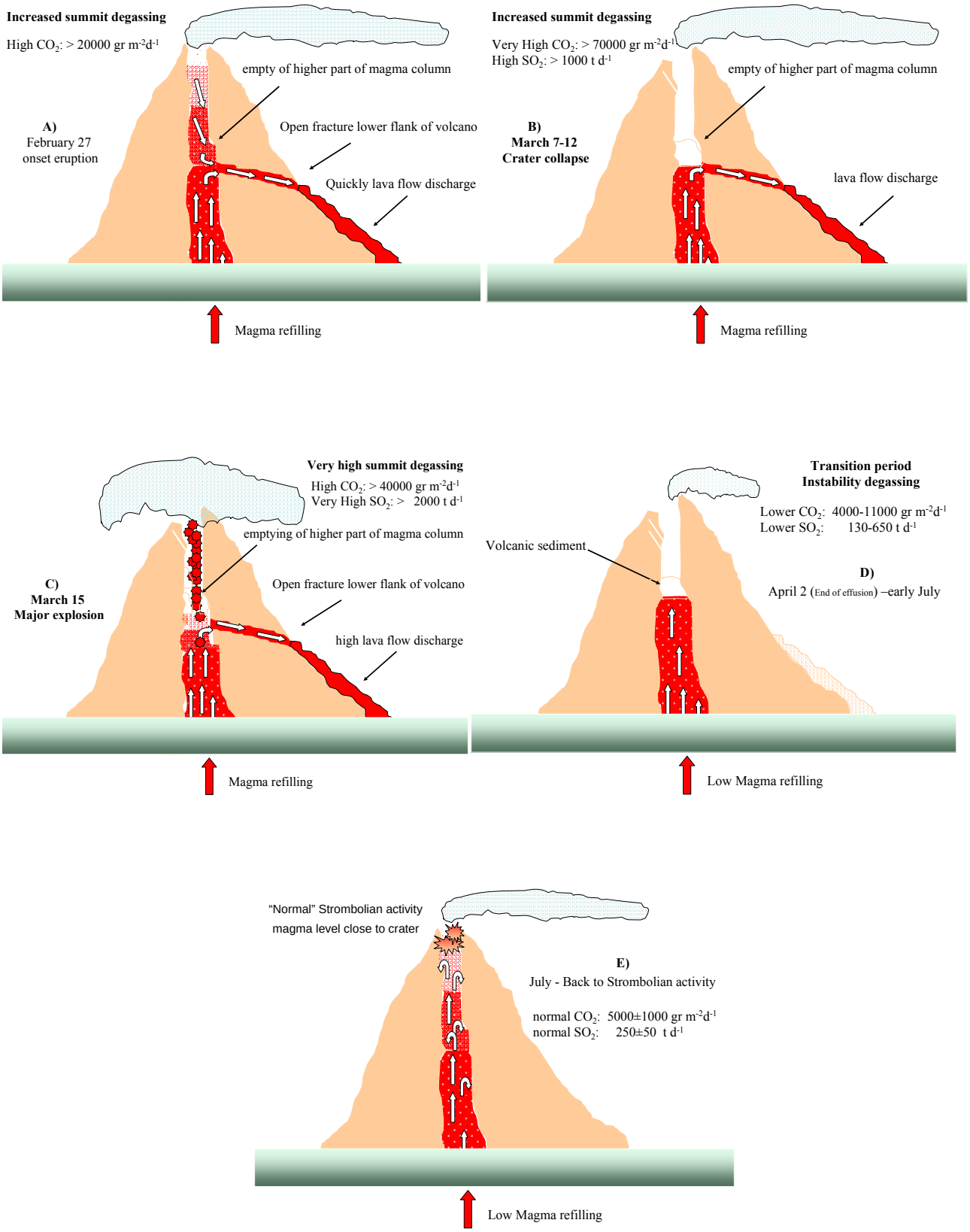

Fig 6 - **b)** Sketch map of volcanic activity: A)Onset of eruption, B)Crater collapse, C)Major explosion; D)End of effusive activity, transition period with unstable degassing; E) Return to normal strombolian activity.

The emptying of the summit part of the conduit lead to the collapse of the crater walls inside the conduit (7-12 March). The structurally weakened summit part resulted in the "opening up" of the summit area, favouring summit soil CO_2 degassing. The increase in summit degassing during the

first half of March 2007 produced the maximum values of the CO_2 (around 80000 g m^{-2} d^{-1}, 5-8 March) and SO^2 (2900 t d^{-1}, 14 March) fluxes, which preceded the paroxysm that occurred on 15 March (***Fig. 6a***). After this explosion summit degassing showed a decreasing trend, caused by the lack of significant magma refilling, that lasted until the end of March when it dropped to its minimum values of 4500 g m^{-2} d^{-1} (28 March) and 370 t d^{-1} (30 March) for CO_2 and SO_2 fluxes respectively. This announced the end of the effusive activity (2 April).

After the end of the effusive activity there was a true instability in the degassing regime characterized by CO_2 fluxes up to 11000 g m^{-2} d^{-1} and SO_2 fluxes up to 500 t d^{-1}(***Fig. 6a***). This period (April-early July) represents the transition from effusive to Strombolian activity when slow magma refilling caused the steady up-lift of the magma level towards the central craters. "Normal" Strombolian activity resumed in July 2007 (***Fig. 6a,6b***).

This last eruption was studied in detail and other new parameters were monitored on a continuous basis. In particular, Aiuppa et al. 2009, on the basis of the C/S monitored in the plume, estimated the depth of the magma degassing source. These depth values were inferred by considering the differences in solubility of these volatiles in the magma. We found it of great service to compare and combine the information regarding extensive parameters (CO_2 and SO_2 flux in this paper) with the intensive parameter (C/S by Aiuppa et al. 2009) data set acquired during the 2007 eruption.

We analyzed the behaviour of these parameters in the overlapping observation period (January 2006-December 2007). In particular, the year 2006 was considered by Aiuppa et al. 2009 as a period of relatively "normal" activity at Stromboli with the lowest C/S ratios at around 5. On the contrary, the daily average soil CO_2 flux featured, mainly in the first semester of 2006, a significant increase of up to 12,000g m^{-2} d^{-1} that was corroborated by an increase in the seismic activity.

This apparent discordant behaviour could be related to the acquisition of the C/S discontinuity data set.

On the contrary, the year 2007 showed a good relationship between these two data sets. In fact, we simultaneously recorded a strong increase both in the CO_2 and SO_2 fluxes (up to 80,000g m^{-2} d^{-1}, 2800 t d^{-1} respectively) and the highest C/S ratio (up to 25). Therefore, by combining these data we obtained reliable information regarding the evolution of the magma degassing system in terms of amount and depth, which allowed us to evaluate the budget of the magma involved, the origin of the degassing magma batch and the movement of it from depth to the shallow part of the volcanic edifice.

Moreover, by utilizing the plume SO_2 flux measured and the corresponding CO_2/SO_2 ratio (Aiuppa et al. 2009) it was possible to compute the CO_2 flux of the plume taking into consideration three different periods of volcanic activity: before, during, and after the 2007 effusive activity. Therefore,

we coupled these different data sets: C/S = 3-5 with SO2 flux= 250 t d^{-1} for normal Strombolian activity; C/S= 11-21 with SO_2 flux = 400-2800 t d^{-1} for effusive and paroxysmal periods; C/S= 4-20 with SO_2 flux = 200-500 for transition effusive-Strombolian periods. The CO_2 flux from the plume computed for these different periods are respectively 700±200, 15000±4000 and 3000±1500 (***fig. 7***). Subsequently, we observed that the effusive and paroxysmal period was characterized by an increase in the CO_2 flux from the plume of over one order of magnitude compared to that of normal Strombolian activity. These very interesting results are comparable to the soil CO_2 flux increase recorded at the summit (STR02) that went from 5000 to 80000 (over one order of magnitude too; ***fig. 7***).

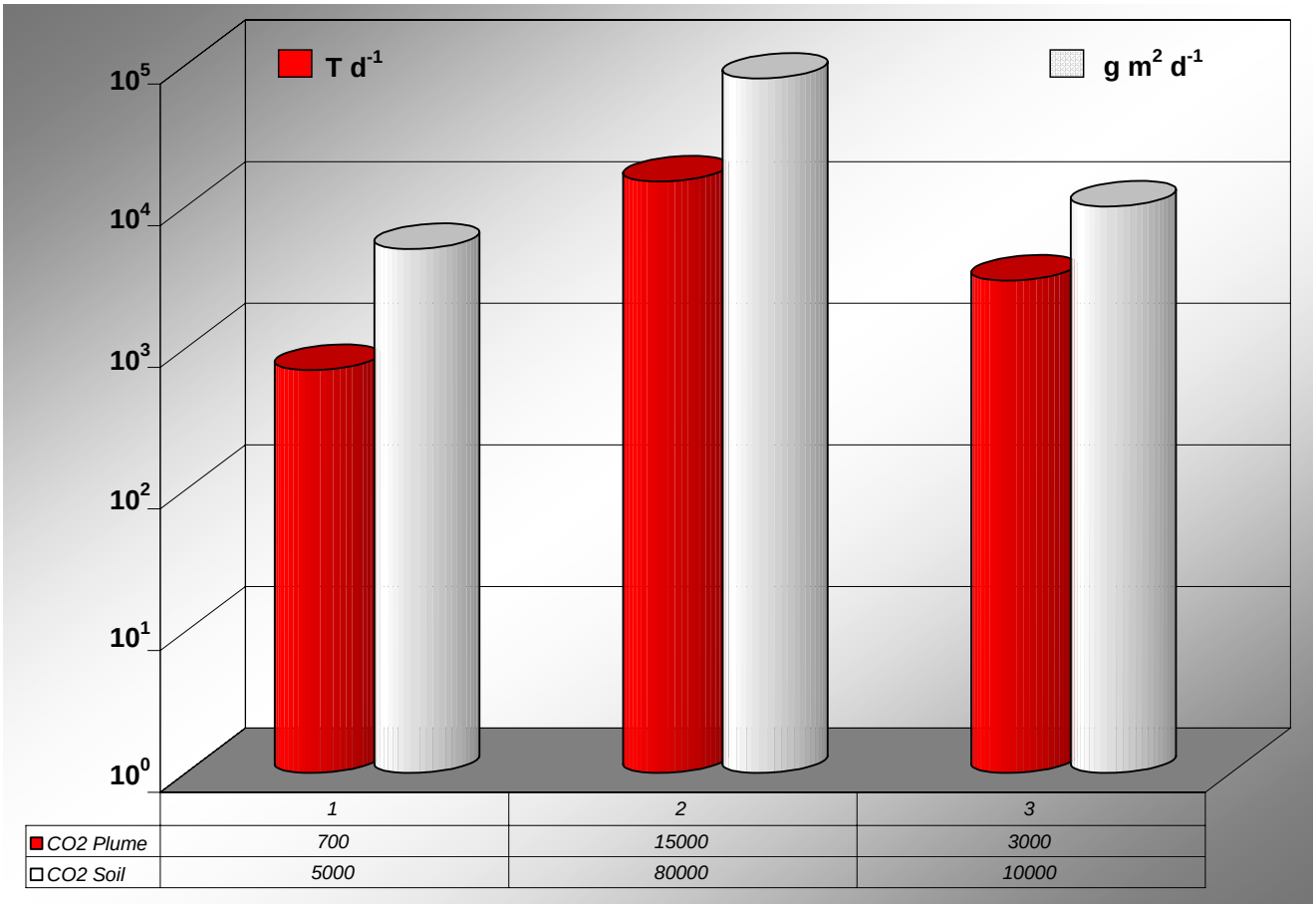

Fig. 7 - Estimated CO_2 flux of plume calculated combining the SO_2 flux (this paper) with the C/S ratio (Aiuppa et al. 2009) for three distinct periods of volcanic activity: "normal" strombolian, effusive and transition;
$\Phi CO_{2\ plume} = C/S_{ratio} * \Phi SO_{2\ plume}$

The measured CO_2 flux of summit soil degassing (STR02) has been plotted for comparison. The good correspondence between the behaviour of the three distinct pairs of data sets highlights the useful information that can be acquired from the monitoring of these parameters.

Therefore, the implications for surveillance activities are the following. Firstly, soil CO_2 summit degassing gives us information regarding the plume degassing system and, just as importantly, the STR02 site represents the whole degassing system and therefore gives us good indications of the changes in the volcanic activity.

Summarizing all the information acquired from the Stromboli discharged fluids (both plume that soil anomalous degassing) highlights the importance of obtaining the extensive parameters to identify and evaluate changes in the volcanic activity. Five years of soil CO_2 flux data have allowed us to establish the real natural thresholds for Stromboli's summit area (STR02- Pizzo sopra La Fossa) that can be used for future monitoring. Both CO_2 flux from the soil and SO_2 flux from the plume varied simultaneously during the 2007 eruption, although the degassing processes were clearly different. In this case, geochemical signals of volcanic unrest were clearly identified both in the plume degassing as well as in the soil degassing at the summit area.On the basis of these promising results we decide to improve the frequency of data acquisition of the SO_2 in the plume. For this reason, inside of this PhD work we starting a joint collaboration with the Heidelberg University research group to install a UV-scanning DOAS prototypes to measure in continuous the SO_2 flux of the Stromboli plume. ***fig. 8.***

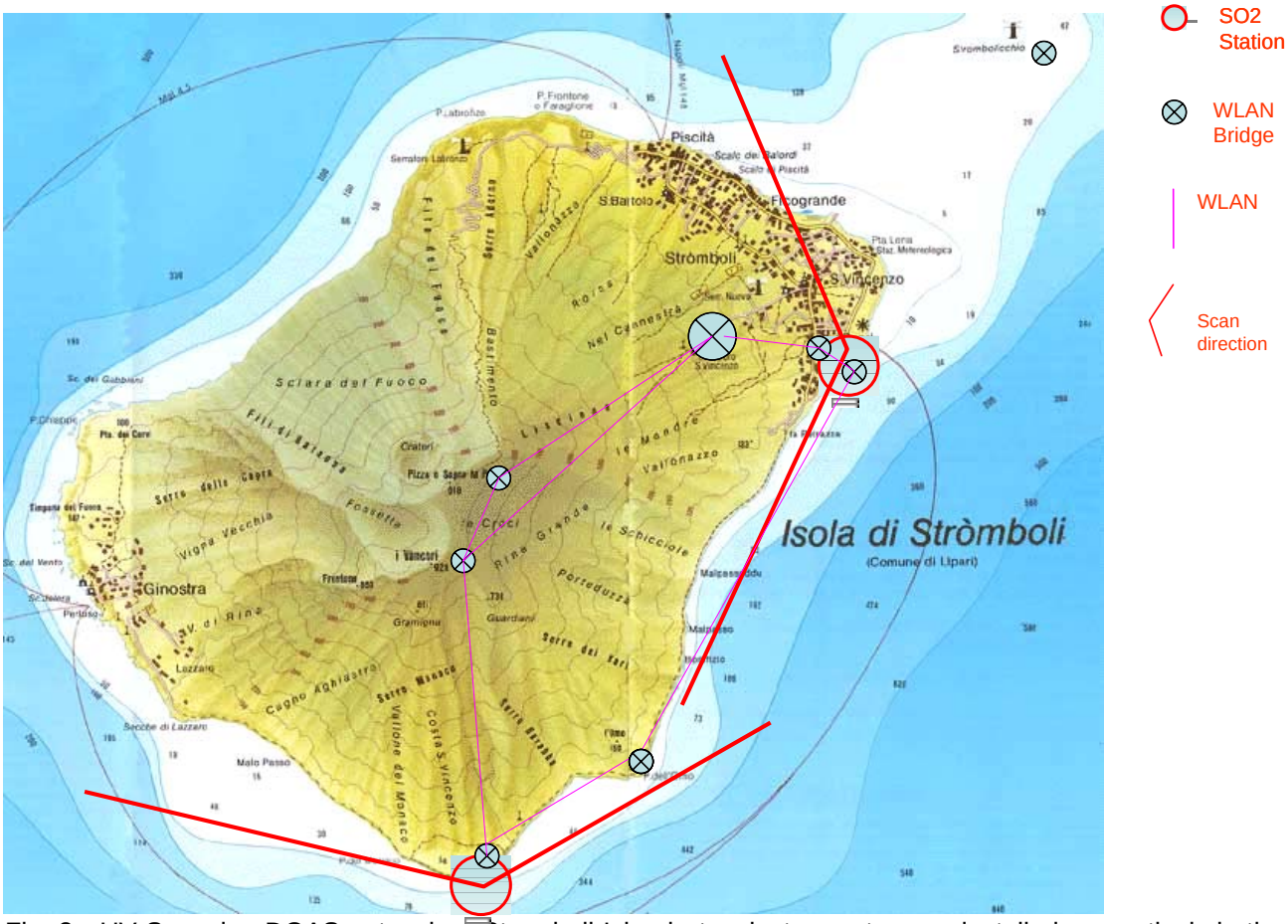

Fig. 8 - UV-Scanning DOAS network at Stromboli Island; two instruments were installed respectively in the northeast (Saibbo) and southern side (Punta Lena) of the island.

The first two NOVAC mark II instruments were installed on the island in the beginning of March 2007 (Kern 2009). The installations were conducted in cooperation with the Istituto Nazionale di Geofisica e Vulcanologia (INGV) Palermo and University of Heidelberg. The two instruments were installed respectively in the northeast (Saibbo) ***fig. 9a)*** and southern side (Punta Lena) ***fig. 9b)*** of the island.

Fig 9 - **a)** Images show the NOVAC installation at Saibbo Well, near the village of Stromboli. The NOVAC mark II instrument is installed on an aluminium tower on the beach;

Fig 9 - **b)** Installation at Punta Lena. The NOVAC mark II instrument is mounted on an aluminium structure on the roof of a small building. An additional housing contains the 100 Ah solar battery, which in turn is charged by a solar panel. The instrument is switched off at night with a 12V DC timer.

The instrument was configured to perform a folded scan in two planes. Before each scan, one spectrum is taken in the zenith (later used as a reference for the evaluation). Afterwards, the dark current and offset are measured. The scan then begins at an azimuth of 215° relative to north, thereby pointing directly towards the other installation on the southern side of the island. Once the zenith is reached, the instrument rotates and the scan continues in an azimuth direction of 335°. 15 exposures are taken in each viewing direction.

This geometry enables the instrument at Saibbo Well to measure the plume during wind directions between about 225° and 350°(Kern 2009). The second installation was performed on the southern tip of Stromboli Island. This site is called Punta Lena and is accessible either by boat or 3 km foot path from the town of Stromboli. This second instrument covers a range of wind directions between about 45° and 260° relative to north. A timer turns the instrument off at night to save power and reboot the system once per day. The temperature stabilization was set to 23°C, the approximate average day-time temperature in spring (Kern 2009).

The acquired SO_2 fluxes data highlight the good performances of the UV-scanning DOAS. The continuous SO_2 data (2009-2010) are reported in the graph of ***fig. 10*** (blue symbols) together with the discontinuous data (red symbols) acquired with mobile DOAS during 2006-2008 (Inguaggiato et al. 2011).

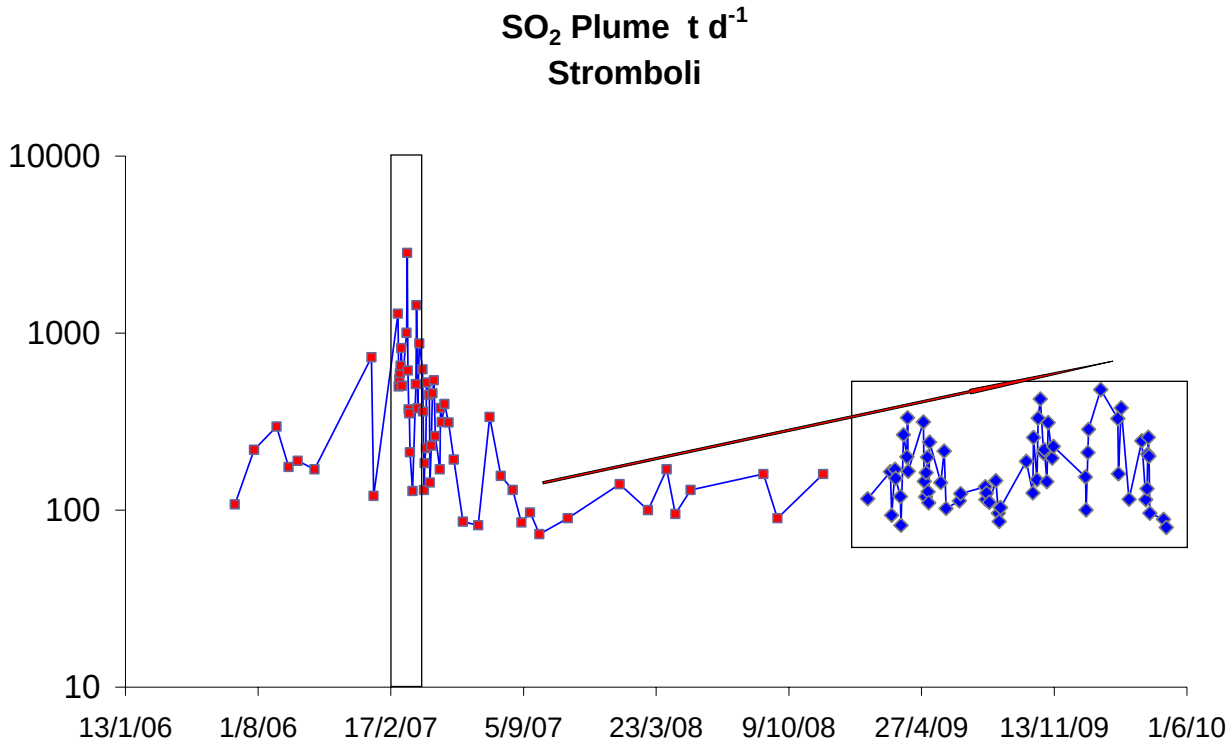

Fig. 10 - Plume-SO_2 flux long-time variations expressed in t d^{-1}. The continuous SO_2 data (2009-2010) acquired with UV-scanning DOAS Mark II are reported (blue symbols) together with the discontinuous data (red symbols) acquired with mobile DOAS during 2006-2008 (Inguaggiato et al. 2011).

The continuous data of SO_2 flux ranging from 80 to 480 t d^{-1} during all the 2009-2010 period showing a coherent behaviour with the variation observed in the other geochemical parameters (soil CO_2 flux) acquired in continuous too. The totality of acquired data showed a big increase of SO_2 flux in coincidence of the paroxysm of February-April 2007 up to 2800 t d^{-1} . After the end of this effusive period we recorded a decrease of SO_2 flux up to 70 t d^{-1} in September 2007. Then we recorded a slow but continuous increasing trend of SO_2 flux from the end-2007 to the end of 2010 (70 and 480 t d^{-1} respectively).

Both these parameters are well correlate with changes of volcanic activity observed..

3 VULCANO ISLAND

3.1 Geological setting

Vulcano is a small volcanic island located at the southernmost of the Aeolian Islands in the southern Tyrrhenian Sea in Italy (***Fig. 11***). Vulcano is one of the largest and the southernmost of the seven Aeolian Islands.

The main activity at Vulcano are related to sin-eruptive pyroclastic surges, bombs and block fallout, phreatic explosions, gas hazard, debris flows, and landslides of altered flanks and the subsequent formation of tsunamis. In ancient times, the Romans believed that Vulcano was the chimney to the forge of the god Vulcan. The earthquakes that either preceded or accompanied the explosions of ashes were considered to be due to Vulcan himself making weapons for the other gods.

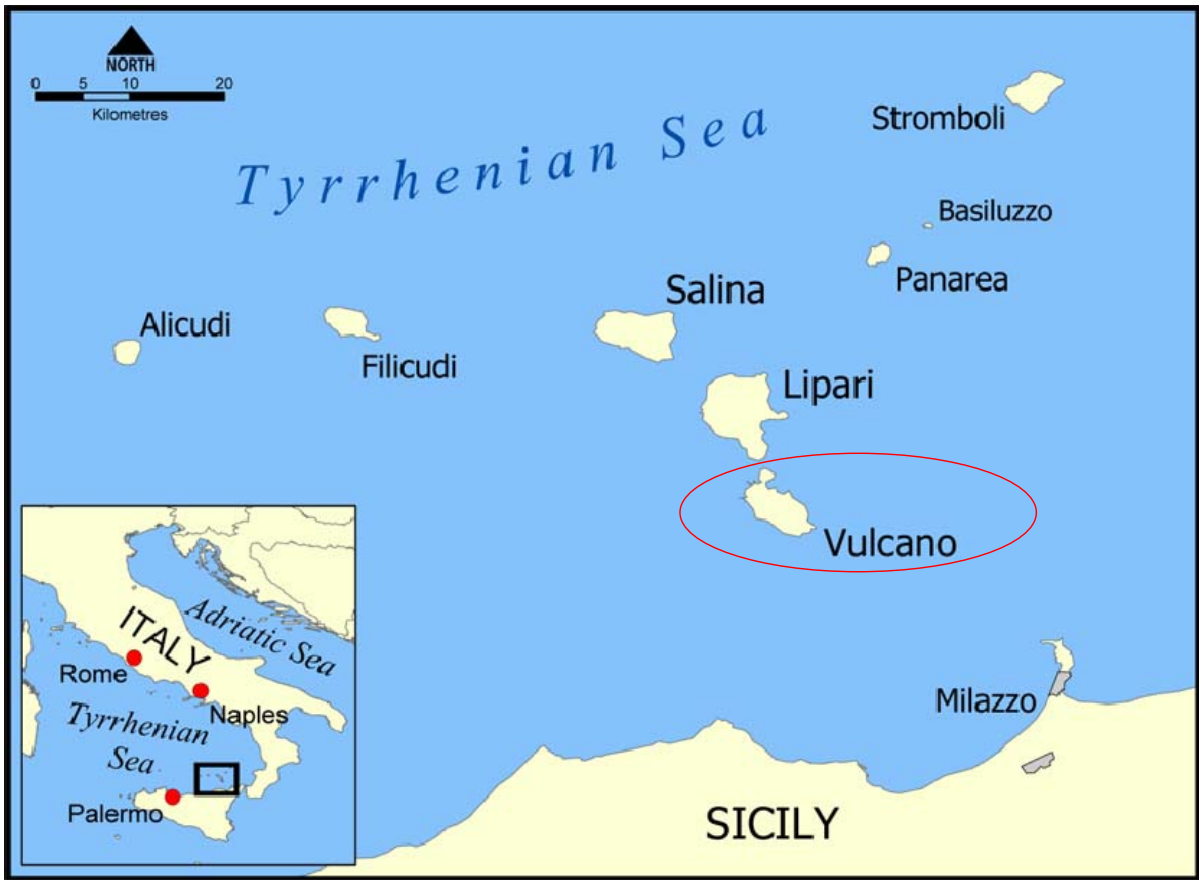

Fig. 11 - Aeolian Island map with Vulcano island, the southernmost island of archipelago.

Vulcano Island, as we see now is the result of five major episodes during the past 120,000 years.
First are Vulcano Primordiale, Piano Caldera, Lentia Complex, La Fossa Caldera, and Vulcanello. The history of Vulcano begins with the formation of a stratovolcano. The collapse of this stratovolcano produces the Piano caldera ,(Santacroce et al. [2003]). Then, this caldera was partially filled with pyroclastic deposits and lava flows. The stratovolcano and its caldera form the southern part of the island of Vulcano.
The Fossa cone is a small stratovolcano with an altitude of 391 m a.s.l. and diameter is about 2 kilometers. The history began form 6,000 years ago [Dellino and La Volpe, 1997; De Rosa et al., 2004]. Six volcanic successions: Punte Nere, Palizzi, Caruggi, Forgia Vecchia, Pietre Cotte and Gran Cratere, with different vent locations and eruptive histories, shaped the edifice [Dellino and La Volpe, 1997; De Rosa et al., 2004, De Astis et al.,2007].
Vulcanello was formed as an island beginning in 183 BC and was connected to the Vulcano island in 1550 AD during its last eruption.
Each succession follows the same evolution starting with pyroclastic surges and ending with the emission of highly viscous lava flows.
All the explosive and effusive products of La Fossa cone have high potassium contents and a chemical composition ranging from trachytic to the more evolved rhyolitic composition [Keller, 1980]. The latest eruption from Vulcano consisted of explosive activity from the Fossa cone from 1888 to 1890 [e.g., Frazzetta et al., 1983, 1984].
In the same century, Vulcano produced three eruptions lasting more than one month (1822–1823, 1873 and 1886). The violence of the last eruption (1888–1890) was marked by the fall of volcanic bombs and blocks, about 1 m in diameter, at 1 km from the vent. Breadcrust bombs, distinctive of this style of eruption, were ejected about 500 m.

Vulcano Island, is an active volcano that has been in state of solphataric activity, since the last eruption (1888-1890). At present, the main exhalative activity is in the northern part of the island ***fig. 12***, it is revealed by: a) a wide fumaroles field, on the active edifice of "La Fossa" crater, (100°C <450°C); b) low temperature fumaroles (T<100°C) and sea-bubbling gases in the Baia Levante area. Moreover, strong soil degassing occurs in the Vulcano Porto area and around the volcanic edifice, where the active tectonic discontinuities drive CO_2 to the surface (Capasso et al 1997, Diliberto et al 2002). Finally, numerous carbon-rich thermal wells (up to 80°C) in the Vulcano Porto Area, testify the presence of a geothermal system with equilibrium temperature around 200°C (Federico et al. 2010).

In the last decades Vulcano Island has showed indication of renewal activity, highlighted by increase of temperatures and volatile fluxes of fumarolic area (Chiodini et al.1996 a,b; Paonita et al. 2002); strong variations of chemical and isotopic compostion of crater fumaroles and thermal waters (Capasso et al., 1997, 1998), probably due to increase of deeper fluid fluxes.
In fact, volatiles discharged from a volcanic system represent the exsolved volatiles from the batch of magma located beneath of it.

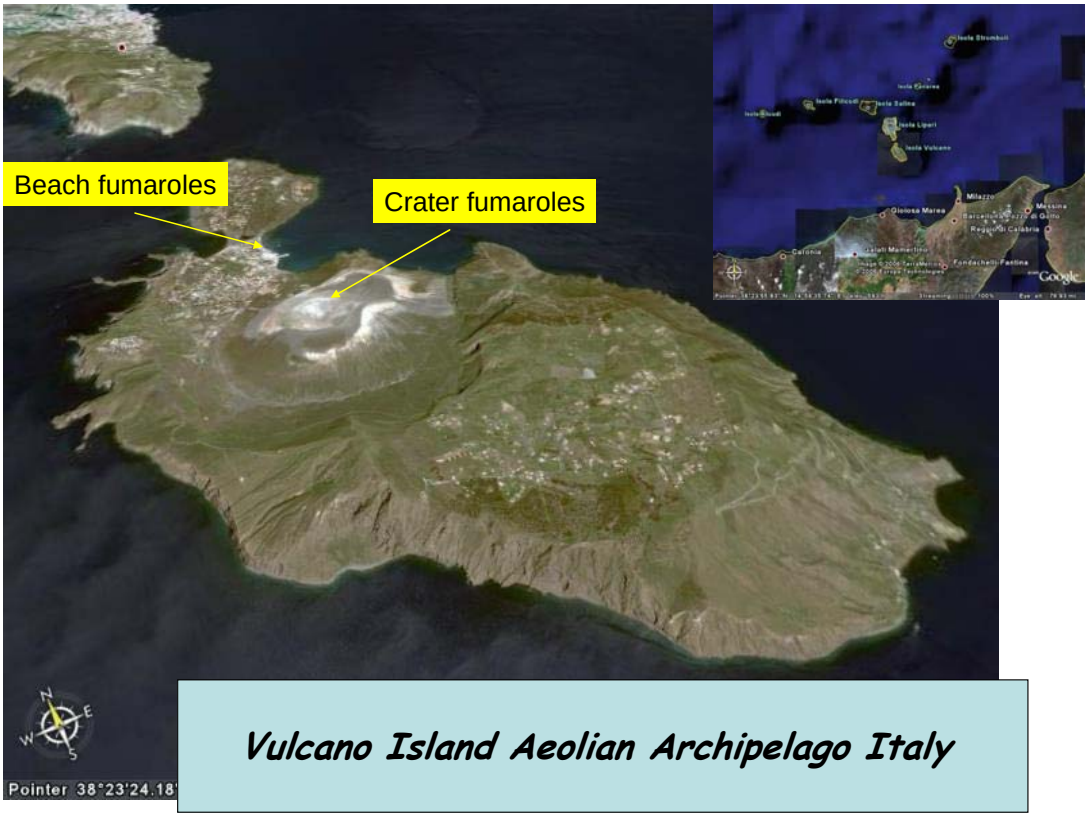

Fig 12 – Vulcano Island. Main exhalative activity: Fumarolic field on the summit crater; Beach fumaroles; Thermal waters; strong soil degassing in the Vulcano Porto area and around the volcanic edifice.

Usually, a decrease in pressure caused by rock fracturation or rising of magma batch towards the surface determine an over pressure of volatiles in the magma and consequently their exsolution. These volatiles, reaching the surface, interact with superficial fluids like aquifer and produce also increase in soil degassing and fumarolic activity (Taran et al. 1986; Capasso et al. 1997; Nuccio and Paonita 2001; Inguaggiato et al. 2000, 2004, 2011).

3.2 Previous geochemical studies

In the last few years many geochemical investigations on volcanic systems were focused on the study of extensive parameters, as tools to quantify the involved masses during the degassing processes both during active and quiescent phases (Allard et al. 1994; Italiano et al. 1997; Aiuppa et al. 2005, 2010; Allard et al. 2005, Inguaggiato et al. 2011).

Generally, the carbon dioxide represents the main constituent of anidrous gases discharged in the summit areas of the volcanoes through the plume or crater fumaroles (Chiodini et al. 2005; Inguaggiato et al. 2005).

This parameter has been applied successfully to studies the volatiles budget in many volcanic systems (Chiodini et al. 1996; Favara et al. 2001; Cardellini et al. 2003; Chiodini et al. 2005; Pecoraino et al. 2005; add more Mazot et al.2010), and in the geochemical monitoring program to be aim to individuate changes in the volcanic activity (Brusca et al. 2004; Carapezza et al. 2004; Werner et Cardellini 2006).

The goal of this part of thesis-work was the CO_2 budget estimation of discharged fluids from the summit area of Vulcano Island. Moreover, the realization of a CO_2 flux map allowing us to individuate the anomalous degassing areas and idoneous sites future installation of geochemical monitoring systems to control the volcanic activity. To reach this aim a geochemical campaign for measuring the soil CO_2 fluxes was performed in September 2007 covering the whole summit area of Vulcano Island. Moreover, the installation of continuous soil CO_2 fluxes equipment on the summit area and the UV-Scanning DOAS system and the relative long-time acquisition data will be presented.

The estimation of CO_2 degassing budget from volcanic systems have relevant aspect both for geochemical monitoring activity and for the role of magmatic-CO_2 in the Carbon world global cycle. The volcanic activity represents the main natural contributor of CO_2 emitted in to the atmosphere, consequently many authors worked to estimate it (Brantley and Koepenick, 1995; Morner and Etiope, 2002). For this reason any work aimed to estimate the CO_2 degassing in a volcanic system represent a contribution to refine the previous global estimation and to achieve a realistic value of a total world global budget of CO_2 volcanic .

Great amount of soil, fumaroles and plume CO_2 fluxes were observed during quiescent activity (inter-eruptive periods) from the volcanoes (Carbonnelle et al. 1985; Allard et al. 1987; Baubron et al.1990; Allard et al. 1991, Baubron et al. 1991, Aiuppa et al. 2010; Inguaggiato et al. 2011). Changes in the CO_2 fluxes have been correlated with important variations in the volcanic activity

and in several cases forecast the renewal of the paroxystic volcanic activity like increase of explosion activity and/or onset of effusive activity (Carapezza et. al 2004; Brusca et al. 2004; Aiuppa et al. 2010; Inguaggiato et al. 2011).

The Vulcano Island was studied from many authors to characterize and estimate the discharged carbon dioxide. In particular, many studies was aimed to estimate the CO_2 emitted from the summit area (Chiodini et. al. 1996a), and from the peripheral area (Diliberto et al. 2002). Moreover, studies aimed to highlight relationship between changes in the CO_2 rate flux and the volcanic activity level were also performed (Chiodini et. al. 1996b; Diliberto et al. 2002).

The diffuse soil degassing estimation in the Porto area (north-east side of Vulcano) was carried out from different authors since 1984 (Badalamenti et al 1998). The estimations shown a wide range of values, in fact in the 1984-1988 period (Badalamenti et al. 1998). On the basis of 55 points of measurement covering an area of 2.2 Km^2 report a range of values between 70 and 1000 t d^{-1}. In 1993, a flux of 75 t d^{-1} was reported from the same area utilizing 420 points of measurement performed with accumulation chamber method (Chiodini et al, 1995).

Regarding to the diffuse soil degassing from the summit area an estimation of 115 t d^{-1} (150 measurement's point) and 200 t d^{-1} (91 measurement's point) have been calculated respectively in 1990 and 1995 (Baubron et al., 1991; Chiodini et al. 1996).

In 1990 the carbon dioxide discharged from the fumaroles of the Istmo area was estimated to be 6.5 t d^{-1} (Italiano and Nuccio, 1994).

Vulcano Island was also studied for the chemical composition of a volcanic "plume". In fact, nevertheless the Vulcano Island does not show a real plume like an open conduct degassing volcano (only a summit degassing fumarolic field around 400°C) in the last few years many scientists utilized Vulcano as natural laboratory to test new remote sensing techniques and different prototypes. In particular, Toshiya Mori et al.(1995) used FT–IR Spectral Radiometer on the Vulcano's plume; Aiuppa et al. (2004), carried out an inter-comparison of different methodologies (FTIR, Filter-packs, direct sampling) on the plume of Vulcano Island; Real-time measurement of volcanic H2S and SO2 concentrations have been measured by a UV spectroscopy prototype (M. O'Dwyer et al. GRL, 2003); moreover, an intercomparison of H2S fluxes from Vulcano with those of Etna and Stromboli volcanoes was made to the aim of estimate the total sulfur budget at volcanoes (Aiuppa et al., 2005) Finally, Aiuppa et al. 2004, 2005a, 2005b, 2006 and McGonigle 2008 carried out measurements to determine H_2S/SO_2 and CO_2/SO_2 and relative fluxes of SO_2 with DOAS, Infra Red and electrochemical sensors equipments.

3.3 CO_2 fluxes budget

On the basis of previous geochemical information about the kind of fluid manifestations (Chiodini et al. 1996; Italiano & Nuccio 1994; Italiano et al. 1997) we tried to estimate the total CO_2 output discharged from Vulcano Island by fluids in different way. In particular, we measured the discharged CO_2 from both the fumaroles and soil degassing summit areas.

The crater area is characterized by a wide fumarolic field with temperature ranging between 100 and 450 °C. The fumaroles show a chemical composition with ratios values of H_2O/CO_2 and CO_2/SO_2 (Capasso et al. 1997, Paonita et al. 2002; Aiuppa et al. 2005a; McGonigle et al. 2008) between 4-11 and 30-67 respectively. Moreover many studies have been focused on determining the H_2S/SO_2 ratio (Aiuppa et al., 2005b; Aiuppa et al., 2006) and show values between 0.4 and 2.3.

To estimate the CO_2 flux emitted from the fumarolic field we utilize an indirect method based on "plume" SO_2 flux measurements and CO_2/SO_2 fumaroles ratio (McGonigle et al. 2008, Aiuppa et al. 2010; Inguaggiato et al. 2011). The SO_2 flux measurements were carried out by a portable UV-DOAS system on September 2009. Six traverses by car were performed below the "plume", allowing us to estimate an average SO_2 flux value of 12 t d^{-1} ±2. This value represents the back-ground level of SO_2 flux for the "normal" solfataric activity of Vulcano like measured by other authors in the past (Aiuppa et al., 2005a, McGonigle et al. 2008; Diliberto 2002).

In order to determine the CO_2/SO_2 ratio, 2 fumarolic gas samples, FA and F0, were collected using pre-evacuated glass flasks containing an alkaline solution ($AgNO_3$ in ammoniacal solution) in which steam condenses and CO_2 is absorbed. These fumaroles are located respectively in the inner part (FA) of fumarolized area and on the rim (F0) of the crater.

On the basis of the average CO_2/SO_2 ratio of fumarolic gases and of the SO_2 plume flux measured with mobile DOAS instruments we estimated the CO_2 flux from the fumarolic area (Farea) by the following relation:

$$QCO_{2Farea} = QSO_{2Plume} * [CO_2]/[SO_2]_{fumaroles}$$

Where, QCO_{2Farea} is the flux of CO_2 plume of the fumarolized area; $[CO_2]/[SO_2]_{fumaroles}$ is the average weight ratio of CO_2/SO_2 in the fumaroles and QSO_{2Plume} is the SO_2 flux in the plume.

$$QSO_{2Plume} = 12 \text{ tday}^{-1}$$

$$(CO_2/SO_2)_{fumaroles} \sim 30$$

$$QCO_{2Farea} = 362 \text{ tday}^{-1} \div 40$$

Soil summit degassing:

Soil flux measurements have been carried out through 248 measures of CO2 fluxes from the entire summit area of Vulcano Island, performed by means of the accumulation chamber method (West Systems equipment. Soil gas data were processed for surface mapping using the sequential Gaussian simulation (sGs), which produces maps flux contour lines. The 248 measured CO_2 fluxes in randomly distributed points on the Crater surface were interpolated by a distribution over a grid of 2823 square cells (5x5 m2) covering an area of 238,150 m2 using the so-called exponential variogram model. Then, 100 simulations of the CO_2 fluxes with the obtained distribution were performed (***Fig. 13***). For each simulation, the CO_2 flux estimated at each cell is multiplied by 25 m2 and added to the other CO_2 fluxes estimated at the other cells of the grid to have a total CO_2 output for the simulation. The average flux of the 100 simulation is 206 g m^{-2} d^{-1} with a standard deviation of 42 g m^{-2} d^{-1}. The mean of the 100 total simulated CO_2 outputs, 49 t d^{-1}, represents the estimation of the total CO_2 output from the Crater area. (The total area of the crater is 440,755 m^2, if we remove the fumaroles area (32,755 m^2) we have a total CO_2 output of 91 t d^{-1} for an area of 408, 000 m^2.

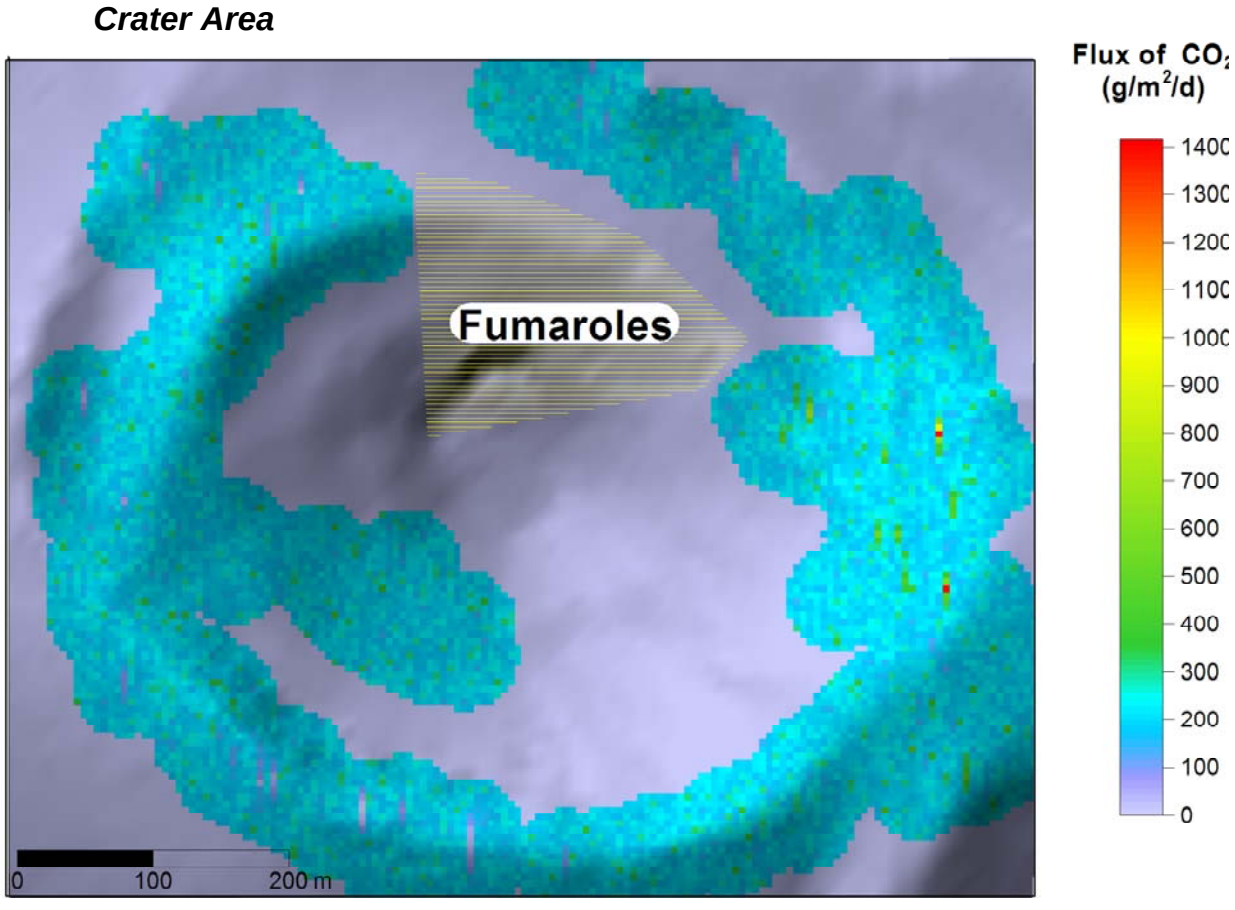

Fig. 13 - Map of CO2 flux of crater area.

The total CO_2 output of 532 t d^{-1} was estimated for the summit area of active crater, with 362 and 91 t d^{-1} from crater fumaroles (indirect method) and crater soil anomalous degassing areas (direct measurements) respectively.

The estimation of the CO_2 output discharged from the summit allowed us to improve the comprehension of degassing system of Vulcano and to compare with other volcanic systems in the world (Fig 14). This comparison shows that Vulcano Island emits 532 t/d of CO2 into the atmosphere similar to other quiescent volcanoes such as Pantelleria (1071 t d^{-1}), Ischia (1313 t d^{-1}) and Teide (Tenerife) (432 t d^{-1}).

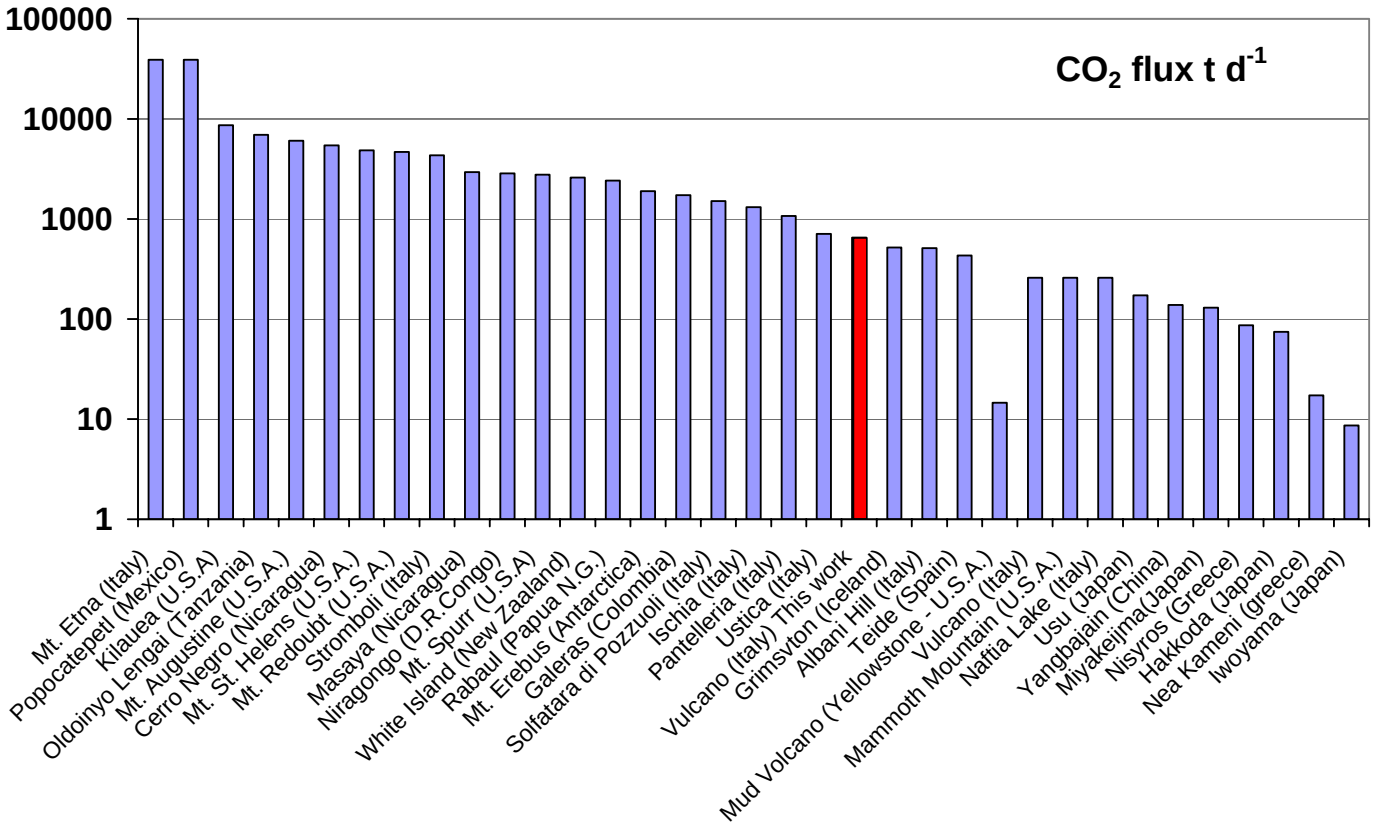

Fig. 14 – Comparison of CO2 fluxes for some active volcanoes. The red bar shows the mean fluxes measured in Vulcano Island during the PhD thesis period (2007- 2010).

Moreover, the map of summit soil degassing allowed us to find the suitable sites for the installation of continuous monitoring system to measure the CO_2 flux continuously.

On the basis of the acquired information it has been decided to install a CO_2-flux equipment on the north-east side of the crater (***fig. 15***) in a point close to the fumarolic area but outside to avoid processes of corrosion with acid fumarole condensates.

Fig. 15 - Picture of CO2 soil equipment installed at the summit of Vulcano (La Fossa Crater).

3.4 Summit CO_2-flux: long-time variations

Since November, 2007 the continuous monitoring of CO_2 fluxes emitted from the soil at La Fossa crater (VCS) has been carried out on an hourly basis by means of an accumulation chamber (Fig.15) (West Systems LTD, Chiodini et al. 1998). Data is transmitted directly to INGV-Palermo geochemical monitoring centre by GSM service.

We analyzed the complete soil CO_2 flux hourly data set from station VCSCS during the 2007-2010 period, in order to improve our knowledge of the behaviour of summit soil CO_2 flux and to try to relate the fluxes variations to the different degassing regimes of solfataric activity of Vulcano Island.

We processed the CO_2 flux data through a cumulated probability graph (Sinclair 1974). In this graph ***(fig. 16*a)** the log CO_2 flux is plotted against the cumulated probability for the entire data set of CO_2 flux at La Fossa crater (2007-2010). This graph highlights a continuous degassing process, without any "break slope" in the curve, indicating a single family of degassing. The histogram of the totality of the acquired data (***fig. 16b***) confirm it showing an unimodal distribution of log CO_2 centred around 3.2 value (~1600 g m^{-2} d^{-1}). The average values of CO_2 flux, 1600±250 g m^{-2} d^{-1}, computed from the acquired data, represents the background value to be found during "normal" Solphataric activity at the permanent station.

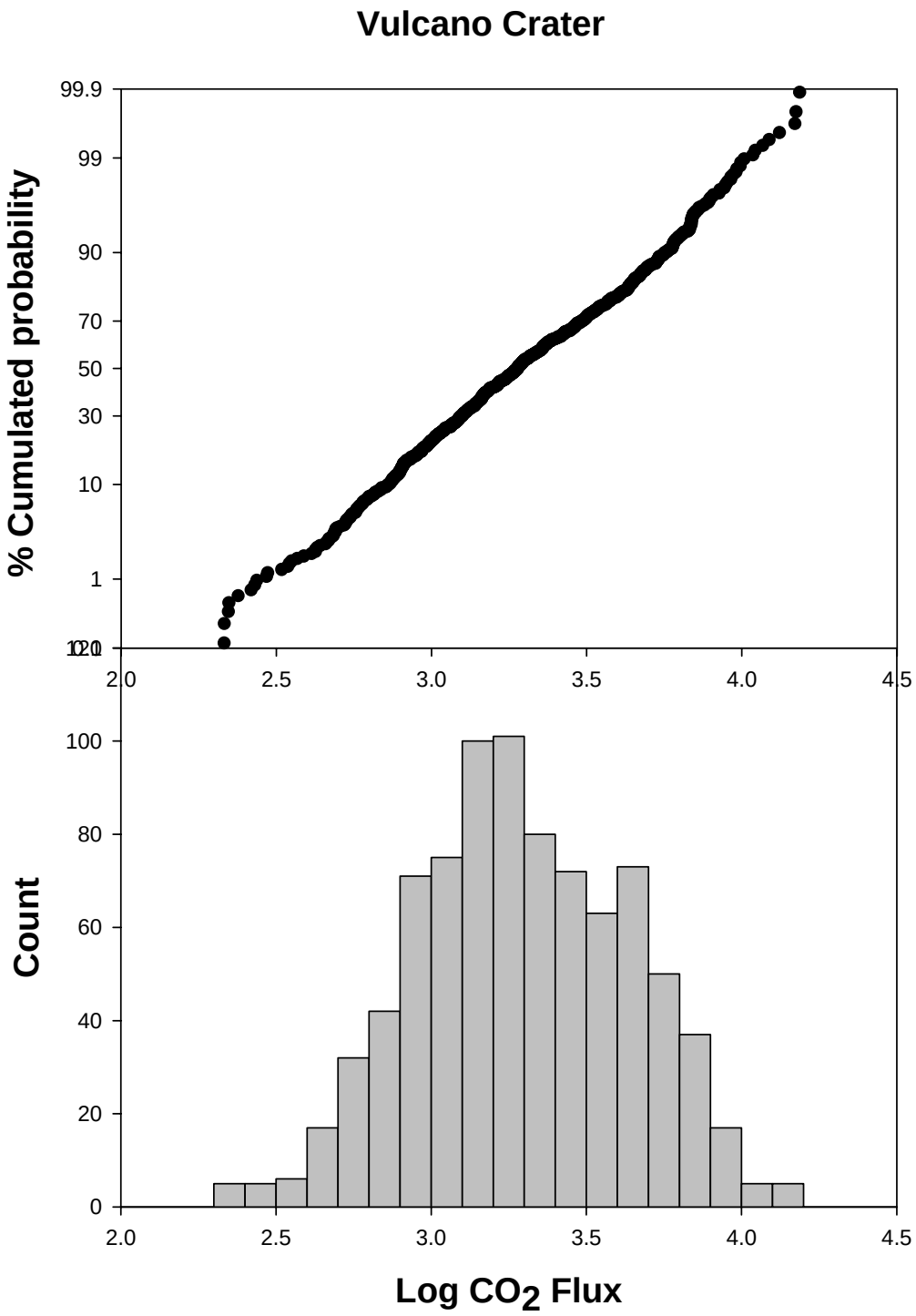

Fig. 16 a) VCS Log CO_2 flux vs cumulated probability – period 2007-2010; The distribution of the plotted data show a single degassing family. b) - Histogram of VCS log CO_2 flux data. The plotted data show a unimodal distribution centred at 3.2 value.

The daily average of the CO_2 flux for the whole period (2007-2010) was reported in Fig. ***fig. 17***. The daily average of degassing flux showed a slow decreasing trend of CO2 from 9000 to 500 g $m^{-2}d^{-1}$ from November 2007 to August 2008 with an average value of about 1200 g $m^{-2}d^{-1}$ recorded in the period August 2008 to September 2009. In Mid-September 2009 we observed a great and rapid

positive trend of CO2 flux that increased up to 16,000 g $m^{-2}d^{-1}$ with hourly peaks of 20,000 g $m^{-2}d^{-1}$, recorded on November-December, 2009. The anomalous degassing period terminated at the early January with fluxes coming back to the "normal" values of about 2000 g $m^{-2}d^{-1}$.

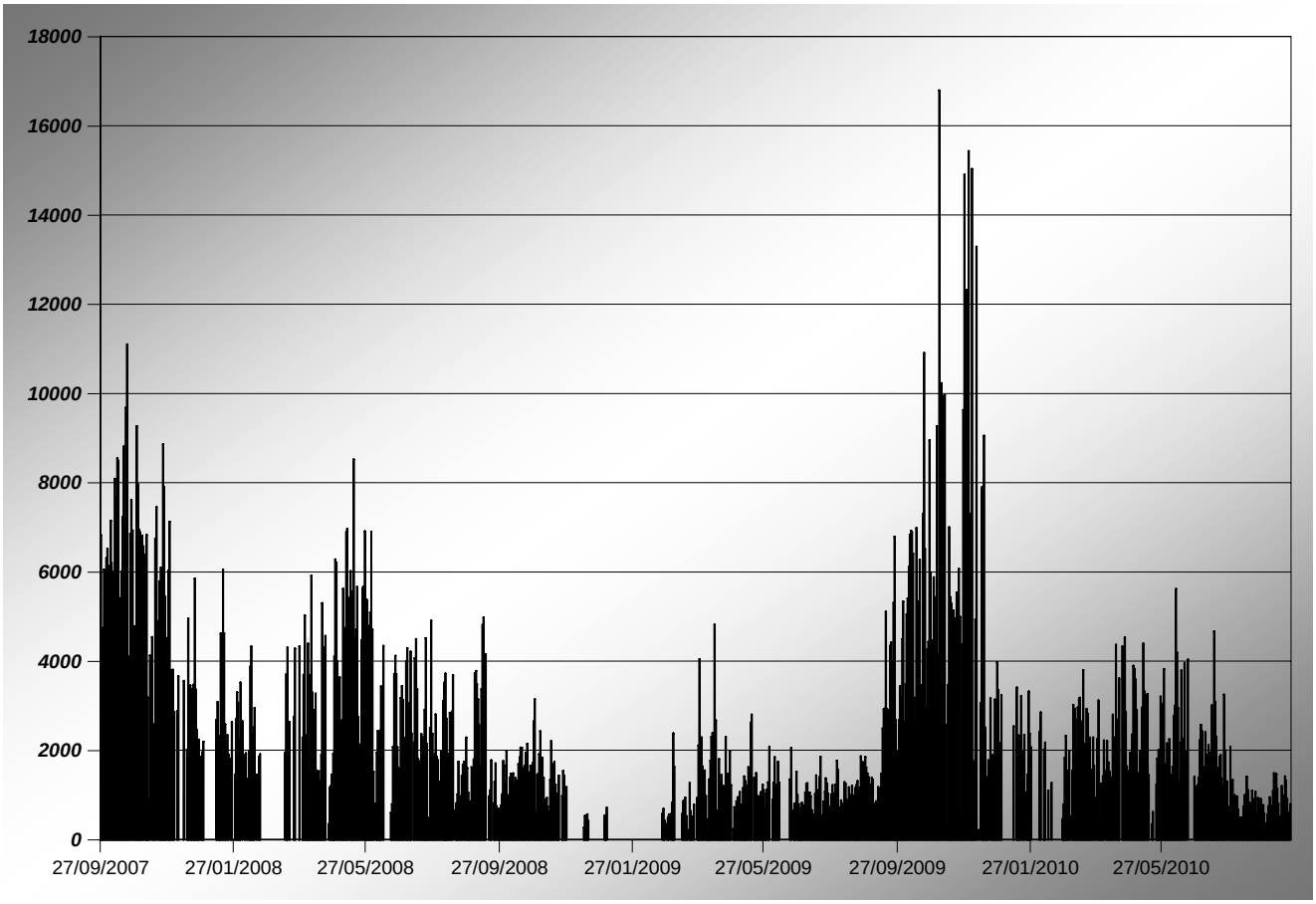

Fig. 17 - Daily average values (g $m^{-2}d^{-1}$) of summit CO_2 flux (VCS) for the period 2007-2010;

The great variations of CO_2 fluxes recorded in the summit during the solphataric activity were similar (one order of magnitude) to the changes observed in the Stromboli volcano (open conduct degassing system) in coincidence of the paroxystic activity occurred in the 2007 effusive activity. This big variation observed indicate change in the degassing regime of solphataric activity due to increase of volatiles input arriving from depth.

Nevertheless, this variation is of the same order of magnitude than this recorded at Stromboli during changes in the strombolian activity, the flux variation recorded in Vulcano island show different way of degassing.

In this particular case (VCS) we observe that the big variation of summit CO_2 flux recorded in Vulcano occurred in the wide time interval (about 2 months) and do not reveal the presence of other

degassing families. Probably, it is due to the different way of degassing processes that the summit soil degassing reveals.

In the case of Strombolian activity the anomalous CO_2 degassing in the summit area occurred in few days (Inguaggiato et al.2011), because it's directly connected to the exsolving volatiles from the magma inside the open conduct where new batches of magma refilling it.

Conversely, the anomalous degassing processes visible on the summit area of Vulcano Island are linked to degassing processes of volatiles exsolved from the huge hydrothermal system (Federico et al. 2010) feed from magma batch located below La Fossa crater. This hydrothermal system does not allow sharp variation in soil CO_2 flux in short time because the volatiles exsolved from the magna batch *underwent* a buffering processes that smooth the deep input variation in a wide time.

3.5 SO_2 fluxes

Vulcano Island is a closed conduct volcano and in a state of solphataric activity whit no real "plume" but only a wide fumarolic field degassing on the summit area (La Fossa crater). On the basis of this consideration the telemetric measurements of SO_2 fluxes in the "plume" were not performed systematically in the past. In the framework of NOVAC (Network for Observation of Volcanic and Atmospheric Change) we decided to improve our knowledge on SO_2 fluxes at Vulcano and we installed a scanning DOAS at Palizzi in March 2008 ***fig. 18***.

The NOVAC project is started in 2005, a worldwide network of permanent scanning DOAS instruments (Galle et al. 2010) was installed at 19 volcanoes around the world for measuring volcanic SO_2 emission fluxes, and now use this technology for real-time monitoring and risk assessment (***fig. 19***).

The equipment installed is an Differential Optical Absorption Spectroscopy-instrument designed by the Optical Sensing Group in Chalmers University of Technology in Göteborg, Sweden.

The system contents a single spectrometer from Ocean Optics Company, an embedded PC, a GPS receiver, a fibre, and a telescope. Technical aspects of continuous monitoring with scanning DOAS systems such as instrument design, station networking, and measurement geometries were described in Zhang 2005, Galle et al. 2010, Johansson 2009a.

Data analysis was significantly improved by identifying and considerably reducing the two main sources of error: wind speed at plume height and radiative transfer effects (Johansson et al. 2009b, Kern et al. 2009). New software for data evaluation was specifically implemented for the NOVAC network (Johansson 2009b).

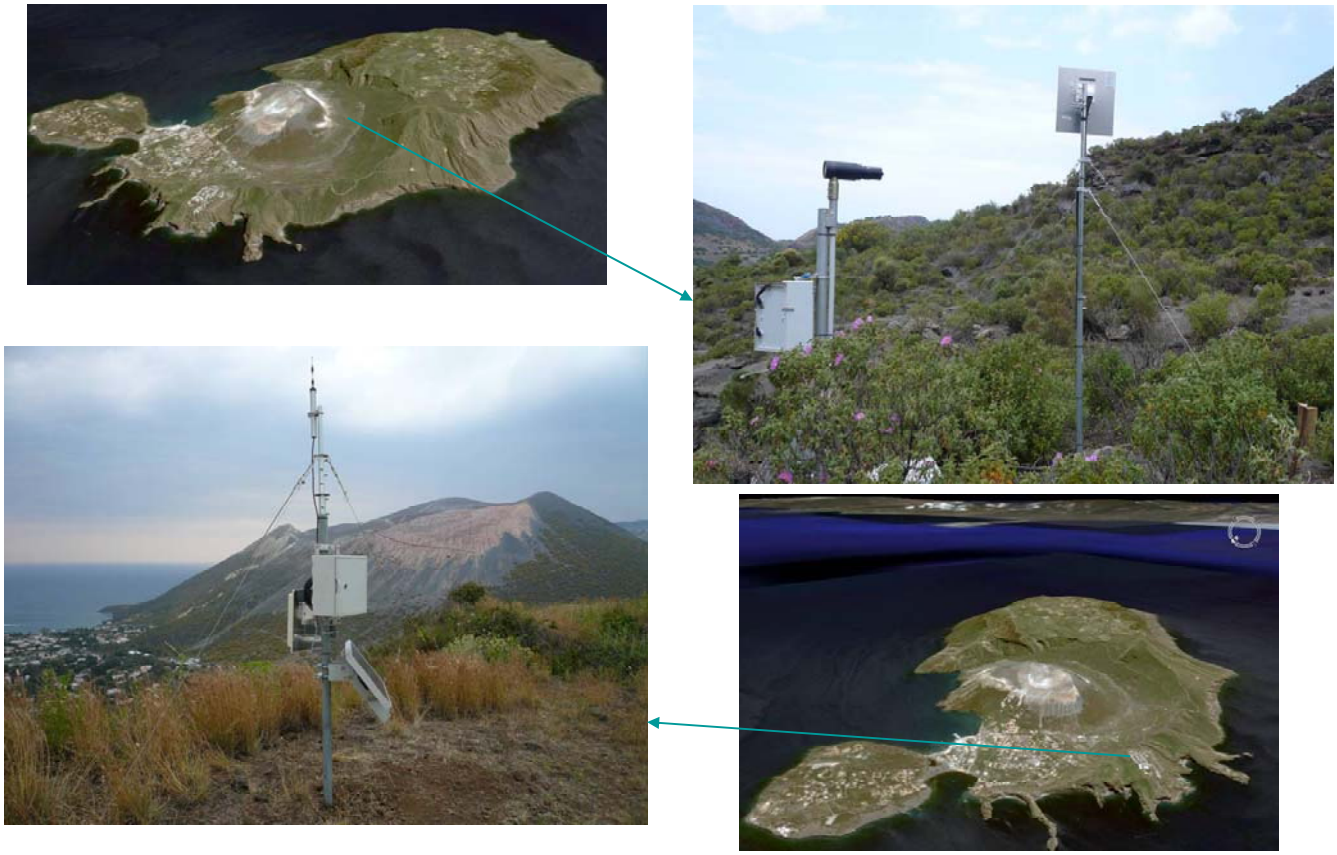

Fig. 18 - Picture of UV-Scanning DOAS equipment installed at Palizzi area south-east flank of Vulcano island.

Further two weather stations were installed, one directly at the la Fossa crater and the second one at Lentia, an area with nearly the same height as the la Fossa crater, around 2 km away from it (***fig. 20***)

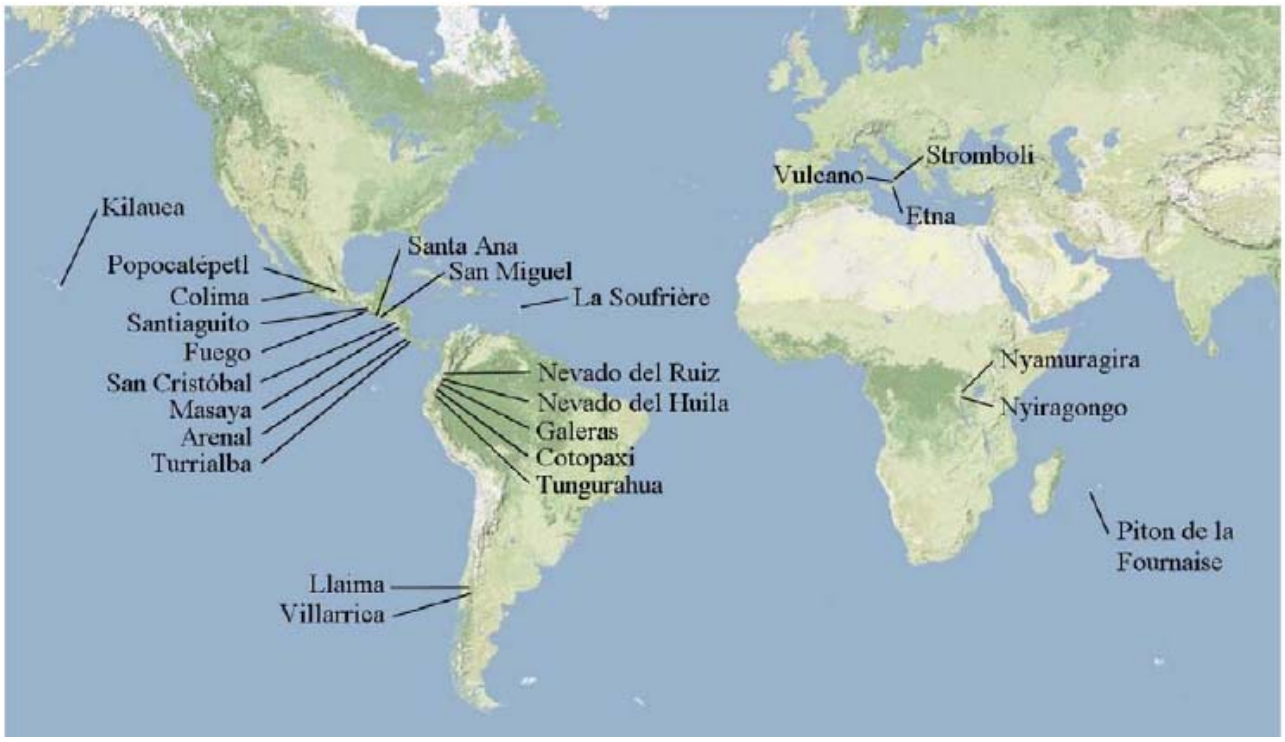

Fig. 19 - Geographical location of the volcanoes involved in the NOVAC project as of March 2009. The project is open to participation by any interested institution, so the network may be expanded in the future.

Fig. 20 - Weather station at Lentia, an area with nearly the same height as the la Fossa crater, around 2 km away from it.

The continuous SO2 flux measurements were recorded from March 2008 up to October 2010, the results are reported in ***fig. 21***.

Vulcano Island is characterized by very low SO_2 flux considering the absence of a real "plume". Nevertheless this anomaly respect to the open conduct volcanoes characterized by higher SO_2 fluxes, we were able to measure in continuous and calculate the SO_2 fluxes at Vulcano Island. This was possible because Vulcano island is a very small volcano with an altitude of only 320 masl and a diameter of 500 m. UV-scanning DOAS could be install at Palizzi area, very close to the source of SO_2 (La Fossa crater), the distance between this two points is only 400 meters and the relative SO_2 slant column is high enough (50 to 250 ppmm) to well calculate the flux. In the diagram of ***fig.21*** is reported the SO_2 flux with the time. We observe a quite constant value of SO_2 flux around 12 t/d in the period of August 2008-August 2009. In mid September 2009 a great increase in SO_2 emission was recorded with fluxes up to 100 t d^{-1} reached in November 2009. These anomalous values were recorded in the period 15 September 2009 - end December 2009. Then, the values of SO_2 flux decreased to the normal values of about (12 t d^{-1}) and remained constant until October 2010.

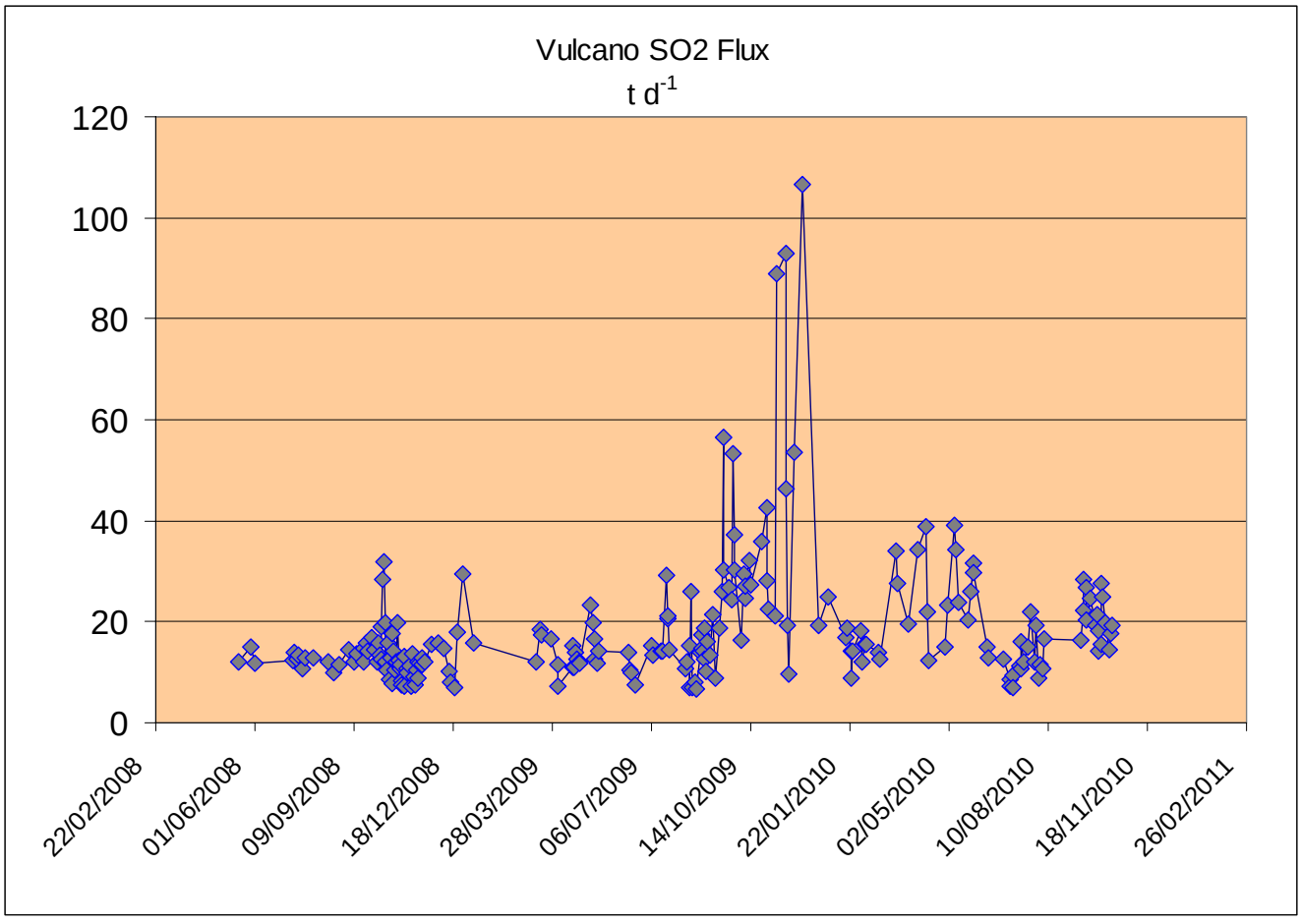

Fig. 21- Plume-SO_2 flux expressed in t/d^{-1} , time variation for the 2008-2010 period of continuous data set.

It is very interesting to observe that the anomalous values of SO_2 fluxes that increased about one order of magnitude occurred in the same period of the anomalous degassing processes of soil CO_2 recorded with a VCS monitoring station, located at the summit of the La Fossa crater (see ***fig 22)***.

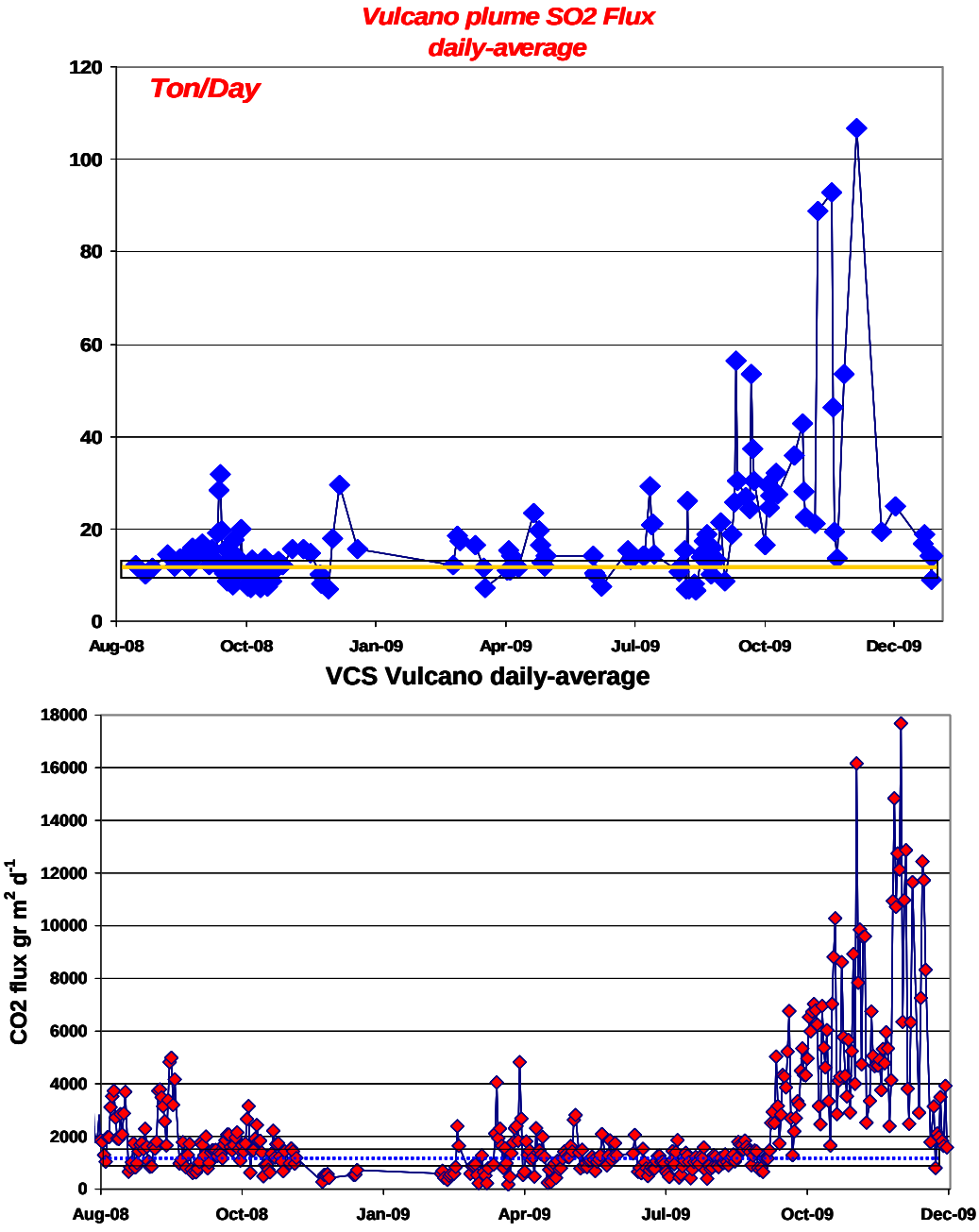

Fig 22 Comparison between the CO_2 soil flux and SO_2 plume flux in Vulcano Island

This indicate that independent parameters like CO_2 soil flux and "plume" SO_2 flux give us the same indication and reveal an increase of volatiles "masses" involved in the solphataric degassing processes at Vulcano Island due to an increase of volatiles arriving from the deep.

These are the first continuous data set of geochemical parameters acquired in continuous directly from the summit crater at Vulcano Island. This approach is very promising to better investigate the geochemical processes responsible of the plumbing degassing system of Vulcano Island and will help us to formulate a more complete geochemical fluids model.

3.6 Analysis of data evaluation of fluxes

3.6.1 Evaluation of spectra

The collect spectra are analyzed according to standard procedures DOAS; each spectrum is corrected for electronic offset and dark current signal.

To obtain the optical density, the logarithm is taken at each measurement spectrum. A polynomial is used to compensate any broadband extinction structures caused by Rayleigh molecular and Mie aerosol scattering (Platt and Perner 1983; Platt 1994). High and low pass filter are applied. For a best fit ,a shift and squeeze of the absorption cross-sections are allowed to compensate for any small optical error. (Stutz and Platt 1996) and then fitted to a library reference spectrum of SO_2 (Vandele et al. 1994).

In the way to improve and find the best solutions for data evaluation, several tests were performed on data from the station "scanning DOAS" on Vulcano Island. The data set of the 14th of August 2008 was chosen to carry out various sensitivity studies on the SO_2 evaluation. On this day the plume was clearly inside the geometrical plane of the instrument. For all performed tests the NOVAC-software was applied and the data of all scans on this day are compared below.

The presented results, discussed and shown in the various figures, are always based and compared to an evaluation done in the 305.26-318.22 nm range, and include SO_2, ozone (O_3) and a Ring correction in the fit with a polynomial of 5th degree, which is illustrated as black rectangles. The first test was done expanding slightly the wavelength evaluation range from 305.26 - 318.22 nm to 305.26 - 321.40 nm, the second one was performed by shifting the evaluation range to 310.00 - 320.00 nm. In ***fig*** 23(a) the results are expressed as kg/s of SO_2 over the day analysed in the above described wavelength regions. The different results obtained by the analysis in various wavelength ranges are displayed with different colours and symbols. Neither the slight nor the larger shift analyzed showed glaring difference of SO_2 fluxes although a systematic increase can be noted for the shift to the larger wavelength region. ***Fig*** 23(b) reports the different results, again displayed with different colours, gained by applying various polynomial degrees (2, 3 and 5 degree) in order

to remove the broadband extinction structures from the spectra. No differences are notable in these results. In ***fig*** 23(c) are reported the results considering correction or non correction of the Ring effect as well as taken into account or not the O_3 absorption. If only the Ring effects is considered (red circle) the SO_2 fluxes are generally larger, instead considering only the O_3 presence (blue triangle) and leaving the Ring effect out of considerations leads to comparable results as considering both (Ring effect and O_3 absorption).

Fig 23d shows the last sensitive study carried out in this work; two different SO_2 references were utilized (273 K and 293 K) and the results compared. The data obtained are almost overlapping, in contrast with earlier studies performed by Bobrowski 2005, where a difference of 7 % was observed.

The most notable difference, the effect of the O_3 absorption, is shown in more detailed in ***fig*** 23(e). displays two plume scan examples, one at midday and the other in the afternoon, comparing the fit results obtained with and without included ozone (O_3). From this figure can be noted that without including O_3 in the evaluation process the SO_2 values obtained are generally higher, especially when the telescope is looking closer to the horizon. In the afternoon this effect gets even stronger showing a difference of up to 10 ppmm. This is expected, because of an increased ozone column due to a longer light-path in the stratosphere when the sun light is entering the earth atmosphere under a higher solar zenith angle (Hönninger et al. 2004).

3.6.2 Weather measurements:

In order to have correct information about wind speed and wind direction, a weather station was installed at Vulcano Island in a site called Lentia located at the same elevation of the crater ***fig20***. The weather station was built by Davis and model and Vantage Pro 2 and provides us, as well as wind speed and direction, including rainfall, temperature, relative humidity, sunburn and UV. Communication is ensured by a wireless system, the data passing via the Vulcano Observatory arrived in Palermo at the National Institute of Geophysics and Volcanology in a real time.

The wind data for the measurement at Stromboli island arrived from the station Str02 located at the summit area(Pizzo sopra la Fossa) in real-time.

In some cases wind data provided by global model from European Centre for Medium-Range Weather Forecasts (ECMWF) or the National Oceanic and Atmospheric Administration (NOAA) can be referred.

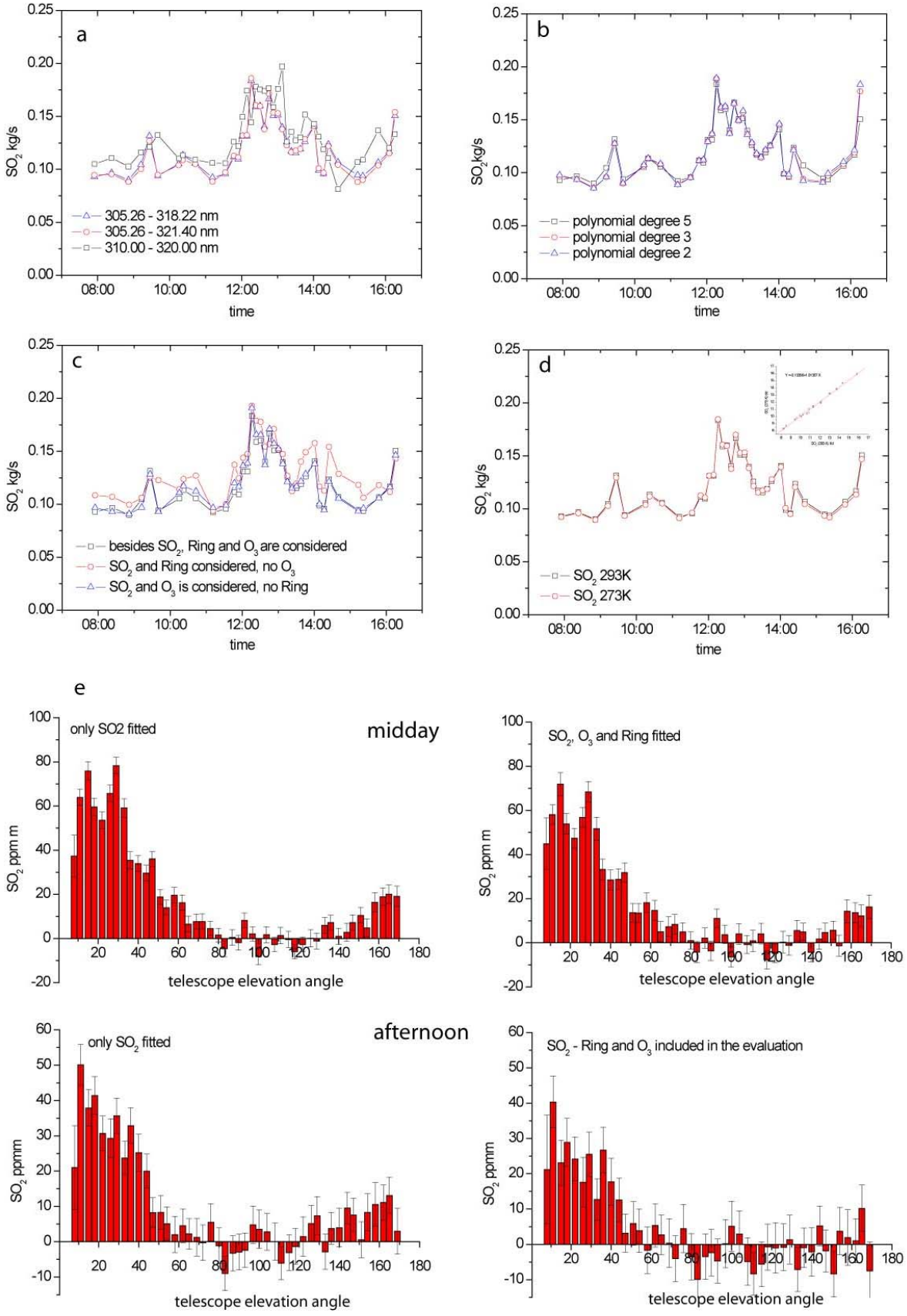

Fig. 23 - Sensitivity studies on the SO2 evaluation a) The different results obtained by the analysis in various wavelength ranges are displayed with different colours and symbols;b) the different results, gained by applying various polynomial degrees (2, 3 and 5 degree);c) are reported the results considering correction or non correction of the Ring effect as well as taken into account or not the O_3 absorption;d) two different SO_2 references were utilized (273 K and 293 K) and the results compared; e) displays two plume scan examples, one at midday and the other in the afternoon, comparing the fit results obtained with and without included ozone (O_3).

3.6.3 Error Analysis

The errors identified in these measurements are mainly: spectroscopy, atmospheric scattering and wind parameters.

Spectroscopic error is related to non linear absorption, errors in absorption cross section, stray light and temperature changes in the spectrometer.

While the errors in absorption cross section and nonlinear behaviour in Beer's low are documented, (C. Kern et al 2010) the major spectroscopy errors from stray light and change in temperature are different to each spectrometer. For reducing the stray light error we use a filter (Hoya U330). In some of these instruments, like Dual-axis scanning DOAS and the Active DOAS, the temperature effects are reduced by active temperature stabilization of the spectrometer.

Atmospheric scattering errors:

Solar light scattered by molecules and particles in the air like volcanic ash, condensed water and others molecules, giving an extended path length in the plume and this effect is detected by the instrument.

The scattering error strongly depends on meteorological condition, also depends on the distance between the instrument and the plume, to a lesser distance is less the error *(Kern* 2009).

Wind parameters error

To calculate the flux the concentration of the molecules in a cross section perpendicular to the direction of propagation of the plume shall be multiplied by the wind speed. If the speed and direction of propagation is not real you will have an under or overestimation of the flux measurement. To reduce the wind speed and wind direction have to be measured directly on the summit areas of the emission point. Although the measurements made at long distances downwind from the point of emission may not reflect the real conditions of speed and wind direction.

4. Realization of an Active DOAS prototype

4.1 Introduction active DOAS

The Active-DOAS utilize the artificial light as source. The first active DOAS instruments were developed in the 1970s as research tools for the measurements of various radicals, in particular OH. This type of technology has now found place in the study of trace gases, air pollution from anthropogenic emissions, and study of natural phenomena such as gaseous emissions as natural volcanic systems like O_3, NO_2, and SO_2, as well as NO_3 and HONO. Technology has seen the new source light of the LED (light emitting diodes) as a great alternative to Xenon arc lamps for low power consumption, longevity and high stability.

4.2 Prototype idea and realization

My research project included the realization of an instrument called Long Path Active DOAS. The new active DOAS ideated and assembled at the INGV PA followed the plans of the first models manufactured at the University of Heidelberg with little but substantially improvements. The new Active DOAS is designed primarily for measurements in volcanic areas, as opposed to models made before. In fact, this new model is characterized by reduced weight and dimensional geometry in order to allow easy transport up to the volcanic summit areas. Were also treated some aspects of the optical system tracking allowing a fast focus, reducing than the operational time spent in the no safe summit areas. The optical system of light sources and the size of the optical fiber were replaced too. In fact, while in previous models the optical system of the light source was prepared and focused in the laboratory while with the new system, we can make a quick focus in the field. The aperture size of optical fiber has been reduced for a narrower beam of light and to reduce intensity losses.

In detail the Active-Doas consists of the following items ***(fig. 24)***:

- telescope,
- optical fiber,
- UV LED sources,
- Spectrometer,
- retro-reflector
- notebook

Fig. 24 - NewActive Doas composed by one telescope, a optical fiber, three UV LED sources, one Spectrometer, a retoreflector and one notebook

Telescope: is composed of a spherical mirror (6" Ø) with a radius of curvature (R) of 800 mm and a focal length (f) 400 mm. This mirror (BK7 material), covered with Aluminium and MgF2 UV enhanced, mounted on a special support that allows the movement along the X Y directions ***(fig. 25)***.

An aluminium optical bench allows the position in line between the mirror and the optical fiber positioner, that allows the movement along the Z direction. Moreover, the telescope is supported by an adjustable tripod.

Optical fiber: is a bundle of 7 fibers (AS 100/110 UVPI-2,5m N.A 0.10 micron) (***fig. 26)*** with a transmissivity greater than 90% at the wavelengths involved (***fig. 27)***. Six transmitting fibers (two fibers for each LED) were arranged in a ring around a central receiving fiber in the focal point of the telescope, thus allowing radiation at three different wavelengths (***fig. 28***).

Fig. 25 - Detail of the telescope consists of a Spherical mirror mounted on a special support that allows the movement along the X Y directions. An aluminium optical bench allows the position in line between the mirror and the optical fiber positioner, that allows the movement along the Z direction.

Fig. 26 - Section of a bundle of 7 fibers, six transmitting fibers (two fibers for each LED) were arranged in a ring around a central receiving fiber.

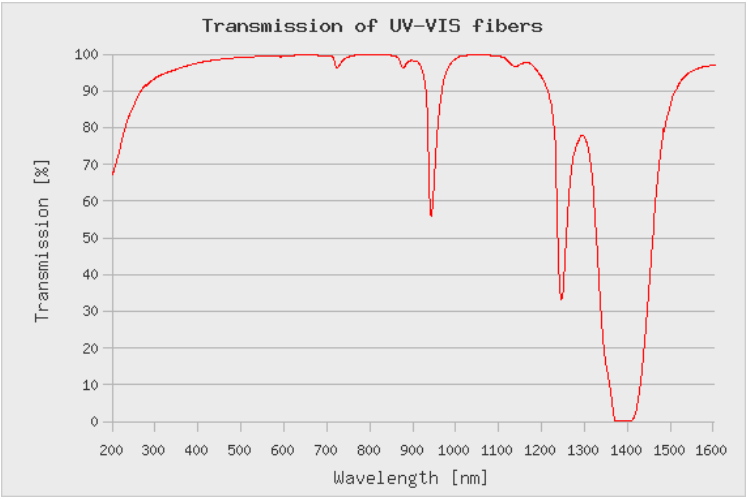

Fig. 27 - Transmissivity of the fiber, greater than 90% at the wavelengths involved.

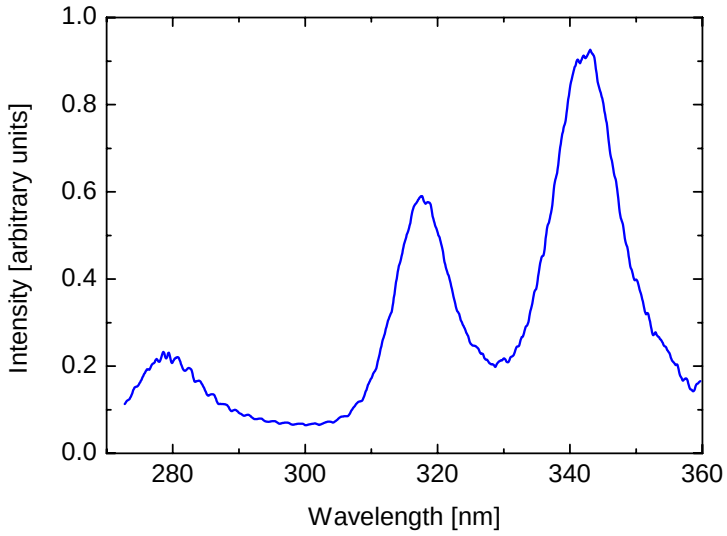

Fig. 28 - Example of radiation at three different wavelengths.

Source: Multi-UV-LED light source is composed by three separate optical systems ***(fig. 29)***, each one of which is composed by one LED (***fig. 30)*** with a different wavelength placed in an XY positioner, connected to a optical tube (1" Ǿ) where two plane-convex lenses focus the beam into the fiber. An electronic system allows to adjust the intensity of the each beam.

The wavelengths 280, 310 and 315 nm were chosen to the absorption of SO2, ClO, CS2 structures mainly.

Fig. 29 - Multi-UV-LED light source is composed by three separate optical systems with electronic system for the intensity variation.

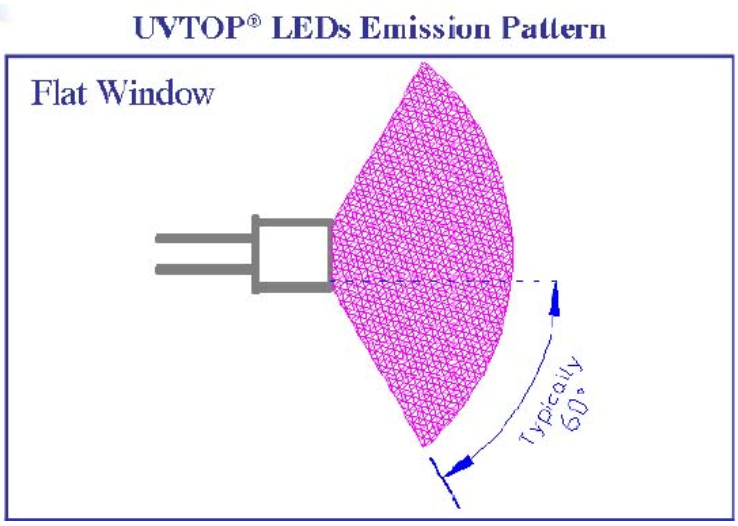

Fig. - 30 UV Top LED pattern emission

Spectrometer: Ocean Optics© QE65000 spectrometer ***(fig. 31)***: spectral range between 260 and 340 nm; w/scientific-grade detector Grating H7installed; select 70-100 nm; best: 200-500nm; SLIT-100: installed optical bench entrance aperture 100.

The spectrometer is maintained at a stable temperature using a SuperCool© PR-59 thermoelectric cooling/heating whit digital control unit (***fig. 32***).

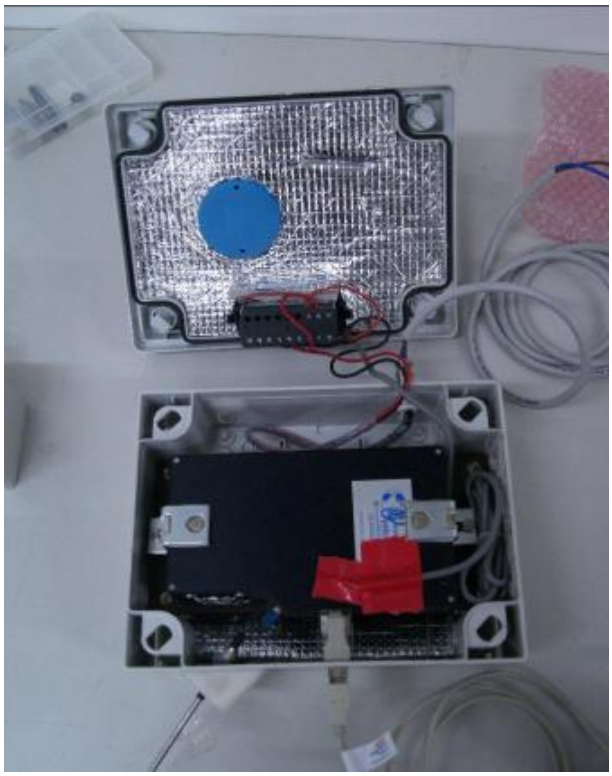

Fig. 31 - Ocean Optics© QE65000 spectrometer with a spectral range between 260 and 340 nm w/scientific-grade detector Grating H7installed, select 70-100 nm, SLIT 100

Fig. 32 - Isothermal box whit SuperCool© PR-59 thermoelectric cooling/heating and digital control unit

Retroreflector : it is composed by 10 UV Fused Silica Corner Cube Retroreflectors ***(fig. 33)***. 520mm Ø by Edmund Optics© inserted into appropriate housing ***(fig. 34)***, and placed on a stand of triangular shape, in turn mounted on an adjustable tripod ***(fig. 35)***.

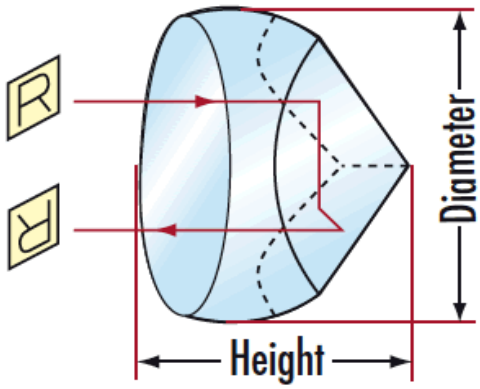

Fig. 33 - UV Fused Silica Corner Cube Retroreflector 520mm

Notebook: The spectra are collected by a small notebook computer with the help of specific programs like: OOIB Base 32 (Ocean Optics) and DOASIS (DOAS Intelligent System By Institute of environmental Physics, University of Heidelberg) for working with spectral data, data acquisition, mathematical operations, species evaluation. A 12 V battery is necessary to power the entire setup.

The operation is described in more detail in the experiment on the plume of Vulcano Island (paragraph 5: Geochemistry of molecular traces).

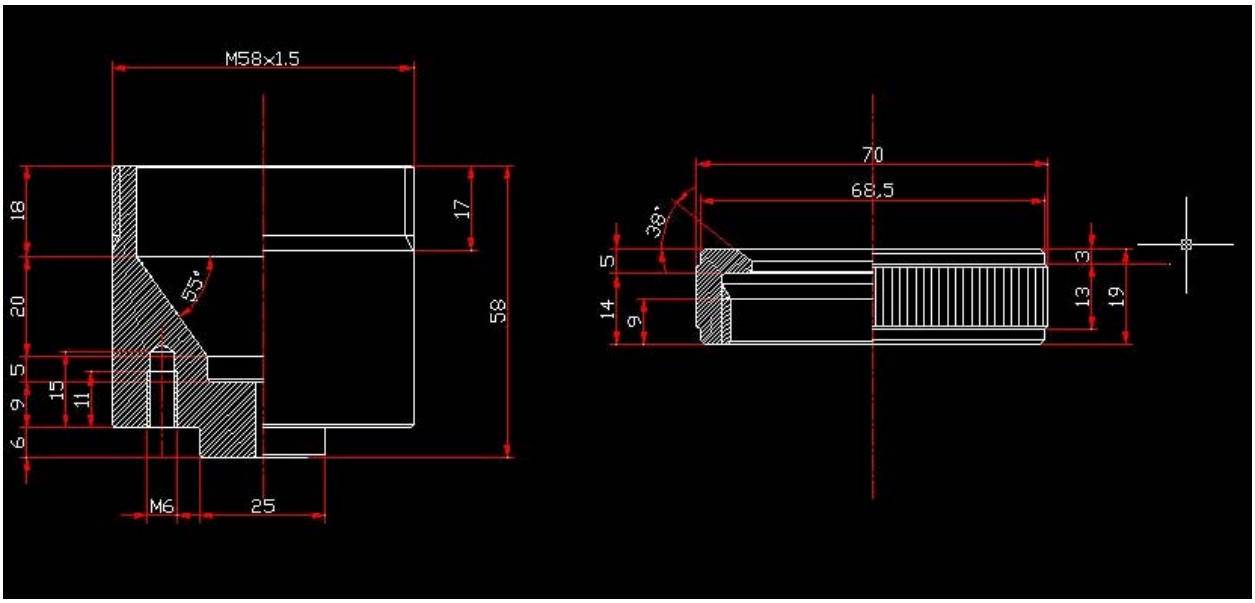

Fig. 34 - Drawings for the construction of retro-reflectors PVC supports

Fig. 35 - Triangular shape mounted on an adjustable tripod.

In summary the light beam produced by the artificial source (LEDS) is coupled in to the fiber and arrive at the mirror; then the light through the gas masses is reflected by retro-reflector back to the mirror, and by the fiber into the spectrometer. The signal converted from analog to digital, is collected by the notebook.

5 Geochemistry of molecular traces

LP-DOAS measurements conducted at Vulcano Island (Italy) - February 2010

5.1 Measurement Setup

5.1.1 Instrument design

Long path differential optical absorption spectroscopy (LP-DOAS) measurements were conducted on the west rim of the Gran Cratere on Vulcano Island (Italy) on February 24 and 25, 2010. The goal of these measurements was to test a novel LP-DOAS instrument especially designed for measurements of volcanic gas emissions. Features of the instrument include a fiber-optic-based Newtonian telescope (as described by Merten 2008, Merten et al. 2010) with a smaller than usual 15 cm main mirror, as shown in Fig. . The compact design specifically targets short light paths (order of several hundred meters, not several kilometers) usually used in volcanic environments. In addition, the compact setup reduces weight and space limitations therefore enabling use in remote locations.

Fig. 36 – Image of the LP-DOAS setup. The compact design of the telescope is specifically targeted at applications in which small, light instrument is necessary. The spectrometer is located in a temperature controlled housing. The current driving each of the three LEDs can be regulated individually on the power supply (seen in the lower part of the image). The entire setup is powered by a standard 12 V battery.

Ultra violet LEDs served as a light source for the measurements (see Kern et al. 2006, Sihler et al. 2009 for details). Three different LEDs were connected to two fibers each. These six transmitting fibers were arranged in a ring around a central receiving fiber in the focal point of the telescope,

thus allowing radiation at three different wavelengths to be used. For these first measurements, the wavelengths 280, 310 and 315 nm were chosen, where the absorption structures of SO_2, ClO, and CS_2 are located.

An array of retro-reflectors was used to reflect the transmitted radiation back to the telescope after having crossed the sampling area. An Ocean Optics© QE65000 spectrometer with a spectral range between 260 and 345 nm was used to measure the spectrum of this incident radiation at intervals of a few seconds. The spectrometer was kept at a stable temperature of 20° using a SuperCool© PR-59 thermoelectric cooling/heating unit. The spectra were recorded on a small netbook computer. A 12 V battery was used to power the entire setup.

Fig. 37– Location of the array of retro reflectors during the first measurement period (Position 1) on February 25, 2010. The array is visibly reflecting the flash of the camera with which the picture was taken. The reflectors are positioned directly behind a low-temperature fumarole on the western rim of the Gran Cratere.

5.1.2 Measurement geometry

The measurements on February 24, 2010 were not successful, as the onset of rain caused the experiment to be abandoned shortly after setting up the instrumentation. However, on February 25, successful measurements were performed using two different light paths. During the first measurement period from approximately 12:00 to 12:45 local time, the array of retro reflectors was positioned behind a low temperature fumarole about 150 m from the telescope (see **Fig.**). During this time, the gases being emitted by this fumarole were sampled. Little or no disturbance from other fumaroles is expected in this dataset, as favorable winds were blowing the gases from other

fumaroles in the area away from the light path. Depending on the wind, the light path length through the fumarolic gases was between 0 and 15 m one way, so a total light path of between 0 and 30 m resulted (see **Fig. 1**8).

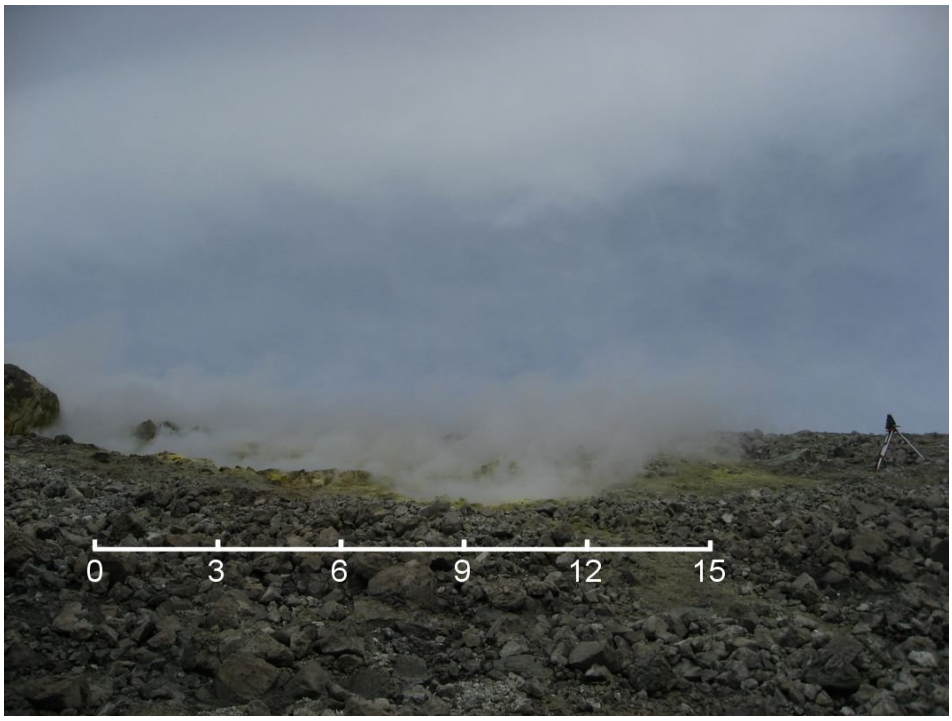

Fig. 18 – Side view of the location of the retro reflector array during measurements at Position 1 on February 25, 2010. A length scale was added to demonstrate the extent of the fumarolic gases during the measurements. The one way light path through the fumarolic gases was between 0 and about 15 m during the measurements, depending on the wind direction. Therefore, peaks in the SO_2 column density are thought to correspond to a total light path of 30 m through the fumarolic gases.

During the second measurement period, the reflectors were then moved to a position further down in the crater to enable the measurement of gases being emitted from the higher temperature fumaroles located on the edge of the crater floor (see **Fig.**). The light path length inside the fumarolic gases varied considerably due to variations in wind direction as well as variations in the degassing strength of the fumaroles themselves. Therefore, obtaining volatile concentrations from these measurements is difficult, but concentration ratios between different species are accessible with the LP-DOAS technique.

5.2 Sulfur dioxide (SO_2) evaluation and results

5.2.2 DOAS retrieval of SO_2 column densities

Sulfur dioxide is the volcanic gas with by far the most dominant absorption structures in the analyzed wavelength range. Therefore, measuring SO_2 is the first experiment conducted to prove

the functionality of the novel LP-DOAS instrumentation. SO_2 was evaluated in all recorded spectra in the wavelength range between 280 and 290 nm. This evaluation range was chosen because several strong absorption lines of SO_2 are found here. However, the most important argument for choosing this range was the absence of solar radiation in this wavelength region. Below about 300 nm, solar radiation is completely blocked by the ozone layer. Since the fumarolic plume studied in these experiments was rich in highly scattering aerosol, solar radiation was scattered into the light path of the LP-DOAS to a varying degree depending on the aerosol optical density in the light path during a particular measurement. The spectrum of the scattered solar radiation was therefore superimposed on the transmitted LED spectrum. By using an evaluation range below 300 nm, however, interference between the two could be avoided.

Fig. 39 – The arrow indicated the location of the retro reflector array during the second measurement period on February 25, 2010 (Position 2). The reflectors are now located further down in the crater to enable the measurement of gas being emitted from the high temperature fumaroles in the crater floor.

For each measurement spectrum, the offset and dark current of the spectrometer were first corrected. Then the logarithm was taken. In order to obtain the optical density, the logarithm of the average of 150 spectra recorded under conditions in which no SO_2 was in the light path was fit to each measurement spectrum together with the absorption cross-section of SO_2 (Vandaele et al. 2009). Also, a 5^{th} order polynomial was included to remove any broadband structures and a spectrum of the background solar spectrum as well as a Ring spectrum were included to allow the fit to be adapted to other wavelength later on. An example fit is shown in Fig. .

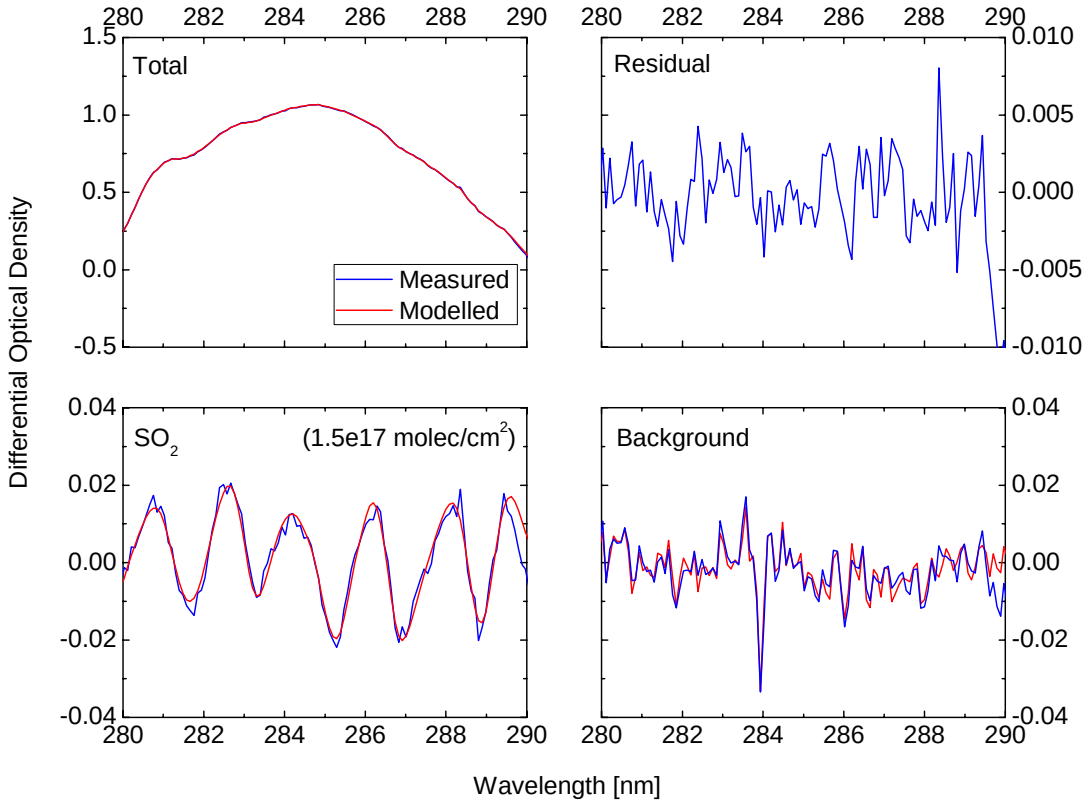

Fig. 40 – Example evaluation of SO_2 between 280 and 290 nm. The residual is still slightly structured, a result of the short total integration time used for the measurement (see text for details).

5.2.3 Retrieved SO_2 column densities

The results of the SO_2 evaluation for the spectra recorded during the first measurement period at Position 1 (low temperature fumarole) are shown in Fig. . The time series is characterized by a strong fluctuation of SO_2 column densities. These fluctuations are mainly caused by winds blowing the fumarolic gas into or out of the light path of the LP-DOAS instrument. In part, fluctuations of the degassing strength of the fumarole itself could also be responsible.

The errors of the individual measurements are considerable. This is due to the very short (order of seconds) integration time of the instrument for an individual measurement. While it is desirable to use a longer integration time to enhance the signal to noise ratio, this is not possible for measurements such as these in which the measurement conditions change at such a rapid pace. It is not advisable to average consecutive spectra obtained under drastically different measurement conditions (SO_2 column density, aerosol optical density…) as this will distort the results of a DOAS evaluation. Instead, statistics can be improved by co-adding or averaging spectra that were obtained under similar measurement conditions, as will be discussed later on.

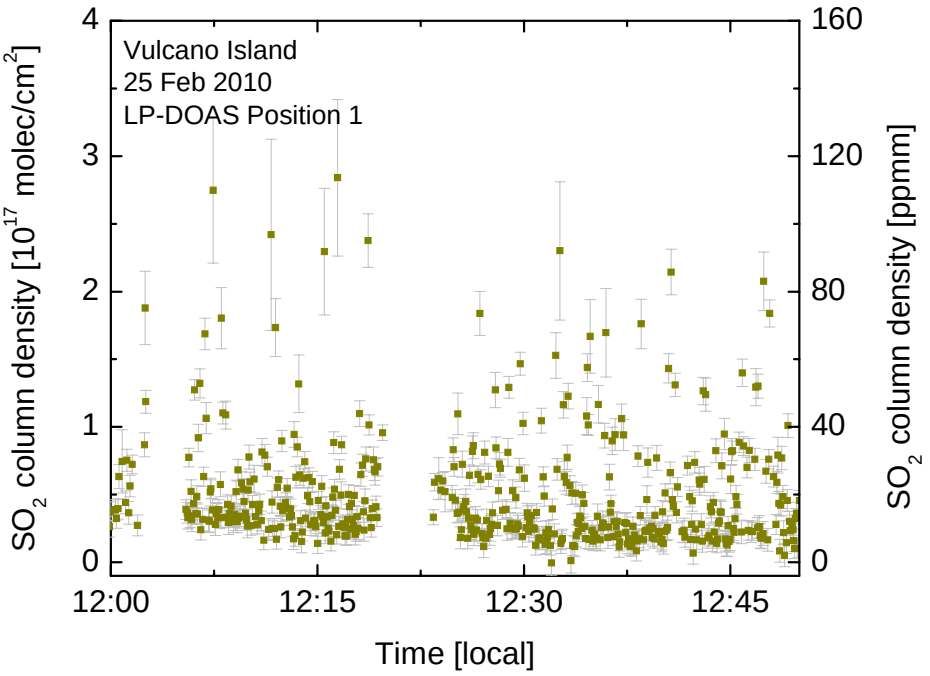

Fig. 41 – Time series of SO_2 recorded during the first measurement period on February 25, 2010. The SO_2 column density fluctuated between 0 and 2.8×10^{17} molec/cm^2. The fluctuation is mainly caused by winds blowing the fumarolic gas into or out of the light path. The maximum values correspond to an average SO_2 mixing ratio of about 3.7 ppm in the fumarolic gas along the light path (assuming a light path length of 30 m for these measurements, see text for details).

While DOAS measurements always yield integrated column densities, it is possible to estimate an average mixing ratio of SO_2 from the obtained results in this case. As shown in Fig. 18, the one-way light path length in the fumarolic gases was between 0 and 15 m during the experiment, depending on the wind during a particular measurement. Assuming that the highest column densities (2.8×10^{17} molec/cm^2) were measured at a time in which the fumarolic gases filled out the entire 15 m (thus yielding a total light path length of 30 m in the gases), the average SO_2 mixing ratio along the 30 m light path amounts to about 3.7 ppm.

Fig. depicts the time series of SO_2 column densities obtained from the LP-DOAS measurements of the fumarolic gases emitted by the higher temperature fumaroles located at the base of the Gran Cratere (Position 2). Measurements were conducted in this set up from about 13:00 to 15:30 local time on February 25, 2010. Again, favorable wind conditions allowed the more-or-less exclusive sampling of the gases emitted from the fumaroles at the base of the volcanic crater. While the LP-DOAS light path was several hundred meters, only a fraction of this path was filled with the gases of interest. Variations in the amount of gas in the light path due to fluctuating winds and emission strength of the fumaroles led to a highly variable time series. The highest SO_2 column densities were measured during the first 45 minutes of the measurements. In this time period, up to 1.2×10^{18}

molec/cm^2 were detected. After this time, a shift in wind direction towards the south caused less gas to be blown into the light path and lower columns (up to about 5×10^{17}molec/cm^2) were measured.

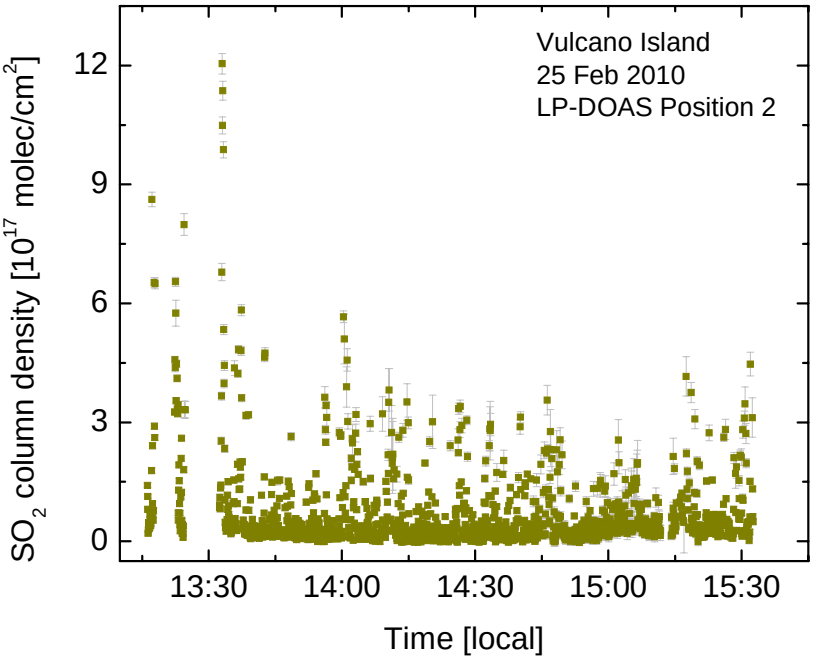

Fig. 42 – Time series of SO_2 column density in the light path of the LP-DOAS instrument during the second measurement period (Position 2). Here, the fumarolic gases from the higher temperature fumaroles located in the base of the Gran Cratere were sampled. Fluctuations are due to varying wind directions leading to varying amounts of fumarolic gas in the light path and fluctuations of the emission strength.

The measurement errors were significantly reduced during the measurements conducted at Position 2 compared to those at Position 1. This was due to an improved alignment of the instrumentation leading to an increased light throughput of the system. More photons could be recorded in each measurement interval, thus improving the statistics of the measurement. The time series recorded at Position 2 thus demonstrates the ability of the novel LP-DOAS to measure SO_2 at high accuracy (errors on the order of a few percent) and time resolutions on the order of a few seconds.

5.3 Quantification of CS_2 with active Long Path DOAS

5.3.1 Background

It was shown above that the novel LP-DOAS is capable of measuring SO_2 at high accuracy and temporal resolution. The experiment conducted at Vulcano Island had another goal as well. The instrumentation was to be applied in an attempt to measure carbon disulfide (CS_2). While this compound has never before been detected at a volcano using the DOAS technique, its differential absorption structure (see **Fig.**) makes it potentially detectable with an LP-DOAS instrument.

Vulcano Island was chosen for this experiment because the low temperature of its fumaroles causes a substantial amount of the emitted sulfur to be degassed in a reduced form. Recent measurements have shown that H_2S / SO_2 ratios are typically between 0.15 and 2.5 (Aiuppa et al. 2005, Aiuppa et al. 2006), depending on the degassing temperature and extent of re-equilibration of gases with the hydrothermal system. The authors report that the lowest values for the H_2S / SO_2 ratio were obtained during heating events, and that periods of low degassing temperature resulted in ratios close to unity.

5.3.2 Spectroscopy

The ultra-violet absorption cross-section of CS_2 is well known today, although the most recent publication in a major journal dates back to 1981 (Wu and Judge 1981). However, more recent unpublished measurements (Schneider and Moortgat 1990, Vandaele et al. 2000) confirm the original cross-section within reasonable errors. As shown in **Errore. L'origine riferimento non è stata trovata.**, the cross-section exhibits a number of differential absorption structures between 280 and 330 nm, with the strongest absorption bands lying between 315 and 330 nm. Therefore, measurement with differential spectroscopy is in principle possible in this wavelength region.

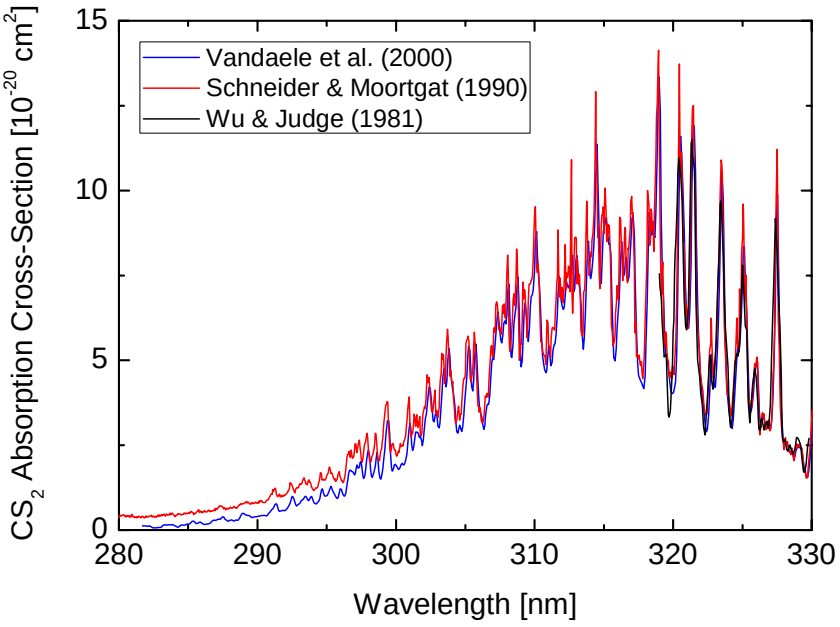

Fig. 43 - Absorption cross-section of CS_2 between 280 and 330 nm according to 3 separate studies (Wu and Judge 1981, Schneider and Moortgat 1990, Vandaele et al. 2000). The strongest differential absorption bands are found between 315 and 330 nm.

The absorption cross-section of SO_2 is also very prominent for wavelengths between 280 and 320 nm, as can be seen in Fig. , and although it is an order of magnitude weaker above 320 nm (Fig.), the differential structures still reach depths of approximately 1.5×10^{-20} cm^{-1} between 320 and

330 nm. As the differential absorption structures of CS_2 are about 1 order of magnitude larger in this wavelength range, the sensitivity of a DOAS instrument will typically be 1 order of magnitude higher for CS_2 than for SO_2 at these wavelengths. However, the CS_2 / SO_2 ratio in the plume of La Fossa crater fumarolic field on Vulcano Island is expected to be between 10^{-4} and 10^{-3} (S. Inguaggiato, personal communication). Therefore, the measured DOAS optical density of CS_2 is expected to be approximately 100 to 1000 times smaller than that of SO_2 in any particular measurement. The detection limit of the instrument in respect to CS_2 will in large part be determined by the ability to fully account for SO_2 absorption in the CS_2 absorption region.

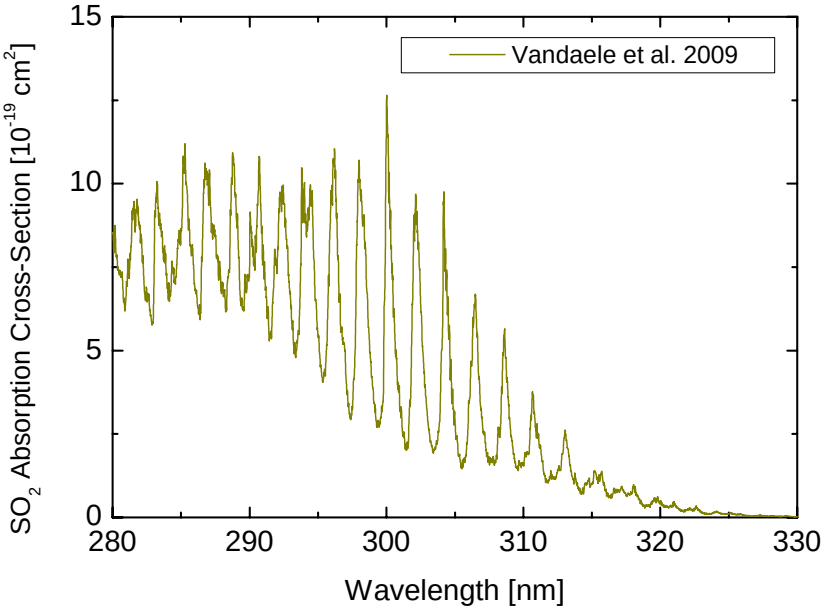

Fig. 44 – Absorption cross-section of SO_2 between 280 and 330 nm according to Vandaele et al. 2009. The strongest differential absorption lines are between 280 and 310 nm.

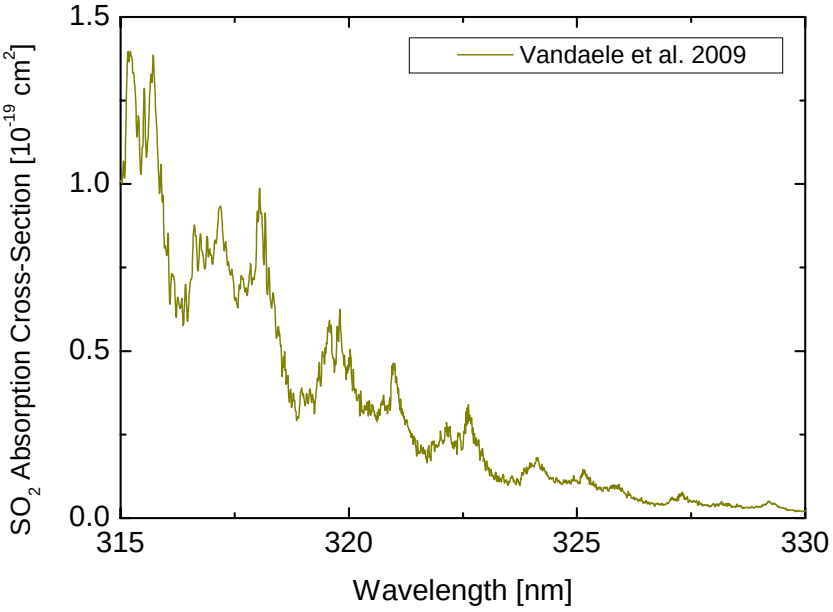

Fig. 45 – Absorption cross-section of SO_2 between 315 and 330 nm according to Vandaele et al. 2009. While the differential absorption becomes weaker towards higher wavelengths, the differential structures still reach depths of approximately 1.5×10^{-20} cm^{-1} between 320 and 330 nm

5.3.3 DOAS retrieval of the CS_2 detection limit

A DOAS retrieval was set up to retrieve the column density of CS_2 in the spectra recorded during the measurements on February 25, 2010. The wavelength region between 314 and 321 nm was chosen for the retrieval. This region contains three absorption bands of CS_2. While several additional strong absorption bands are located above 321 nm, this region was not accessible with the available LEDs (see Outlook for more details). In addition to the cross-section of CS_2, the cross-section of SO_2 (the strongest absorber in the evaluation range) was included in the fit as well as a background spectrum, a Ring spectrum and a reference spectrum compiled from 60 spectra without SO_2 absorption. A 5^{th} order polynomial was used to account for any broad band structures in the retrieval. To improve the statistics of the measurement, between 10 and 20 spectra with similar SO_2 column densities were co-added before the fit was applied.

Unfortunately, it was not possible to retrieve CS_2 in any of the measured spectra. The noise superimposed on the measurement was larger than any potential CS_2 absorption structures at all times. Instead of a specific CS_2/SO_2 ratio, only an upper limit for this ratio could be retrieved. This upper limit was obtained from the detection limit of CS_2 in each spectrum. In order for a species to be measured using the DOAS technique, the differential optical density τ of this species must be larger than the noise R in the DOAS fit residual (see Kern 2009 for details).

$$\tau = \sigma' \cdot S > R \qquad \text{Eq. 1.}$$

The trace gas column density S must therefore be larger than the ratio of the noise N and the differential absorption cross-section σ' in order for it to be measured. The detection limit S_{det} of a specific gas is thus given by the relation

$$S_{det} = \frac{R}{\sigma'} \qquad \text{Eq. 2.}$$

Fig. 2 demonstrates the retrieval of the CS_2 detection limits for the LP-DOAS measurements. To obtain an upper limit for the CS_2 column density in each spectrum, the DOAS fit described above was performed in the absence of the CS_2 absorption cross-section. After the fit was applied, the fit residual was analyzed. The fit residual gives the difference between the measurement optical density and the modeled optical density obtained from the DOAS fit. IF CS_2 were present in the optical path of the instrument, the respective absorption structures would be visible in the fit residual. If no such structures are visible, the optical density of potential CS_2 absorption must be smaller than the differential optical density of the residual (see Eq. 1 and 2). Therefore, the upper limit can be estimated from the residual. The dotted red line in the lower left panel of Fig. 2 depicts the maximum differential CS_2 absorption deemed to be possibly hidden by the noise in the residual. In this case, the upper limit was 3.7×10^{14} molec/cm^2. This results in an upper limit for the CS_2/SO_2 ratio of about 5×10^{-4}.

In this manner, each of the compiled spectra was evaluated in regard to the individual detection limits of CS_2. The results are shown in Fig. and Fig. . The resulting upper limit for the CS_2/SO_2 ratio at Position 1 (the low temperature fumarole) was 7×10^{-4}. The enhanced light throughput at Position 2 enabled the retrieval of a lower detection limit. Here, the CS_2/SO_2 ratio was below 5×10^{-4} during the measurement time period. Hence, although CS_2 could not positively be identified during the measurements, hard upper limits can be given both in total column and relative to the abundance of SO_2. If the CS_2/SO_2 ratio had been higher, the instrument would have positively identified the species.

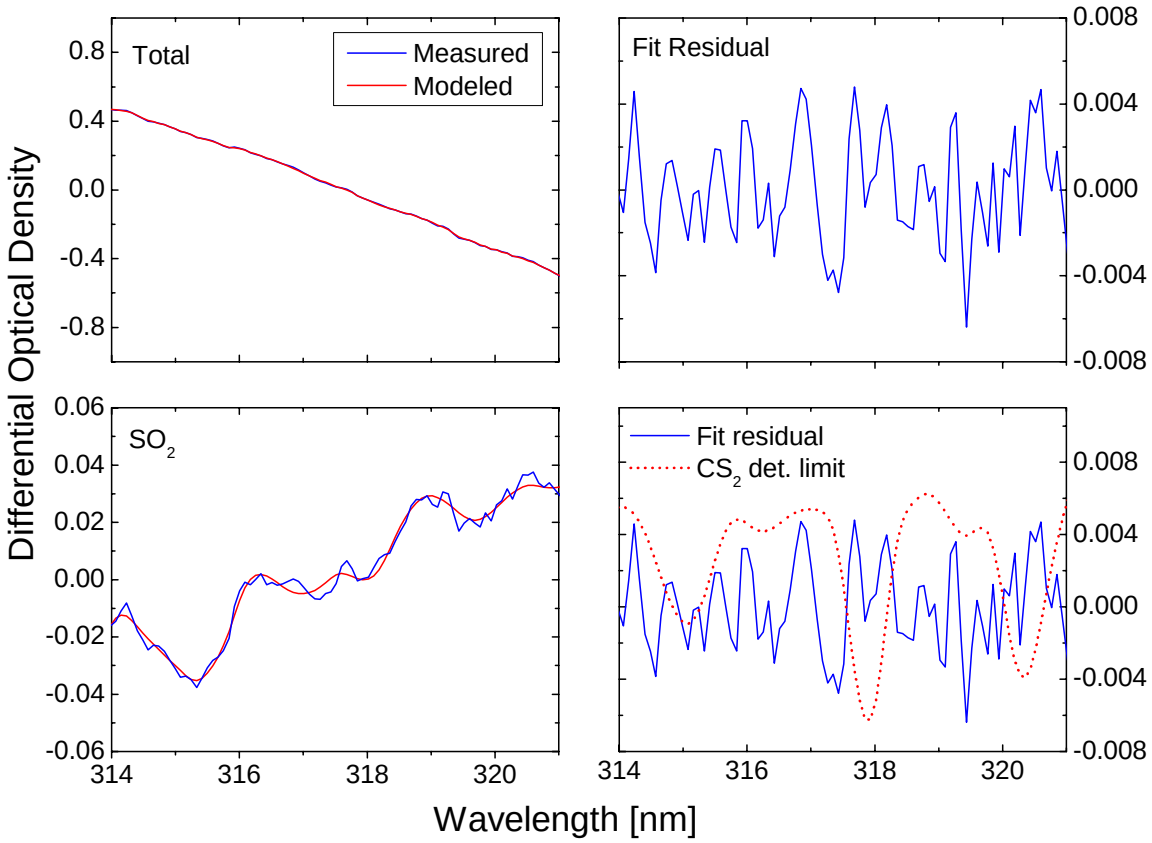

Fig. 2 – Example of the retrieval of the CS_2 detection limit for the LP-DOAS measurements conducted at Vulcano Island on February 25, 2010. The fit residual shows the difference between measurement and model spectra after fitting SO_2 to the measurement. The residual is of random nature and doesn't show an indication of CS_2 absorption. The detection limit of CS_2 is determined by the differential optical density of the noise. The red dotted line shows the maximum CS_2 signal that is deemed to possibly be hidden by the noise. This is the detection limit. In this case, the detection limit was calculated to 3.7×10^{14} molec/cm^2. By dividing this value by the SO_2 column density, a maximum for the CS_2/SO_2 ratio of about 5×10^{-4} is obtained.

5.4 DISCUSSION

First and foremost, this study confirms the functionality of the newly developed LP-DOAS instrument specifically designed for application in remote volcanic environments. Despite its small size, weight and power consumption compared to typical LP-DOAS instruments, it allows the remote sensing of a multitude of gases in the ultra violet wavelength region. As a proof of principle, stable measurements of SO_2 were performed at two positions on the crater rim of the Gran Cratere of Volcano Island on February 25, 2010. The resulting SO_2 time series illustrated the instruments capability to measure SO_2 absorption at high accuracy and time resolution.

The second objective of the experiment was to quantify CS_2 in the fumarolic gases on Vulcano Island. Unfortunately, the abundance of CS_2 was below the instrument's detection limit at all times during the experiment. However, upper limits of the CS_2/SO_2 ratio could be retrieved. In the low temperature fumarole, the CS_2/SO_2 ratio was below 7×10^{-4}. In the fumarolic gases emitted near the base of the Gran Cratere, the ratio of CS_2/SO_2 was below 5×10^{-4} during the experiment. Combined

with the SO_2 flux measurements conducted at Vulcano Island in the scope of the NOVAC project, an upper limit for the CS_2 flux can be calculated.

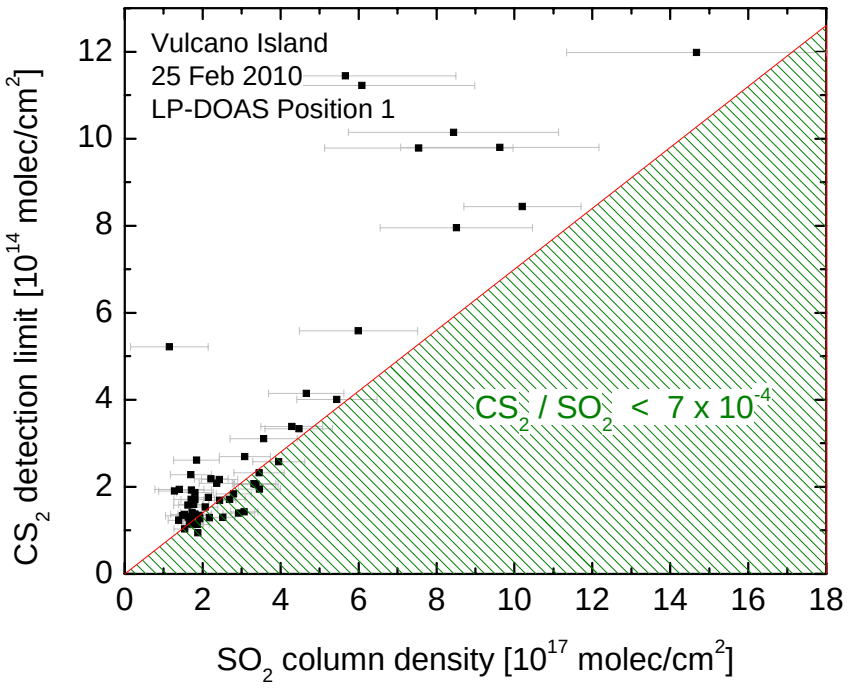

Fig. 47 – Upper limits for the CS_2 column density as a function of the SO_2 column density retrieved in the same spectrum for measurements conducted at Position 1. The CS_2 detection limit increases towards higher SO_2 column densities, as the strong absorption of SO_2 can not be perfectly compensated in the CS_2 retrieval. The measurements yield an upper limit for the CS_2/SO_2 ratio of about 7×10^{-4}.

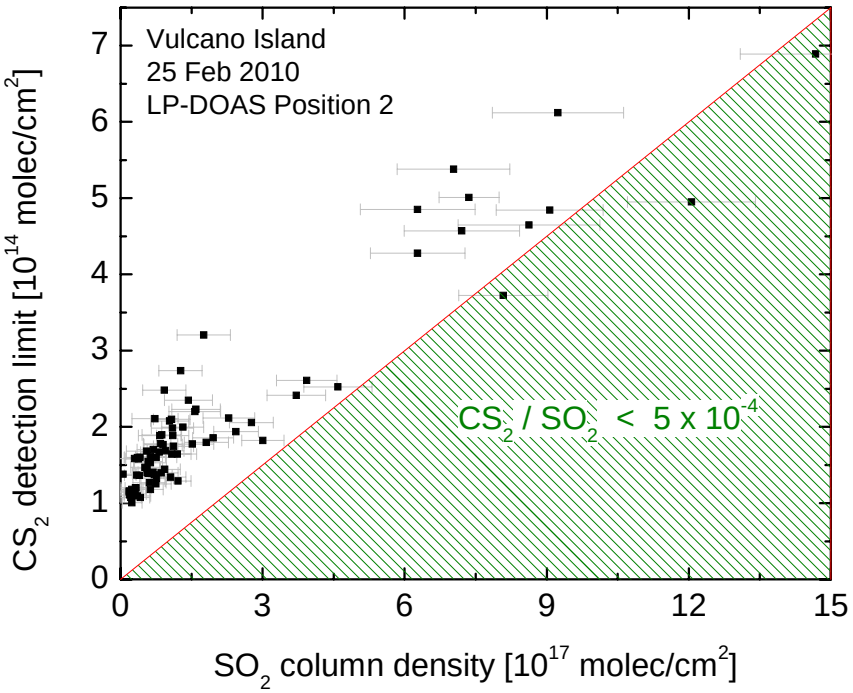

Fig. 48 – Upper limits for the CS_2 column density as a function of the SO_2 column density retrieved in the same spectrum for measurements conducted during the second measurement period at Position 2. Here, the measurements yield an upper limit for the CS_2/SO_2 ratio of about 5×10^{-4}.

Of course it is desirable to further improve the instrument's sensitivity towards CS_2 in order to be able to actually measure the true ratio of CS_2 to SO_2 at Vulcano Island. To this extent, several modifications of the instrumentation are suggested. First, at least one if not two LEDs emitting in the wavelength region between 320 and 330 nm should be used. This will reduce the interference of SO_2 in the spectra, as the differential absorption cross-section of SO_2 is weaker at wavelengths above 320 nm. Also, it will enable the detection of a number of strong yet currently inaccessible CS_2 bands. Finally, the maximum intensity of these LEDs will be higher than with the current LEDs, as technical production is more evolved.

At the same time, an automated, software-driven switch should be designed to switch on and off the LEDs. This would allow the recording of a background spectrum in close temporal proximity to each individual measurement spectrum. The compensation of scattered solar radiation in each of the measurement spectra could thus be improved. This is especially important if longer wavelengths are used, as the solar spectrum becomes increasingly intense towards 400 nm.

In total, it is expected that these changes should increase the light throughput of the LP-DOAS by a factor of 2 due to the brighter LEDs (this corresponds to a reduction of noise by a factor of 1.5) as well as reducing the SO_2 disturbances by a factor of 2 in optical density. Therefore, the CS_2 detection limit should be reduced by at least a factor of 3, thus hopefully making a positive detection of the species possible in future measurements.

6. APPLIED METODOLOGIES

6.1 Telemetry State of art

Differential optical absorption spectroscopy (DOAS) is based on the principle that different molecules absorb light in different wavelength regions and are characterised by typical absorption structure, which can be related to the kind and the number of gas molecules, in the light path between the source and the spectrometer collecting in the spectra (Platt and Perner, 1980).

The DOAS is distinguished in two main types depending on the kind of light source used, Active DOAS use artificial light sources, while passive DOAS uses light from natural sources (Sun, Moon, or hot lava in the infrared).

NOXON in 1975 was among the first to make measurements of scattered sunlight, to better understand both ozone and NO_2 in the stratosphere. The DOAS was considered as a fundamental tool to study and understanding the halogen-catalysed ozone destruction mechanisms and the budget of nitrogen species in the atmosphere.

The measurements of BrO and OClO by Solomon et al.(1987b,) revealed that chlorine and bromine chemistry played a crucial role in the formation of the ozone hole in the stratosphere.

The rapid development of MAX-DOAS offers a large number of practical applications: monitor the level of air pollution, information about pollution transport, measurements of emissions from individual industrial point sources, as well as from area sources such as traffic, monitoring of emissions from forest fires, measurement of SO_2 ,BrO, and other gases emitted from volcanoes, used in the monitoring of the state of a volcano(Bobrowski et al., 2003).

MAX-DOAS also expands the use of passive DOAS systems from mainly stratospheric applications, to the measurements of tropospheric trace gases (NO_2, HCHO...)

Recent development in several models and instruments using the DOAS technique to monitor and study the gases of both natural and anthropogenic origin in the atmosphere has been improved:1) Mobile Mini Doas, 2) simple Scanning DOAS, with fixed location, using a motor and a prism where viewing direction can be changed in a vertical plane or on a conical surface that intersects the plume, 3) Dual beam scanning Doas collecting column data from two different directions, 4) Multi-Axis DOAS, multiple viewing angles and 5)Imaging DOAS (IDOAS) basically combining two principles, imaging spectroscopy and DOAS technique (I.Louban et al. 2007).

Many of these instruments are now automated, thanks to special software that can simplify the process of extraction and processing the data (concentration of gases), and are very important for remote sensing. gas monitoring.

Developments over the past ten years was projected on a global scale thanks to the launch of the satellite systems that Global Ozone Monitoring Instrment GOME on board Earth Research Satellite 2 by ESA (ERS-2) in 1995 has extended explorations of local or regional to global coverage allows us to study simultaneously several chemical species such as O_3, NO_2 , BrO, HCHO, and SO_2 present in the atmosphere. Scanning Imaging Spectrometer (SCIAMACHY) for Atmospheric Cartography was launched in 2002 and is now will likely go offline soon. The next generation of satellite instruments, OMI and GOME2 are now operational.

6.2 *DOAS TECHNIQUES*

The Differential Optical Absorption Spectroscopy is based on the Lambert Beer's law:

$$I(\lambda) = \mathbf{Io}(\lambda) \exp(-\sigma(\lambda)\cdot c\cdot L) \qquad (6.2.1)$$

which describes the diminution of light when light passes through matter. **Io**(λ) is the intensity before the light passes through matter, **I**(λ) the light intensity after the light has passed the matter (i.e. volcanic plume), σ(λ) is the absorption cross section of molecules at wavelength(λ) , **c** the

concentration and **L** the length of the light path, beside absorption of light due to molecules, also scattering (Rayleigh and Mie) takes light out of the light path, ..

A schematic diagram of the basis of Lambert Beer's law

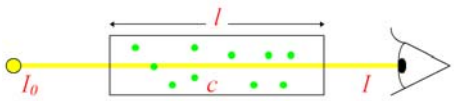

If the length of the light path **L** , is known, the concentration **c** of the species can be calculated as:

$$c = \frac{\ln\left(\frac{Io(\lambda)}{I(\lambda)}\right)}{\sigma(\lambda)\cdot L} \qquad (6.2.2)$$

Where , $\ln\left(\frac{Io(\lambda)}{I(\lambda)}\right)$ is defined optical density **D(λ),** and therefore equation can be written :

$$c = \frac{D(\lambda)}{\sigma(\lambda)\cdot L} \qquad (6.2.3)$$

In the real atmosphere, the Lambert Beer's law is more problematical because the intensity of the light is dropped off by the absorption of other trace gases, and scattered by air molecules and aerosol particles.
In addiction the instrument (mirrors, grating, retro-reflectors, etc.) will also decreases the light intensity.

Considering all these factors previously mentioned as a cause of decrease in light intensity, the Lambert Beer's law has been expanded including the absorption of various trace gases with concentration c_j and absorption cross-section $\sigma_j(\lambda)$, Rayleigh and Mie extinction, scattering by aerosol particles and air molecules $[\varepsilon_R(\lambda)]$ and $[\varepsilon_M(\lambda)]$, and instrumental effect A(λ) become:

$$I(\lambda) = Io(\lambda)\cdot\exp\left[-L\cdot(\Sigma(\sigma_j(\lambda)\cdot c_j)+\varepsilon_R(\lambda)+\varepsilon_M(\lambda))\right]\cdot A(\lambda) \qquad (6.2.4)$$

While in the laboratory it is possible to reduce these effects by subtracting the absorber from the light path, in the open atmosphere these corrections are very difficult. In this case we measure the "differential absorption", defined as the difference between absorption at two different wavelengths (Platt and Stutz,2008).

Basically the DOAS technique makes it possible to isolate the structures of trace gases separated by broad and narrow band using a filtering method,

$$\sigma_j(\lambda) = \sigma_{j0}(\lambda) + \sigma_j'(\lambda) \qquad (6.2.5)$$

In these Equation $\sigma_{j0}(\lambda)$ represent slow variation with wavelength(λ) , and $\sigma_j'(\lambda)$ rapid variations with wavelength (λ)

The meaning of 'rapid' and 'slow' variation of the absorption cross-section as a function of wavelength is, of course, a question of the observed wavelength interval and the width of the absorption bands to be detected. (Platt and Stutz,2008).

The expanded Lambert Beer's Law can then be rewritten in the following equation:

$$I(\lambda) = I_0(\lambda) \cdot \exp\left[-L \cdot \left(\sum_j (\sigma_j^{'}(\lambda) \cdot c_j) \right) \right] \cdot \exp\left[-L \cdot \left(\sum_j (\sigma_{j0}(\lambda) \cdot c_j) + \varepsilon_R(\lambda) + \varepsilon_M(\lambda) \right) \right] \cdot A(\lambda)$$

(6.2.6)

The first exponential function represent the rapid structured differential absorption of trace gas species, the second exponential function represent the slow absorption due to the influence to Rayleigh and Mie scattering.
Considering the instrument factor $[A(\lambda)]$ dependent of a slow wavelength, the intensity in the absence of differential absorption $I_o^{'}(\lambda)$ can be defined as:

$$I_0^{'}(\lambda) = I_0(\lambda) \cdot \exp\left[-L \cdot \left(\sum_j (\sigma_{j0}(\lambda) \cdot c_j) + \varepsilon_R(\lambda) + \varepsilon_M(\lambda) \right) \right] \cdot A(\lambda) \qquad (6.2.7)$$

The differential optical density $D^{'}(\lambda)$ can be defined as:

$$D^{'}(\lambda) = \ln \frac{I_0^{'}(\lambda)}{I(\lambda)} = L \cdot \sum_j \sigma_j^{'}(\lambda) \cdot c_j \qquad (6.2.8)$$

The equation (6.2.3) can be rewritten

$$c_j = \frac{D^{'}(\lambda)}{\sigma_j^{'}(\lambda) \cdot L} \qquad (6.2.9)$$

Where the concentration of atmospheric trace gases can be calculated replacing $D(\lambda)$ and $\sigma(\lambda)$ by $D^{'}(\lambda)$ and $\sigma^{'}(\lambda)$.

6.3 Soil degassing accumulation chamber method

The most diffuse techniques to measure the soil CO_2 flux is the accumulation chamber method. This method is based on the measurements of CO_2 concentration on the time utilizing normally an Infra-Red spectrometer. The flux is proportional to the slope of concentration in the time (Fig. 49).

$$dC_{CO2}/dt$$

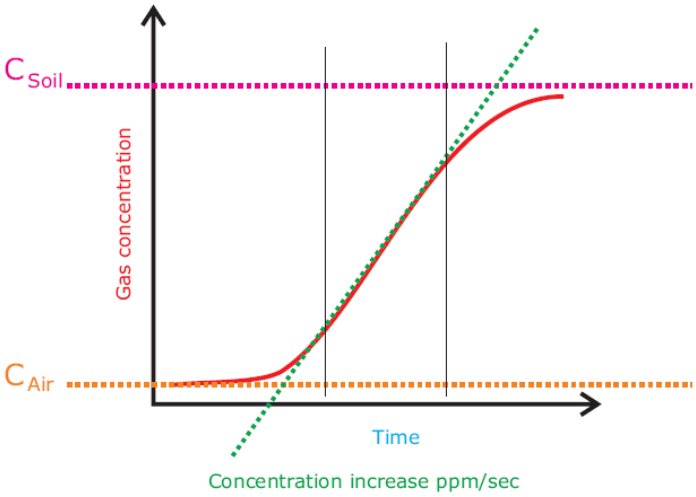

Fig 49 Graphical resolution of CO2 flux measurements.CO_2 concetration vs time the sloop it's proportional to CO2 flux

The amount of CO2 measurements was performed in ppm s^{-1} and on the basis of proportionality factor the CO2 flux was calculate in moles m^2 d^{-1}. The proportionality factory (K) depends on the chamber volume/surface ratio as well as the barometric pressure and the air temperature inside the accumulation chamber. The most common unit is grams/square meter per day, but using the same instrument for two gas species to express the flux using this unit means to have two different conversion factors. Actually we use the unit *moles/square meter per day* that has two advantages: A single conversion factor for every gas specie and an easy conversion of the flux in grams/sm per day simply multiplying the result expressed in moles/sm per day for the molecular weight of the target gas. The accumulation chamber factors A.c.K.:

$$K = \frac{86400 \cdot P}{10^6 \cdot R \cdot T_k} \cdot \frac{V}{A}$$

Where

P is the barometric pressure expressed in mBar (HPa)
R is the gas constant 0.08314510 bar L K-1 mol-1
T is the air temperature expressed in Kelvin degree **k**
V is the chamber net volume in cubic meters
A is the chamber inlet net area in square meters.

The dimensions of the A.c.K. are:

$$K = \frac{moles \cdot meter^{-2} \cdot day^{-1}}{ppm \cdot sec^{-1}}$$

7 Instrumentations

7.1 CO_2 soil portable flux-meter

The WEST Systems fluxmeter is a portable instrument for the measurement of diffuse degassing phenomena ***fig50*** , based on the accumulation chamber method, suitable for volcanic and geothermal areas as well as soil respiration rate in agronomy. This method studied for soil respiration in agronomy and for soil degassing in volcanic areas (Chiodini et al. 1998), has been designed by WEST Systems to obtain a portable instrument that allows the performance of measurements with very good accuracy in a short time. The instrument allows a wide range evaluation of the amount of soil gas flux, and can be also used for the survey of biogas non controlled emissions on landfills.

The instrument is extremely versatile and allow measurement of flux in 2/4 minutes.

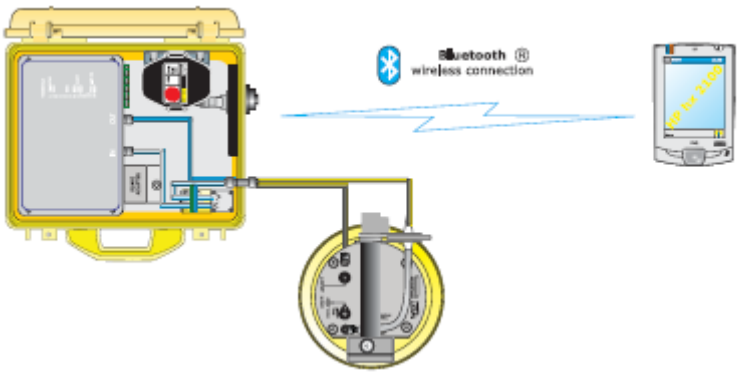

Fig 50 In the drawing CO_2 soil portable flux-meter, the accumulation chamber, electronic IR spectrometer and Gps, palm recorder data.

7.2 CO2 Soil permanent flux-meter

The station, in the default configuration (Fig. 51), record and store the barometric pressure, the air temperature and the soil temperature. The variation of few degrees of temperature do not affect the evaluation of flux very much, then it's possible to use the air temperature instead of the temperature of the gas mixture into the accumulation chamber. The instrument measures the barometric pressure, using the VAISALA barometric pressure gauge, with a good accuracy. A platinum Pt100 it's used to measure the soil temperature and a digital solid state based device measure the air temperature.

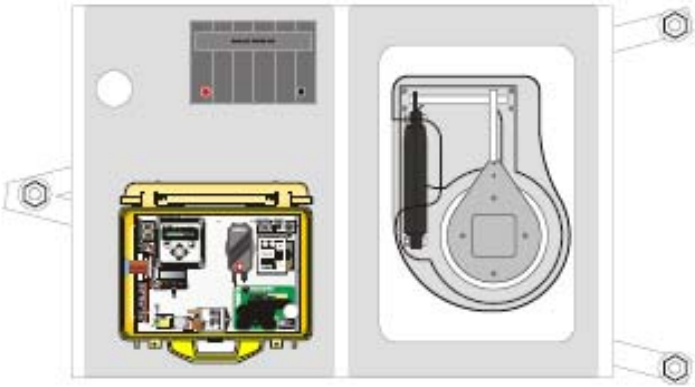

Fig 51) In the drawing the top view of box with the station, the battery and the accumulation chamber in measuring position.

7.3 MiniDOAS

The mobile mini-DOAS instrument includes a telescope, an optical fibre, one spectrometer, one GPS and a PC ***fig. 52***.

The telescope consists of a quartz lens, a U330 filter is used in order to reduce stray light, blocking visible light with wavelength higher then 360 nm (Galle et al. 2003).

The optical quartz fibre connects the telescope to the spectrometer in order to transfer the light beam. The spectrometer used was a Ocean Optics SD 2000 with spectral range from 280nm to 420nm.

Spectrometer and GPS are connected to a computer controlled by software (Mobile Doas) which collects and evaluates acquired spectra in real time (Zhang and Johansson2004-2008)

The telescope is installed in a vehicule and positioned vertically with the aim of measuring the total number of molecules in a cross section of a plume. The transects are carried out in a perpendicular direction to the plume.

For each measurements the exposure time is recorded and automatically calculated in order to regulate the amount of light entering the detector, the exposure time depending of the weather conditions and by solar position during the day.

One reference spectrum is collected at the beginning of every measurement, it is preferable to collect the reference spectrum or “sky spectrum” outside the plume, since the measurement was referred to this initial spectrum. The second spectrum is the dark spectrum collected in the absence of light and used during the evaluation for removing the instrumental noise.

Global Position System (GPS) data is recording for each collect spectrum giving both time and position of each spectrum collected.

To get the flux from traverses the SCD slant column density must be multiplied by the distance perpendicular to the wind direction and by the wind speed at plume height.

Fig. 52 - Mobile mini-DOAS instrument essentially formed by a telescope a optical fibre, one spectrometer, one GPS, and a PC.

7.4 UV-Scanning DOAS

Also called NOVAC Version 1 instrument was designed to be a robust and simple instrument for measurement of volcanic emissions fluxes at high time resolution with minimal power consumption.

Composed predominantly as the mini DOAS described above but with a substantial difference, it work in a fixed position and the scanning of the plume is ensured by a motorized device that allows to take measurements from horizon to horizon in a 180°.

In particular, a composite system from a rotating part driven by a step motor controlled by the electronics, allows the reception of the light beam, that is reflected by a mirror and directed into the telescope. This UV light is coupled to optical fiber, which transmits the signal to the spectrometer. By placing the mirror at 60 degrees a conical scan surface can be performed instead of over a vertical plane. In this condition the instrumental coverage is more than the models with upright position(mirror at 90°). ***fig. 53***

The spectrometer is an Ocean Optics S2000, which incorporate a high-sensitivity 2048-element linear CCD array detector, coupled with an Ocean Optics ADC1000-USB A/D analogue to digital converter, is connected with the electronics based on an embedded computer. The wavelength range is set at 280–420 nm.

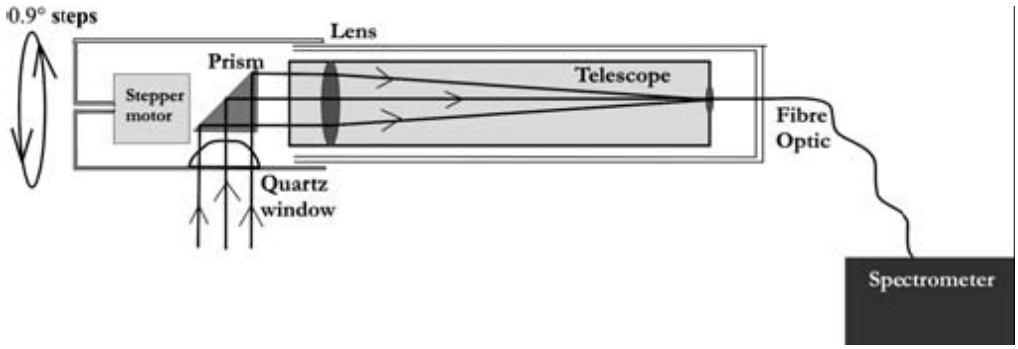

Fig. 50 - UV Scanning DOAS (modified by Galle et al 2010)

The integration time (the time the CCD array is exposed to light) is adjusted automatically throughout the day by the software, in the range 200 to 1,000 ms, to account for changes in the intensity of sunlight throughout the day and to prevent saturation of the data stream.

The integration time is linked to the angular velocity of the stepper motor such that, for any integration time, there is the same number of data points per scan (i.e. the prism rotates faster for faster measurement times).

A (GPS) provides latitude and longitude of the instrument and the exact time for each measurement.

A web-server, and a FTP-server allow by network-interface the transmission data.

The scanning systems are powered by solar panels and a 12-V battery. Electronic timer switching the power on in the morning and off at night, data collection is programmed to begin at 08:00 and continues until 16:00 h.

The spectrometer and the electronic part of the scanning system are housed in insulated boxes, and a Peltier cooling system technology prevents changes in temperature.

Free Wave radio modems; transfer the data from embedded pc back to the observatory.

7.5 UV- scanning DOAS Mark II

The Dual-axis scanning DOAS, also called NOVAC Version II instrument, was designed to allow the best possible spectroscopy and enhanced flexibility in regard to measurement geometry of the plume. ***fig. 47***.

The difference that distinguishes it from scanning DOAS described above is the ability to perform scanning in all directions.

The Dual-axis scanning Doas in fact has two motors step, one (elevation motor), that allows scan from zenith to zenith and the second motor or (Azimuth motor) that allows movements in the horizontal plane.

The geometry of this device is totally different from scanning mini DOAS, in this case, both the optical and the electronics are in the same box that can be used in a fixed position or discontinuous measurements mounted on a tripod.

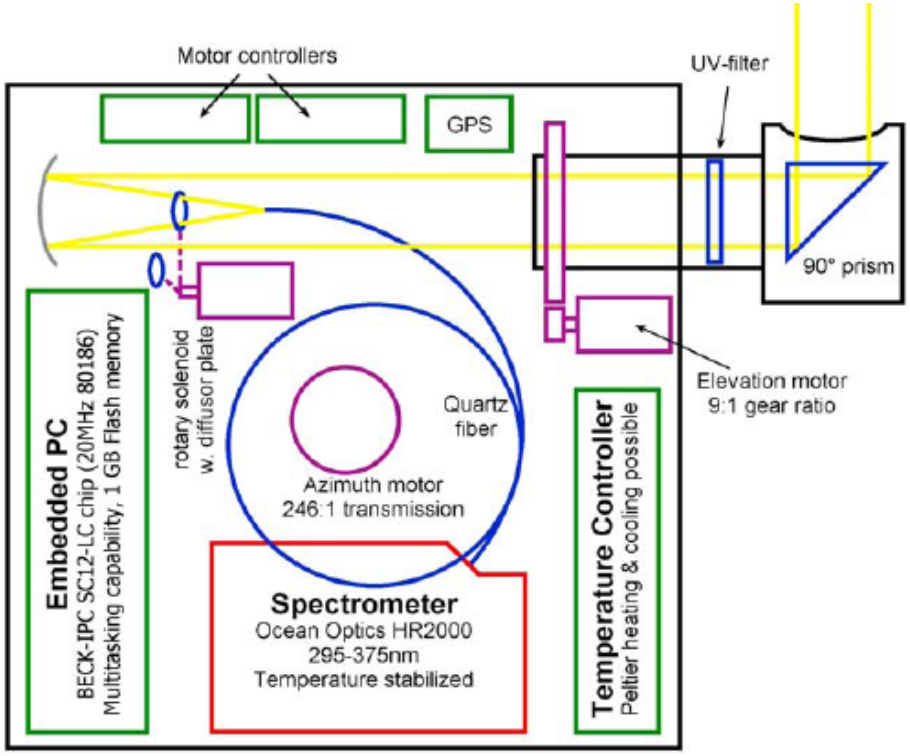

Fig. 47 UV- scanning DOAS Mark II (Modified by Galle et al.2010)

From the instrumental point of view this device contain a spectrometer Ocean Optics HR2000 with a focal length of 101.6 mm at f/4, a 100 mm entrance slit, and a 2400 groove/mm grating, yielding a wavelength range of 295–390 nm. The spectrometer optical bench temperature
is controlled by a thermoelectric Peltier module regulated using a Super Cool PR-59 temperature controller with constant voltage pulse width modulation.

The entry of light is ensured by the presence of an optical system composed of: a prism which replaces the mirror, an Hoya U330 UV filter and 25 mm diameter spherical mirror that focused the beam onto a single 400 mm fused silica fiber positioned in the focal point 75 mm away and leading to the spectrometer.

The electronic consists of a An embedded PC that controls the peripheral components in the sensor, with the assistance of a software package especially developed to control spectra collection, read out information from the GPS receiver and temperature sensor, handle data communication, and manage the file system. (Galle et al. 2010).Data transmission is ensured by a wireless system.

8. Conclusions

The main goal of this PhD thesis have been focused on the importance of extensive parameters in the study of volcanic systems. In particular, anomalous degassing of CO_2 from the soils and SO_2 fluxes from the plume have been investigated. The measurements of these kind of parameters were carried out on Stromboli and Vulcano islands. These volcanoes, characterized respectively by Strombolian and Solphataric activities, give us the opportunity to investigate the relationships between some recorded geochemical variations and the changes observed in the stage of volcanic activity.

In particular we have reported data of SO_2 and CO_2 fluxes emitted respectively from the plume and degassed from the soils in the upper part of the Stromboli area in the period February-April 2007, concomitant to a period of effusive eruption. The entire data set of CO_2 and SO_2 fluxes recorded during the 2007 eruption, highlights the relationship between extensive parameters (fluxes measured) and observed changes in volcanic activity.

The same geochemical approach was utilized at Vulcano Island even if this volcano is actually in a stage of solphataric activity. The results of our preliminary investigation shows huge variations (order of magnitude) in the SO_2 and CO_2 fluxes in coincidence of some other geochemical parameters acquired discontinuously (Gas/H_2O ratio of fumaroles) and geophysical parameters (increase of shallow seismic activity). These promising results open new prospective for the strengthening of geochemical monitoring of volcanic activity and for the constraints regarding the construction of a "geochemical model", necessary condition to better understand the functioning of volcanic systems.

Moreover, another part of the investigation of this PhD thesis was focused on the realization of a innovative telemetric equipment " Active-DOAS" that give us the possibility to improve both, in number and sensitivity, the determination of some geochemical parameters (SO2, BrO, ClO and OClO) to better investigate the composition of fluids emitted from volcanic systems to the atmosphere.

9 References

Aiuppa A, Burton M, Muré F, Inguaggiato S (2004) Intercomparison of volcanic gas monitoring methodologies performed on Vulcano Island, Italy. Geophys Res Lett 31:L02610. doi:10.1029/2003GL018651

Aiuppa A, Federico C (2004) Anomalous magmatic degassing prior to the 5th April 2003 paroxysm on Stromboli. Geophys Res Lett L14607. doi:10.1029/2004GL020458

Aiuppa A, Federico C, Giudice G, Giuffrida G, Guida R, Gurrieri S, Liuzzo M, Moretti M, Papale P (2009) The 2007 eruption of Stromboli volcano: Insights from real-time measurement of the volcanic gas plume CO_2/SO_2 ratio. J Volcanol Geotherm Res 182:221–230

Aiuppa A, Federico C, Giudice G, Gurrieri S, Valenza M (2006) Hydrothermal buffering of the SO_2/H_2S ratio in volcanic gases: Evidence from La Fossa Crater fumarolic field, Vulcano Island. Geophys Res Lett 33:L21315, doi:10.1029/2006GL027730

Aiuppa A, Inguaggiato S, McGonigle AJS, O'Dwyer M, Oppenheimer C, Padgett MJ, Rouwet D, Valenza M (2005) H_2S fluxes from Mt. Etna, Stromboli, and Vulcano (Italy) and implications for the sulfur budget at volcanoes. Geochim Cosmochim Ac 7:1861-1871

Aiuppa, A., Federico, C., Giudice, G., Guerrieri, S., (2005b) Chemical mapping of a fumarolic field: La Fossa Crater; Vulcano Island (Aeolian Island, Italy) Geophysical research letters, vol. 32, L13309

Aiuppa, A., Burton, M., Caltabiano, T., Giudice G., Gurrieri S., Liuzzo, M., Murè, F., Salerno, G., (2010) Unusually large magmatic CO_2 gass emission prior to a basaltic paroxysm. Geophysical research letters, vol. 37, L17303

Allard P (1983) The origin of hydrogen, carbon, sulphur, nitrogen and rare gases in volcanic exhalations: evidence from isotope geochemistry, In: Tazieff H, Sabroux Jc (eds) Forecasting volcanic events. Elsevier, Amsterdam, pp 337-386

Allard P, Le Bronec J, Morel P, Vavasseur C, Faivre-Pierret R, Robe MC, Roussel C, Zettwoog P (1987) Geochemistry of soil gas emanations from Mt Etna, Sicily. Terra Cognita 7 :G 17– 52, 407

Allard P, Carbonelle J, Dajlevic D, Le Bronec J, Morel P, RobeMC, Maurenas JM, Faivre-Pierret R, Martin D, Sabroux JC and Zettwoog P (1991) Eruptive and diffuse emissions of CO2 from Mount Etna. Nature 351:387–391

Allard P, Burton M, Muré F (2005) Spectroscopic evidence for a lava fountain driven by previously accumulated magmatic gas. Nature 433:407-410

Allard P, Carbonnelle J, Métrich N, Loyer H, Zettwoog P (1994) Sulphur output and magma degassing budget of Stromboli volcano. Nature 368:326-330

Allard P, Aiuppa A, Burton M, Caltabiano T, Federico C, Salerno G, La Spina A (2008) Crater gas emissions and the magma feeding system of Stromboli Volcano, In: Calvari S, Inguaggiato S, Puglisi G, Ripepe M, Rosi M (eds) The Stromboli volcano: an integrated study of the 2002-2003 eruption. American Geophysical Union Mon 182:65-80

"Annual Mean Growth Rate for Mauna Loa, Hawaii". *Trends in Atmospheric Carbon Dioxide*. NOAA Earth System Research Laboratory. http://www.esrl.noaa.gov/gmd/ccgg/trends/#mlo_growth. Retrieved 28 April 2010.

Badalamenti B., Chiodini G., Cioni R., Favara R., Francofonte S., Gurrieri S., Hauser S., Inguaggiato S., Italiano F., Magro G., Nuccio P.M. Parello F., Pennisi M., Romeo L., Sortino F., Valenza M., and Vurro F. (1991) Special field workshop at Vulcano (aeolian Island) during summer 1988: Geochemical result . Acta Vulcanol. 1,223-227

Baubron JC, Allard P, Toutain JP (1990) Diffuse volcanic emissions of carbon dioxide from Vulcano Island, Italy. Nature 344:51–53

Baubron JC, Allard P, Sabroux JC, Tedesco D, Toutain JP (1991) Soil gas emanations as precursory indicators of volcanic eruptions,J Geol Soc Lond 148:571-576

Barberi F, Rosi M, Sodi A (1993) Volcanic hazard assessment at Stromboli based on review of historical data. Acta Vulcanol 3:173– 187

Barberi F, Gandino A, Gioncada A, La Torre P, Sbrana A, Zenucchini C (1994) The deep structure of the Eolian arc (Filicudi–Panarea–Vulcano sector) in light of gravity, magnetic and volcanological data. J Volcanol Geotherm Res 61:189–206

Barberi F, Rosi M (2007) The chronology of the 2007 Stromboli eruption and the activity of the scientific synthesis group. In: Proceedings of the XXIV IUGG General Assembly, Perugia, Italy

Bertagnini A, Métrich N, Landi P, Rosi M (2003) Stromboli volcano (Aeolian Archipelago, Italy): an open window on the deep-feeding system of a steady state basaltic volcano. J Geophys Res 108. doi:10.1029/2002JB002146

Bertagnini A, Métrich N, Francalanci L, Landi P, Tommasini S, Conticelli S (2008) In: Calvari S, Inguaggiato S, Puglisi G, Ripepe M, Rosi M (eds) The Stromboli volcano: an integrated study of the 2002-2003 eruption. American Geophysical Union Mon 182:19-37

Billi, A., Barberi, G., Faccenna, C., Neri, G., Pepe, F. and Sulli, A., 2006. Tectonics and seismicity of the Tindari Fault System, southern Italy: Crustal deformations at the transition between ongoing contractional and extensional domains located above the edge of a subducting slab. Tectonics, 25, TC2006, doi: 10.1029/2004TC001763.

Bobrowski N (2005) Volcanic Gas Studies by MAX-DOAS. PhD Thesis, University of Heidelberg.

Bobrowski N, Hönninger G, Galle B, Platt U (2003) Detection of bromine monoxide in a volcanic plume. Nature 423:273-276

Brantley, SL; Koepenick, KW (1995) Measured carbon-dioxide emissions from oldoinyo-lengai and the skewed distribution of passive volcanic fluxes. GEOLOGY 23 (10):933-936.

Bruno N, Caltabiano T, Romano R (1999) SO_2 emissions at Mt. Etna with particular reference to the period 1993-1995. Bull Volcanol 60:405-411

Brusca L, Inguaggiato S, Longo M, Madonia P, Maugeri R (2004) The 2002-2003 eruption of Stromboli (Italy): evaluation of the volcanic activity by means of continuous monitoring of soil temperature, CO_2 flux, and meteorological parameters. Geochem Geophys Geosyst 5:Q12001. doi:10.1029/2004GC000732

Burton M, Allard P, La Spina A, Muré F (2007a) Magmatic gas composition reveals the source depth of slug-driven Strombolian explosive activity. Science. doi: 10.1126/science.1141900

Burton MR, Mader HM, Polacci M (2007b) The role of gas percolation in quiescent degassing of persistently active basaltic volcanoes. Earth Planet Sci Lett 264:46-59

Calvari S, Spampinato L, Lodato L, Harris AJL, Patrick MR, Dehn J, Burton MR, Andronico D (2005) Chronology and complex volcanic processes during the 2002–2003 flank eruption at Stromboli volcano (Italy) reconstructed from direct observations and surveys with a handheld thermal camera. J Geophys Res 110:B02201. doi:1029/2004JB003129

Capasso, G. & Inguaggiato, S., 1998. A simple method for the determination of dissolved gases in natural waters. An application to thermal waters from Vulcano Island. Applied Geochem. 13, 631-642.

Capasso G, Carapezza ML, Federico C, Inguaggiato S, Rizzo A (2005) Geochemical monitoring of the 2002-2003 eruption at Stromboli volcano (Italy): precursory changes in the carbon and helium isotopic composition of fumarole gases and thermal waters. Bull Volcanol 68:118-134

Capasso G, Favara R, Inguaggiato S (1997) Chemical features and isotopic composition of gaseous manifestations on Vulcano Island (Aeolian Islands, Italy): an interpretative model of fluid circulation. Geochim Cosmochim Acta 61:3425-3440

Carapezza ML, Inguaggiato S, Brusca L, Longo M (2004) Geochemical precursors of the activity of an open-conduit volcano: The Stromboli 2002-2003 eruptive events. Geophys Res Lett 31:L07620. doi:10.1029/2004GL019614

Carapezza ML, Federico C (2000) The contribution of fluid geochemistry to the volcano monitoring of Stromboli. J Volcanol Geotherm Res 95:227-245

Carbonelle J, Dajlevic D, Le Bronec J, Morel P, Obert JC, Zettwoog P (1985) Etna: composantes sommitales et parietales des emission de gaz carbonique, vol 108. Bull Programme Interdisciplinaire de Recherche sur la Prevision et la Surveillance des Eruptions Volcaniques - Centre National de la Recherche Scientifique

Cardellini C, Chiodini G, Frondini F (2003) Application of stochastic simulation to CO_2 flux from soil: Mapping and quantification of gas release. J Geophys Res 108:2425. doi:10.1029/2002JB002165

Chiodini G, Cioni R, Guidi M, Raco B, Marini L (1998) Soil CO_2 flux measurements in volcanic and geothermal areas. Appl Geochem 13:543-552

Chiodini et al., 1995. G. Chiodini, R. Cioni, L. Marini and C. Panichi , Origin of fumarolic fluids of Vulcano Island, Italy and implications for volcanic surveillance. *Bull. Volcanol.* **57** (1995), pp. 99–110.

Chiodini G, Frondini F, Raco B (1996) Diffuse emission of CO_2 from the Fossa crater, Vulcano Island (Italy). Bull Volcanol 58:41– 50

Chiodini G, Granieri D, Avino R, Caliro S, Costa A, Werner C (2005) Carbon dioxide diffuse degassing and estimation of heat release from volcanic and hydrothermal systems. J Geophys Res 110:B08204. doi:10.1029/2004JB003542

C.Kern ,H.Sihler,L.Vogel, C.Rivera, M.Herrera, U.Platt (2009) Halogen oxide measurements at Masaya Volcano, Nicaragua using active long path differential optical absorption spectroscopy. Bull. Volcanol. 71:659-670

C.Kern, T.Detschmann, L.Vogel, M. Wohrbach, T.Wagner, U.platt (2010) Radiative transfer corrections for accurate spectroscopic measuremens of volcanic gas emissions.
Bull. Volcanol 72:233-247

Kern C (2009) Spectroscopic measurements of volcanic gas emissions in the ultra-violet wavelength region. Ph.D. thesis, University of Heidelberg, Heidelberg

Kern C, Trick S, Rippel B, Platt U (2006) Applicability of light-emitting diodes as light sources for active differential optical absorption spectroscopy measurements. Appl Opt 45:2077-2088

De Astis G, Ventura G, Vilardo G (2003) Geodynamic significance of the Aeolian volcanism (Southern Tyrrhenian Sea, Italy) in light of structural, seismological, and geochemical data. Tectonics 22(4):1040

De Astis, G., P. Dellino, L. La Volpe, F. Lucchi, and C. A. Tranne (2007), Geological Map of the Vulcano Island, scale 1:10000, edited by L. La Volpe and G. De Astis, Ist. Nat. Geofis. Vulcanol., Napoli, Italy.

Dellino, P., and L. La Volpe (1997), Stratigrafia, dinamiche eruttive e deposizionali, scenario eruttivo e valutazioni di pericolosita` a La Fossa di Vulcano in CNR-GNV Progetto Vulcano 1993–1995, edited by L. La Volpe et al., pp. 214– 237, Felici Publ., Pisa, Italy.

De Rosa, R., N. Calanchi, P. F. Dellino, L. Francalanci, F. Lucchi, M. Rosi, P. L. Rossi, and C. A. Tranne (2004), 32nd International Geological Congress, Field Trip Guide Book–P42, vol. 5, Geology and Volcanism of Stromboli, Lipari, and Vulcano (Aeolian Islands), edited by L. Guerrieri, I. Rischia, and L. Serva, Agency for the Environ. Prot. and Tech. Serv., Rome.

Diliberto, Gurrieri, Valenza, (2002) Relationships between diffuse CO2 emissions and volcanic activityon the island of Vulcano (Aeolian Islands, Italy) during the period 1984-1994.
Bull Volcanol (2002) 64:219-228 DOI10.1007/s00445-001-0198-6

Edmonds M, Herd RA, Galle B, Oppenheimer CM (2003) Automated, high time-resolution measurements of SO_2 flux at Soufrière Hills Volcano, Montserrat. Bull Volcanol 65:578-586

Edmonds M, Pyle D, Oppenheimer C (2001) A model for degassing at the Soufrière Hills Volcano, Montserrat, West Indies, based on geochemical data. Earth Planet Sci Lett 186:159-173

Ellam, R. M., C. J. Hawkesworth, M. A. Menzies, and N. W. Rotgers (1989), The volcanism of southern Italy : Role of subduction and the relationship between potassic and sodic alkaline magmatism, J. Geophys. Res., 94, 4589-4601.

Favara R, Giammanco S, Inguaggiato S**,** Pecoraino G (2001) Preliminary estimate of CO_2 output from Pantelleria Island volcano (Sicily, Italy): evidence of active mantle degassing. Appl Geochem 16:883-894

Federico C, Brusca L, Carapezza ML, Cigolini C, Inguaggiato S, Rizzo A, Rouwet D (2008) Geochemical prediction of the 2002-2003 Stromboli eruption from variations in CO_2 and Rn emissions and in helium and carbon isotopes. In: Calvari S, Inguaggiato S, Puglisi G, Ripepe M, Rosi M (eds) The Stromboli volcano: an integrated study of the 2002-2003 eruption. American Geophysical Union Mon 182:117-128

C. Federico, G. Capasso, A. Paonita, R. Favara (2010). Effects of steam-heating processes on a stratified volcanic aquifer: Stable isotopes and dissolved gases in thermal waters of Vulcano Island (Aeolian archipelago) Journal of Volcanology and Geothermal Research 192 (2010) 178–190

Finizola A, Sortino F, Lénat JF, Valenza M (2002) Fluid circulation at Stromboli volcano (Aeolian Islands, Italy) from self-potential and CO_2 surveys. J Volcanol Geotherm Res 116:1-18

Finizola A, Sortino F, Lénat JF, Aubert M, Ripepe M, Valenza M (2003) The summit hydrothermal system of Stromboli. New insights from self-potential, temperature, CO_2 and fumarolic fluid measurements, with structural and monitoring implications. Bull Volcanol 65:486-504

Frazzetta, G., L. La Volpe, and M. F. Sheridan (1983), Evolution of the Fossa cone, Volcano, J. Volcanol. Geotherm. Res., 17, 329– 360.

Frazzetta, G., P. Y. Gillot, L. La Volpe, and M. F. Sheridan (1984), Volcanic hazards at Fossa of Volcano: Data from the last 6,000 years, Bull. Volcanol., 47, 105–125.

Galle B, Oppenheimer C, Geyer A, McGonigle AJS, Edmonds M, Horrocks LA (2003) A miniaturised ultraviolet spectrometer for remote sensing of SO_2 fluxes: A new tool for volcano surveillance. J Volcanol Geotherm Res 119:241– 254

Bo Galle, Mattias Johansson, Claudia Rivera, Yan Zhang, Manne Kihlman, Christoph Kern, Thomas Lehmann, Ulrich Platt, Santiago Arellano, and Silvana Hidalgo (2010)
Network for Observation of Volcanic and Atmospheric Change (NOVAC)—A global network for volcanic gas monitoring: Network layout and instrument description. JOURNAL OF GEOPHYSICAL RESEARCH, VOL. 115, D05304, doi:10.1029/2009JD011823, 2010

Gerlach TM (1993) Oxygen buffering of Kilauea volcanic gases and the oxygen fugacity of Kilauea basalt. Geochim Cosmochim Acta 57:795-814

Gerlach TM, Nordlie BE (1975) The C-O-H-S gaseous systems. Part II: temperature, atomic composition, and molecular equilibria in volcanic gases. Am J Sci 275:377-394

Ghisetti, F., 1979. Relazioni tra strutture e fasi trascorrenti e distensive lungo i sistemi Messina-Fiumefreddo, Tindari-Letojanni e Alia-Malvagna (Sicilia nord-orientale): uno studio microtettonico. Geol. Rom. 18, 23–56.

Giammanco S, Inguaggiato S, Valenza M (1998) Soil and fumarole gases of Mount Etna: geochemistry and relations with volcanic activity. J Volcanol Geotherm Res 81:297-310

Giggenbach WF (1980) Geothermal gas equilibria. Geochim Cosmochim Acta 44:2021-2032

Giggenbach WF (1996) Chemical composition of volcanic gases. In: Scarpa R, Tilling R (eds) Monitoring and Mitigation of Volcano Hazards. Springer-Verlag, Berlin:221–256

Grassa F, Inguaggiato S, Liotta M (2008) Fluid geochemistry of Stromboli. In: Calvari S, Inguaggiato S, Puglisi G, Ripepe M, Rosi M (eds) The Stromboli volcano: an integrated study of the 2002-2003 eruption. American Geophysical Union Mon 182:49-64

Hönninger G, Friedeburg Cv, Platt U (2004a) Multi Axis Differential Optical Absorption Spectroscopy (MAXDOAS). Atmos Chem Phys 4:231-254

Louban .I, N.Bobrowski, D.Rowet, S.Inguaggiato, U.Platt (2009) Imaging DOAS for Volcanological Applications. Bull.Volcanol. 71:753-765

Inguaggiato S, Vita F., Rouwet D., Bobrowski N., Morici S., Sollami A. (2011) Geochemical evidence of the renewal of volcanic activity inferred from CO_2 soil and SO_2 plume fluxes: the 2007 Stromboli eruption (Italy) Bull Volcanol DOI: 10.1007/s00445-010-0442-z

Inguaggiato S, Martin-Del Pozzo AL, Aguayo A, Capasso G, Favara R (2005) Isotopic, chemical and dissolved gas constraints on spring water from Popocatépetl (Mexico): evidence of gas-water interaction magmatic component and shallow fluids. J Volcanol Geotherm Res 141:91-108

Inguaggiato S, Pecoraino G, D'Amore F (2000) Chemical and isotopical characterization of fluid manifestations of Ischia Island (Italy). J Volcanol Geotherm Res 99:151-178

Inguaggiato S, Rizzo A (2004) Dissolved helium isotope ratios in ground-waters: a new technique based on gas-water re-equilibration and its application to Stromboli volcanic system. Appl Geochem 19:665-673

Inguaggiato S, Taran YA, Grassa F, Capasso G, Favara R, Varley N, Faber E (2004) Nitrogen isotopes in thermal fluids of a forearc region (Jalisco Block, Mexico): evidence for heavy nitrogen from continental crust. Geochem Geophys Geosyst 5:Q12003. doi:10.1029/2004GC000767

Italiano F, Pecoraino G, Nuccio PM (1997) Steam output from fumaroles of an active volcano: Tectonic and magmatic-hydrothermal controls on the degassing system at Vulcano (Aeolian arc). J Geophys Res 103:29829– 29842

Italiano, F., Nuccio P.M., (1994) Gas/steam ratios and thermal energy release measured at the gaseous emission of thr baia di Levante of Vulcano Island, Italy. Acta Vulcanol 5:89-94

Johansson M, Galle B, Rivera C, Zhang Y (2009a) Tomographic Reconstruction of Gas Plumes Using Scanning DOAS. submitted to B Volcanol

Johansson M, Kihlman M, Norman P, Rivera C, Zhang Y, Galle B (2008) NOVAC Station User Manual.

Keller, J., 1980. The island of Vulcano. Rend. Soc. Ital. Mineral. Petrol. 36,369-414

Louban .I, N.Bobrowski, D.Rowet, S.Inguaggiato, U.Platt (2009) Imaging DOAS for Volcanological Applications. Bull.Volcanol. 71:753-765

Madonia P, Brusca L, Inguaggiato S, Longo M, Morici S (2009) Variations of soil temperature, CO_2 flux, and metereological parameters. In: Calvari S, Inguaggiato S, Puglisi G, Ripepe M, Rosi M (eds) The Stromboli Volcano: An Integrated Study of the 2002-2003 Eruption. American Geophysical Union Mon:269-278

Mazot A, Rouwet D, Taran Y, Inguaggiato S, Nick Varley (2010) CO_2 and He degassing at El Chichón volcano (Chiapas, Mexico): gas flux, origin, and relationship with local and regional tectonics. Bull Volcanol: this volume

McGonigle, A.J.S., Aiuppa, A., Giudice, G., Tamburello, G., A. J., Hodson, Gurrieri S. (2008) Unmanned aerial vehicle measurements of volcanic carbon dioxide fluxes. Geophysical research letters, vol. 35, L06303

Merten A (2008) New design of Longpath-DOAS instruments based on fibre optics and applications in the study of the urban atmosphere. PhD thesis, University of Heidelberg, Heidelberg, Germany

Merten A, Tschritter J, Platt U (2010) Novel Design of DOAS-Long-path Telescopes based on fiber optics. submitted to Appl Opt

Millan MM, Hoff RM (1978) Remote sensing of air pollutant by correlation spectroscopy instrumental response characteristics. Atmospher Environm 12:853-864

Morner, NA; Etiope, G (2002) Carbon degassing from the lithosphere. GLOBAL AND PLANETARY CHANGE, 33 (1-2): 185-203.

Neri M, Lanzafame G, Acocella V (2008) Stromboli (Italy) eruption. Dyke emplacement and related hazard in volcanoes with sector collapse: the 2007 Stromboli (Italy) eruption. J Geol Soc. doi:10.1144/0016-76492008-002

Nuccio PM, Paonita A (2001) Magmatic degassing of multicomponent vapors and assessment of magma depth: application to Vulcano Island (Italy). Earth Planet Sci Lett 193:467-481

Oppenheimer C, Francis P, Burton M, Maciejewski AJH, Boardman L (1998) Remote measurement of volcanic gases by Fourier transform infrared spectroscopy. Appl Phys 67:505-515

O'Dwyer. M., Padgett, M. J., McGonigle, A. J. S., Oppenheimer, C., Inguaggiato, S., (2003) Real-time measurement of volcanic H_2S, and SO_2 concentrations by UV spectroscopy. Geophysical research letters, vol 30, NO. 12, 1652

Paonita A, Favara R, Nuccio PM, Sortino F (2002) Genesis of fumarolic emissions as inferred by isotope mass balances: CO_2 and water at Vulcano Island, Italy. Geochim Cosmochim Acta 66:759-772

Pecoraino G, Brusca L, D'Alessandro W, Giammanco S, Inguaggiato S, Longo M (2005) Total CO_2 output from Ischia Island volcano (Italy). Geochem J 39:451-458

Platt, U., D. Perner, G.W. Harris, A.M. Winer, J.N. Pitts, "Observations of nitrous acid in an urban atmosphere by differential optical absorption", Nature, 285, 312-314, 1980a.

Platt, U., and D. Perner, "Measurements of atmospheric trace gases by long path differential UV/visible absorption spectroscopy", in Optical and Laser Remote Sensing, edited by D.A. Killinger, and A. Mooradien, pp. 95-105, Springer Verlag, New York, 1983.

Platt, U., "Differential optical absorption spectroscopy (DOAS)", Chem. Anal. Series, 127, 27 - 83, 1994.

Platt U, Stutz J (2008) Differential Optical Absorption Spectroscopy - Principles and Applications. Springer, Berlin Heidelberg New York, pp 1-597

Rizzo A, Grassa F, Inguaggiato S, Liotta M, Longo M, Madonia P, Brusca L, Capasso G, Morici S, Rouwet D, Vita F (2009) Geochemical evaluation of observed changes in volcanic activity during the 2007 eruption at Stromboli (Italy). J Volcanol Geotherm Res 182:246-254

Rosi M, Bertagnini A, Landi P (2000) Onset of the persistent activity at Stromboli Volcano (Italy) Bull Volcanol 62:294-300

Santacroce, R., R. Cristofolini, L. La Volpe, G. Orsi, and M. Rosi (2003), Italian active volcanoes, Episodes, 26(3), 227– 234

Schneider W, Moortgat GK (1990) UV/VIS Spectra of Atmospheric Constituents, Version 1," ATMOS User Center at Deutsches Fernerkundungsdatenzentrum (DFD). CD-ROM

Sihler H, Kern C, Poehler D, Platt U (2009) Applying light-emitting diodes with narrow-band emission features in differential spectroscopy. Optics Lett 34:3716-3718

Sinclair AJ (1974) Selection of threshold values in geochemical data using probability graphs. J Geochem Explor 3:129-149

Solomon S, Schmeltekopf AL, Sanders RW (1987) On the interpretation of zenith sky absorption measurements. J Geophys Res 92:8311-8319

Stutz, J., and U. Platt (1996)., Numerical Analysis and Estimation of the Statistical Error of Differential Optical Absorbtion Spectroscopy Measurements with Least-Squares methods, *Appl. Opt., 35*, (30), 6041-6053

Stoiber RE, Malinconico LL, Williams SN (1983) Use of the correlation spectrometer at volcanoes. In: Tazieff H, Sabroux JC (eds) Forecasting volcanic events. Elsevier, Amsterdam, pp 425-444

Taran YA, Esikov AD, Cheshko AL (1986) Deuterium and Oxygen-18 in waters of Mutnovsky geothermal area. Geochem Int 4:458-468

Taran Y, Fisher TP, Pokrovsky B, Sano Y, Armienta M, Macias JL (1998) Geochemistry of the volcano-hydrothermal system of El Chichón Volcano, Chiapas, Mexico. Bull Volcanol 59:436-449

Toshiya Mori, Kenji Notsu, Yasunori Tohjima, Hiroshi Wakita, P. Mario Nuccio, Francesco Italiano. (1995) Remote detection of fumarolic gas chemistry at Vulcano, Italy, using an FT-IR spectral radiometer. Earth and Planetary Science Letters 134 (1995) 219-224

Vandaele AC, Simon PC, Guilmot M, Carleer M, Colin R (1994) SO2 absorption cross section in the UV using a Fourier transform spectrometer. J Geophys Res 99:25599-25605

Vandaele AC, Hermans C, Fally S (2009) Fourier transform measurements of SO_2 absorption cross sections: II. Temperature dependence in the 29000-44000 cm^{-1} (227-345 nm) region. J Quant Spectrosc and Radiat Transfer 110:2115-2126

Vandaele AC, Hermans C, Simon PC (2000) Absorption cross-section of CS_2 measured at a resolution of 16 cm^{-1}. http://www.oma.be/BIRA-IASB/Scientific/Topics/Lower/LaboBase/Laboratory.html

Ventura G (1994) Tectonics, structural evolution and caldera formationon Vulcano Island (Aeolian Archipelago, Southern Tyrrhenian sea). J Volcanol Geotherm Res 60:207–224

Werner C, Cardellini C (2006) Comparison of carbon dioxide emissions with fluid upflow, chemistry, and geologic structures at the Rotorua geothermal system, New Zealand. Geothermics 35:221-238

Wu CYR, Judge DL (1981) SO_2 and CS_2 cross section data in the ultraviolet region. Geophys Res Lett 8:769-771

Zhang Y (2005) Wireless sensor network for volcano monitoring. Masters thesis, Chalmers University of Technology.